

# 1.21

## The Moon

P. H. Warren

*University of California, Los Angeles, CA, USA*

---

1.21.1	INTRODUCTION: THE LUNAR CONTEXT	559
1.21.2	THE LUNAR GEOCHEMICAL DATABASE	561
1.21.2.1	<i>Artificially Acquired Samples</i>	561
1.21.2.2	<i>Lunar Meteorites</i>	561
1.21.2.3	<i>Remote-sensing Data</i>	562
1.21.3	MARE VOLCANISM	564
1.21.3.1	<i>Classification of Mare Rocks</i>	564
1.21.3.2	<i>Chronology and Styles of Mare Volcanism</i>	569
1.21.3.3	<i>Mare Basalt Trace-element and Isotopic Trends</i>	573
1.21.4	THE HIGHLAND CRUST: IMPACT BOMBARDMENT AND EARLY DIFFERENTIATION	577
1.21.4.1	<i>Polymict Breccias and the KREEP Component</i>	577
1.21.4.2	<i>Bombardment History of the Moon</i>	578
1.21.4.3	<i>Impactite and Regolith Siderophile Signatures</i>	581
1.21.4.4	<i>Pristine Highland Rocks: Distinctiveness of the Ferroan Anorthositic Suite</i>	583
1.21.4.5	<i>The Magma Ocean Hypothesis</i>	587
1.21.4.6	<i>Alternative Models</i>	590
1.21.5	THE BULK COMPOSITION AND ORIGIN OF THE MOON	591
	ACKNOWLEDGMENTS	592
	REFERENCES	592

---

### 1.21.1 INTRODUCTION: THE LUNAR CONTEXT

Oxygen isotopic data suggest that there is a genetic relationship between the constituent matter of the Moon and Earth (Wiechert *et al.*, 2001). Yet lunar materials are obviously different from those of the Earth. The Moon has no hydrosphere, virtually no atmosphere, and compared to the Earth, lunar materials uniformly show strong depletions of even mildly volatile constituents such as potassium, in addition to N<sub>2</sub>, O<sub>2</sub>, and H<sub>2</sub>O (e.g., Wolf and Anders, 1980). Oxygen fugacity is uniformly very low (BVSP, 1981) and even the earliest lunar magmas seem to have been virtually anhydrous. These features have direct and far-reaching implications for mineralogical and geochemical processes. Basically, they imply that mineralogical diversity and thus variety of geochemical processes are subdued; a factor that to some extent offsets the comparative dearth of available data for lunar geochemistry.

The Moon's gross physical characteristics play an important role in the more limited range of selenochemical compared to terrestrial geochemical processes. Although exceptionally large (radius = 1,738 km) in relation to its parent planet, the Moon is only 0.012 times as massive as Earth. By terrestrial standards, pressures inside the Moon are feeble: the upper mantle gradient is 0.005 GPa km<sup>-1</sup> (versus 0.033 GPa km<sup>-1</sup> in Earth) and the central pressure is slightly less than 5 GPa. However, lunar interior pressures are sufficient to profoundly influence igneous processes (e.g., Warren and Wasson, 1979b; Longhi, 1992, 2002), and in this sense the Moon more resembles a planet than an asteroid.

Another direct consequence of the Moon's comparatively small size was early, rapid decay of its internal heat engine. But the Moon's thermal disadvantage has resulted in one great advantage for planetology. Lunar surface terrains, and many of the rock samples acquired from them, retain for

the most part characteristics acquired during the first few hundred million years of solar system existence. The Moon can thus provide crucial insight into the early development of the Earth, where the direct record of early evolution was effectively destroyed by billions of years of geological activity. Lunar samples show that the vast majority of the craters that pervade the Moon's surface are at least 3.9 Gyr old (Dalrymple and Ryder, 1996). Impact cratering has been a key influence on the geochemical evolution of the Moon, and especially the shallow Moon.

The uppermost few meters of the lunar crust, from which all lunar samples are derived, is a layer of loose, highly porous, fine impact-generated debris—regolith or lunar “soil.” Processes peculiar to the surface of an atmosphereless body, i.e., effects of exposure to solar wind, cosmic rays, and micrometeorite bombardment, plus spheroidal glasses formed by in-flight quenching of pyroclastic or impact-generated melt splashes, all are evident in any reasonably large sample of lunar soil (Lindsay, 1992; Keller and McKay, 1997; Eugster *et al.*, 2000). The lunar regolith is conventionally envisaged as having a well-defined lower boundary, typically 5–10 m below the surface (McKay *et al.*, 1991); below the regolith is either (basically) intact rock, or else a somewhat vaguely defined “megaregolith” of loose but not so finely ground material. Ancient highland terrains tend to have a regolith roughly 2–3 times than that of the maria (Taylor, 1982). However, in much of the highlands the regolith/megaregolith “boundary” may be gradational. The growth of a regolith can approach a steady-state thickness by shielding its substrate against further impacts (Quaide and Oberbeck, 1975), but there is no reason to believe that the size–frequency spectrum of impactors bombarding the Moon (Melosh, 1989; Neukum *et al.*, 2001) features a discontinuity at whatever size (of order 1–10 m) would be necessary to limit disintegration to ~10 m.

All lunar samples are from the regolith, so the detailed provenance of any individual lunar sample is rarely obvious; and for ancient highland samples, never obvious. The closest approach to *in situ* sampling of bedrock came on the Apollo 15 mission. The regolith is very thin near the edge of the Hadley Rille, and many samples of clearly comagmatic basalts were acquired within meters of their 3.3 Ga “young,” nearly intact, lava flow, so that their collective provenance is certain (Ryder and Cox, 1996). Even the regional provenance of any individual lunar sample is potentially allochthonous. However, most lunar rocks, even ancient highland rocks, are found within a few hundred kilometers of their original locations. This conclusion stems from theoretical modeling of cratered landscapes (Shoemaker *et al.*, 1970; Melosh, 1989), plus observational evidence

such as the sharpness of geochemical boundaries between lava-flooded maria and adjacent highlands (e.g., Li and Mustard, 2000).

Besides breaking up rock into loose debris, impacts create melt. Traces of melt along grain boundaries may suffice to produce new rock out of formerly loose debris; the resultant rock would be classified as either regolith breccia or fragmental breccia, depending upon whether surface fines were important, or not, respectively, in the precursor matter (Stöffler *et al.*, 1980). Features diagnostic of a surface component include the presence of glass spherules (typically a mix of endogenous mare-pyroclastic glasses and impact-splash glasses) or abundant solar-wind-implanted noble gases (e.g., Eugster *et al.*, 2000).

Elsewhere, especially in the largest events in which a planet's gravitational strength limits displacement and the kinetic energy of impact is mainly partitioned into heat (Melosh, 1989), impact melt may constitute a major fraction of the volume of the material that becomes new rock. Rocks formed in this manner are classified as impact-melt breccias and subclassified based on whether they are clast-poor or clast-rich, and whether their matrix is crystalline or glassy (Stöffler *et al.*, 1980). Obvious lithic and mineral clasts are very common in impact-melt breccias, although the full initial proportion of clasts may not be evident in the final breccia. Some of the clasts may be so pulverized, especially in large impact events (Schultz and Mendell, 1978), that they are “lost” by digestion into comingled superheated impact melt (Simonds *et al.*, 1976). By some definitions, the term impact-melt breccia may be applied to products of melt plus clast mixtures with initial melt proportion as low as 10 wt.% (Simonds *et al.*, 1976; Papike *et al.*, 1998).

A few impactites feature a recrystallized texture, i.e., they consist dominantly of a mosaic of grains meeting at ~120° triple junctions. These metamorphic rocks, termed granulitic breccias, may form from various precursor igneous or impactite rocks, and the heat source may be regional (burial) or local, such as a nearby impact melt (Stöffler *et al.*, 1980). But lunar granulitic breccias are almost invariably fine grained, and they tend to be “contaminated” with meteoritic siderophile elements (e.g., M. M. Lindstrom and D. J. Lindstrom, 1986; Warren *et al.*, 1991; Cushing *et al.*, 1999), implying that the precursor rocks were probably mostly shallow impact breccias (brecciation and siderophile-element contamination being concentrated near the surface), and the heat source was probably most often a proximal mass of impact melt.

Besides impactites, which are predominant near the bombarded surface, virtually all other lunar crustal rocks are igneous or annealed-igneous. The super-arid Moon has never produced

(by any conventional definition) sedimentary rock, and most assuredly has never hosted life. Even metamorphism is of reduced scope, with scant potential for fluid-driven metasomatism. Evidence for metamorphism among returned lunar samples is mostly confined to impact shock and thermal effects. Although regional burial metamorphism may occur (Stewart, 1975), deeply buried materials seldom find their way into the surface regolith, whence all samples come. Annealing of lunar rocks is more likely a product of simple post-igneous slow cooling (at significant original depth), dry baking in proximity to an intrusion, or baking within a zone of impact heating.

The Moon's repertoire of geochemical processes may seem limited, but it represents a key link between the sampled asteroids (see Chapters 1.05 and 1.11) and the terrestrial planets. Four billion years ago, at a time when all but monocrystalline bits of Earth's dynamic crust were fated for destruction, most of the Moon's crust had already achieved its final configuration. The Moon thus represents a unique window into the early thermal and geochemical state of a moderately large object that underwent igneous differentiation in the inner solar system, and into the cratering history of near-Earth space.

## 1.21.2 THE LUNAR GEOCHEMICAL DATABASE

### 1.21.2.1 Artificially Acquired Samples

Six Apollo missions acquired a total of 382 kg of rocks and soil. Sampling was mostly by either simple scooping of bulk regolith, or by collection of large individual samples, mostly much bigger than 0.1 kg (four of the six missions collected individual rocks >8 kg). As a result, the particle size distribution of the overall sample is strongly bimodal. Of the total Apollo collection, rocks big enough to not pass a 10 mm sieve comprise 70 wt.%, yet the fraction between 1 nm and 10 mm adds only 2–3 wt.%, and the remaining 27–28 wt.% of the material is <1 mm fines (including core fines) (Vaniman *et al.*, 1991). Three Russian unmanned Luna missions added a total of 0.20 kg of bulk regolith. All nine of the lunar sample-return sites are tightly clustered within the central-eastern region of the Moon's nearside hemisphere. These sites can be encompassed within a polygon covering just 4.4% of the Moon's surface; if limited to rock-sampling (Apollo) sites, the polygon's coverage is merely 2.7%.

#### 1.21.2.2 Lunar Meteorites

In contrast with the Apollo and Luna sites, the distribution of source craters for lunar meteorites

is virtually random. This conclusion is based on the randomness of overall cratering (Bandermann and Singer, 1973), plus celestial-mechanical constraints (Gault, 1983; Gladman *et al.*, 1996) indicating that the vast majority of Moon–Earth journeys are not direct, but involve a phase of geocentric or even heliocentric orbit. All of the lunar meteorites are finds (in some cases significantly weathered), and their masses tend to be curiously low in comparison to other achondrites, including martian meteorites (Table 1). Lunar provenance is proven for these meteorites by a variety of observations, but the single most useful constraint comes from oxygen isotopes (Clayton and Mayeda, 1996).

In addition to the usual potential for pairing among meteorites, lunar meteorites have an important potential for launch (source-crater) pairing. To date, with only ~20 lunar meteorites to cross-compare, launch pairing can often be ruled out based on cosmic ray exposure (CRE) constraints (e.g., Benoit *et al.*, 1996; Thalmann *et al.*, 1996; Nishiizumi *et al.*, 2002; Chapter 1.13). The launch age is the sum of the terrestrial age (usually brief, of order  $10^3$ – $10^4$  yr) plus the “ $4\pi$ ” (all-directional exposure, Moon-to-Earth) CRE age. Unfortunately, the most unambiguous  $4\pi$  CRE constraints, based on radioisotopic methods, become increasingly imprecise for CRE ages much lower than  $10^6$  yr, and hopelessly imprecise for CRE ages much less than  $10^5$  yr, whereas physical modeling shows that, over time, most lunar meteorites have Moon-to-Earth journeys that take less than  $10^5$  yr (Gault, 1983; Gladman *et al.*, 1996). When CRE does not resolve the launch pairing question, it may be possible to virtually rule out launch pairing on the basis that materials from a single source crater will generally show a degree of overall geochemical similarity. This approach is most useful if one or both of the samples is a thoroughly polymict breccia, as exemplified by regolith breccia, i.e., a type of material that is usually representative of its region. In this connection, it is important to realize that the scale of the launch zone is far smaller than the full diameter of a crater, because ejection velocity is a strong function of proximity to the point of impact (Warren, 1993). Unfortunately, uncertainty about launch pairing among lunar meteorites is bound to increase as more and more samples are acquired.

In principle, a thorough sampling of the lunar surface might yield pieces of Earth impact-transported to the Moon (these might be dubbed “retrometeorites”), a large proportion of which would presumably date from the era of heavy bombardment, 3.9 Ga and before (see below). However, Earth's escape velocity is high even compared to the Moon and Mars, and rocks of terrestrial provenance have not been discovered among

**Table 1** Known lunar meteorites, as of early 2003.

Meteorite	Mass (g)	Pair total <sup>a</sup> (g)	Rock type <sup>b</sup>	Year(s) <sup>c</sup> discovered	wt.% Al <sub>2</sub> O <sub>3</sub>	mol.% mg
<i>Highland (and mostly highland) meteorites</i>						
1 <b>ALH81005</b> <sup>d</sup>	31.4	31.4	Rego B, highland	1982	26	73
2 Calcalong Creek	18	18	Rego B, mainly highland	1991	21	?
3 Dar al Gani 262	513	513	Rego B, highland	1997	28	66
4 Dar al Gani 400	1,425	1,425	Polymict B, highland	1998	28	71
5 Dhofar 025	751	772	Rego B, highland	2000–2001	27	71
paired samples	Dhofars 301 (2 g), 304 (10 g), 308 (9 g)					
6 Dhofar 026 (13 stones)	636	636	Polymict B, highland	2000	27	71
7 Dhofar 081	174	564	Polymict B, highland	1999–2001	31	61
paired samples	Dhofars 280 (251 g), 302 (3.8 g), 303 (4.1 g), 305 (34), 306 (13), 307 (50), 490 (34)					
8 Dhofar 489	34.4	34.4	Polymict B, highland	2001	30 (est.)	?
9 <b>MAC88104</b>	61	723	Rego B, highland	1989	28	63
paired sample	MAC88105 (662 g)					
10 NWA482	1,015	1,015	IMB, highland	2001	29	66
11 <b>QUE93069</b>	21.4	24.5	Rego B, highland	1994–1995	28	66
paired sample	QUE94269 (3.1 g)					
12 <b>Yamato-791197</b>	52	341	Rego B, highland	1983–2002	26	63
paired (???) sample	Yamato-983885 (289 g)					
13 <b>Yamato-82192</b>	37	712	Polymict B, highland	1984–1987	28	66
paired samples	Yamato-82193 (27 g), Yamato-86302 (648 g)					
<i>Mare (and mostly mare) meteorites</i>						
1 <b>Asuka-881757</b>	442	442	Gabbro, mare	1990	11	33
2 Dhofar 287	154	154	Basalt + Rego B, mare	2001	8	50
3 <b>EET87521</b>	31	84	Polymict B, mare	1989–1998	13	42
paired sample	EET96008 (53 g)					
4 NWA032	300	456	Basalt, mare	2000	9	40
paired sample	NWA479 (156 g)					
5 NWA773 (3 stones)	633	633	Gabbro + Rego B, mare	2001	6	70
6 <b>QUE94281</b>	23.4	23.4	Rego B, mainly mare	1995	16	52
7 <b>Yamato-793169</b>	6.1	6.1	Basalt, mare	1990	12	31
8 <b>Yamato-793274</b>	8.7	195	Rego B, mainly mare	1987–1999	15	53
paired sample	Yamato-981031 (186 g)					

<sup>a</sup>Aside from the conventional pairings noted in the table, several launch pairs have been inferred: Yamato-793169 with Asuka-881757, and QUE94281 with Yamato-793274 (and possibly also with EET87521) (Arai and Warren, 1999; Korotev *et al.*, 2003). There may be other launch pairs that are not manifested (i.e., the rocks are not sufficiently ideosyncratic). <sup>b</sup>Abbreviations: Rego, regolith; B, breccia; IMB, impact-melt breccia. The classification “polymict breccia” for six of the samples may seem vague, but most of these six samples are either difficult to classify or simply little-studied. EET87521 is clearly a fragmental breccia. <sup>c</sup>Listed “discovery” dates refer to year of discovery of lunar provenance, not year sample was first collected as a meteorite. <sup>d</sup>Samples shown in **bold** font are from Antarctica, and thus generally less weathered than the other (hot-desert) finds.

the meteorites hitting Earth in modern times; only glasses (tektites) are known to have re-entered from space. In any case, to date no “retrometeorite” has been found among the lunar samples.

### 1.21.2.3 Remote-sensing Data

The period since the early 1990s has been a golden age for lunar remote sensing, thanks to the 1994 Clementine mission and the 1997–1998 Lunar Prospector mission. Among the pre-1994 remote-sensing geochemical databases, the most notable (i.e., still not completely superseded) is probably the X-ray spectrometry data obtained for ~10% of the lunar surface on the Apollo 15 and 16 missions. These data were reported as Al/Si, Mg/Al, and Mg/Si ratios, at a spatial resolution of

~50 km (e.g., Adler *et al.*, 1973; Bielefeld *et al.*, 1977; Andre and El-Baz, 1981). The more precisely determined Al/Si ratio data show trends that could be gleaned almost as well from simple albedo variations. Among lunar rocks, aluminum is strongly linked with light-colored feldspar, while silicon is relatively constant (probably as a consequence of the lesser potential to form silicon-free oxides, except “late” ilmenite, in the reducing lunar environment). The Mg/Si and Mg/Al data suffer from poor precision. For example, the average 1 $\sigma$  error in Mg/Si reported for 22 large regions by Adler *et al.* (1973) is 26%.

Clementine used four different cameras to map the global surface reflectance of the Moon at eleven different wavelengths, from the near-ultraviolet (415 nm) to the near-infrared (2,800 nm), in roughly one million images.

The workhorse UV/visible camera had filter center wavelengths and bandpass widths (FWHM) of 415 (40) nm, 750 (10) nm, 900 (30) nm, 950 (30) nm, and 1,000 (30) nm; and a broadband filter covering 400–950 nm. Depending upon orbit parameters and camera, pixel resolution generally varied from 100 m to 300 m. Clementine's highest resolution camera took 600,000 images at typical pixel resolution of 7–20 m, for four different wavelengths (415–750 nm) but covering only selected areas of the Moon.

Exploitation of the vast treasure trove of Clementine data is still at a fairly basic stage. Clementine multispectral images have been used to map surface mineralogy and, for a few elements, chemical composition, and even regolith maturity (i.e., average extent of exposure to surface-regolithic processing) (e.g., [Lucy et al., 2000a,b](#); [Staid and Pieters, 2001](#); [Shkuratov et al., 2003](#)). Translation from spectral data into concentration is most straightforward for iron, using primarily data from 900 m to 1,000 nm, the region of a major  $\text{Fe}^{2+}$  absorption band for pyroxene ([Lucy et al., 2000a](#)). The technique for titanium is less direct, relying on the spectrum slope as determined by the ratio between the 415 nm and longer wavelength (especially 750 nm) reflectances. The technique for soil maturity depends on an even more subtle analysis of slopes in different portions of the spectrum ([Pieters et al., 2002](#)). Plagioclase (or aluminum) is gauged mainly from simple albedo ([Shkuratov et al., 2003](#)). There are a number of complications: e.g., olivine/pyroxene ratio, major opaque phases other than the presumed dominant opaque (ilmenite), the shock state of plagioclase, sunlight phase angle (mainly a function of latitude, but also affected by local slopes), and the maturity grain size and glass abundance (three related parameters) of the regolith ([Lucy et al., 1998](#)). The important database for  $\text{TiO}_2$  has been somewhat controversial, as the early calibration showed poor agreement for a few of the sampled landing sites; [Gillis et al. \(2003\)](#) have proposed an *ad hoc* remedy. The high spatial resolution of the Clementine data can be exploited to address specific lunar geology issues, for example, the petrology of individual cryptomaria ([Antonenko et al., 1995](#); [Hawke et al., 2003](#)), the petrology of uplifted central peaks of moderately large impact craters ([Tompkins and Pieters, 1999](#)), and compositional variations within the colossal and yet remote (in relation to all Apollo and Luna sampling sites) South Pole Aitken basin ([Pieters et al., 2001](#)).

Lunar Prospector's two most important geochemical mapping sensors were designed for gamma-ray spectrometry (GRS) and neutron spectrometry. The neutron spectrometer, a matched pair of  $^3\text{He}$  gas proportional counters, was mainly designed to map the global

distribution of regolith hydrogen ([Feldman et al., 2001](#)). One of the counters was covered by a 0.63 mm sheet of cadmium, making it responsive only to epithermal neutrons. The difference in counting rates between the cadmium-covered counter and the uncovered counter gave a measure of the thermal neutron flux. Locally very high hydrogen concentrations were found near the poles, and [Feldman et al. \(2001\)](#) argue that these must be more than mere accumulations of solar-wind-implanted hydrogen, i.e., that "a significant proportion of the enhanced hydrogen near both poles is most likely in the form of water [ice] molecules." Long ago, [Arnold \(1979\)](#) had conjectured that water liberated in impacts between comets and the Moon might have accumulated in cold traps within permanently shadowed regions near the lunar poles. However, the high hydrogen concentrations found by [Feldman et al. \(2001\)](#) extend over regions far larger than the minor, scattered areas of permanent shadow. As should surprise no one, the water–ice interpretation has been controversial (e.g., [Crider and Vrondak, 2000](#); [Starukhina and Shkuratov, 2000](#)).

The GRS technique measures the upper few decimeters of the regolith, whereas reflectance spectrometry (e.g., Clementine) measures the very surface, and the Apollo orbital XRF data measured the uppermost  $\sim 10\ \mu\text{m}$ . The difference is not very important, because the lunar regolith is so extensively turned over by repeated impacts, or in lunar terminology, gardened. Prospector's GRS detector was of bismuth germanate (BGO) type, with similar resolution to the NaI(Tl) detectors flown on the Apollo 15 and 16 missions. The Prospector GRS database is far superior, however, because of vastly longer detector acquisition times (i.e., better counting statistics), and because Prospector's coverage was global, whereas the Apollo data covered no more than 20% of the surface in two near-equatorial bands.

The two elements most amenable to orbital GRS are iron and thorium. Although initial thorium mapping was done at a spatial resolution of 150 km ([Lawrence et al., 1998](#)), iron and thorium have recently been mapped to a remarkable 15 km ([Lawrence et al., 2002a,b](#)). Spatial resolution of 60 km has been achieved for potassium and titanium ([Prettyman et al., 2002](#)), and also, based on a complex technique involving comparison with data from Prospector's neutron spectrometer, for the rare earth element (REE) samarium ([Elphic et al., 2000](#)). The GRS data have also yielded maps at spatial resolution of 150 km for oxygen, magnesium, aluminum, silicon, calcium, and uranium ([Prettyman et al., 2002](#)). Establishing the full scientific import of all these new data will take some years, but one of the most striking implications is a remarkable degree of global geochemical asymmetry. For example, average surface

concentration of thorium (an exemplary incompatible trace element; on the Moon such elements are strongly concentrated into a potassium, REE- and phosphorus-rich component known as KREEP) is 3.5 times higher on the hemisphere centered over Oceanus Procellarum compared to the hemisphere antipodal to Procellarum, although it should be noted that this conclusion is based on a correction to the initial (e.g., Lawrence *et al.*, 1998) calibration for the Prospector thorium data (Warren, 2003).

### 1.21.3 MARE VOLCANISM

#### 1.21.3.1 Classification of Mare Rocks

The dark basalts that erupted to veneer the Moon's flat, low-lying "seas" (maria) during the waning of lunar magmatism are compositionally distinctive, even compared to other lunar samples. Mare basalts have high (mostly >16 wt.%) FeO, low to moderate *mg* ( $=\text{MgO}/[\text{MgO} + \text{FeO}]$ ), low to high TiO<sub>2</sub>, and low Al<sub>2</sub>O<sub>3</sub> contents (Figure 1 and Table 2). Calling these rocks "basalt" is potentially misleading. Most mare basalts are far more melano-cratic (mafic silicate-rich feldspar-poor) than terrestrial basalt, and arguably more analogous to a relatively leucocratic and low-*mg* komatiite. The contrast with the rest of the Moon's crust is stark. The typical composition of highland crust, as represented by lunar-meteoritic regolith breccias and regolith averages for the Apollo 14, Apollo 16, and Luna 20 sites (Table 3), features ~5 wt.% FeO, ~0.4 wt.% TiO<sub>2</sub>, and ~27 wt.% Al<sub>2</sub>O<sub>3</sub>. The distinction between mare and highland

materials is seldom controversial, but for quick-and-dirty mare versus highland classification based exclusively on bulk-analysis data, Wood (1975) proposed using a combination of wt.% TiO<sub>2</sub> and Ca/Al ratio (Figure 2).

The various subclassifications for mare basalt we describe below may seem arbitrary but, as will be discussed in the next section, mare basalt compositional diversity is in general not systematic, but haphazard. On Earth, volcanic diversity is largely a function of systematic global tectonics, such as upwelling at mid-ocean ridges to generate MORB. But plate tectonics probably never occurred on the Moon; and it surely never occurred during the comparatively late era of mare volcanism.

Mare basalts are classified primarily on the basis of their highly diverse bulk TiO<sub>2</sub> contents. Those with <1.5 wt.% TiO<sub>2</sub> are termed very-low-Ti (VLT), those with 1.5 < TiO<sub>2</sub> < 6 wt.% as medium-Ti, and those with >6 wt.% TiO<sub>2</sub> as high-Ti. In pre-2001 literature (e.g., Neal and Taylor, 1992), these same classes were called "VLT," low-Ti, and high-Ti, respectively. The bizarre usage of "low-Ti" for basalts with up to 6 wt.% TiO<sub>2</sub> was a historical accident: in the first studies of lunar rocks from Apollo 11, the only large igneous rocks happened to all be "high-Ti." Le Bas (2001) has suggested calling these three groups titanium-poor, medium-Ti, and titanium-rich, but judging from more recent publications (e.g., Hiesinger *et al.*, 2002; Gillis *et al.*, 2003; Jolliff *et al.*, 2003), this terminology has not been widely adopted. To minimize confusion, I choose to adopt the Le Bas "medium-Ti" replacement for "low-Ti," but continue using the old and logical terms VLT and high-Ti.

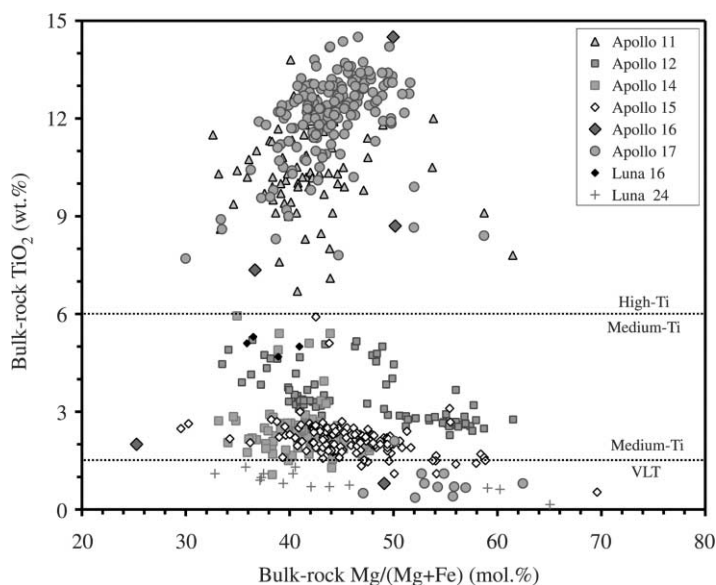


**Figure 1** Mare basalt major elements: *mg* versus TiO<sub>2</sub>. Note that the apparent bimodality in TiO<sub>2</sub> may be misleading (see text) (data are mainly from the compilation of Haskin and Warren, 1991).

**Table 2** Summary of literature compositional data for lunar mare meteorites<sup>a</sup> and other major varieties of mare basalt (see text).

Sample	<i>Na<sub>2</sub>O</i>	<i>MgO</i>	<i>Al<sub>2</sub>O<sub>3</sub></i>	<i>SiO<sub>2</sub></i>	<i>K<sub>2</sub>O</i>	<i>CaO</i>	<i>TiO<sub>2</sub></i>	<i>FeO</i>	<i>Sum</i>	<i>Sc</i>	<i>V</i>	<i>Cr</i>	<i>Co</i>	<i>Ni</i>	<i>Ga</i>	<i>Rb</i>	<i>Sr</i>	<i>Zr</i>	<i>Ba</i>	<i>La</i>	<i>Sm</i>	<i>Eu</i>	<i>Tb</i>	<i>Lu</i>	<i>Hf</i>	<i>Ir</i>	<i>Th</i>	
	(wt.%)	(wt.%)	(wt.%)	(wt.%)	(wt.%)	(wt.%)	(wt.%)	(wt.%)	(wt.%)	( $\mu\text{g g}^{-1}$ )	( $\mu\text{g g}^{-1}$ )	( $\text{mg g}^{-1}$ )	( $\mu\text{g g}^{-1}$ )	( $\mu\text{g g}^{-1}$ )	( $\mu\text{g g}^{-1}$ )	( $\mu\text{g g}^{-1}$ )	( $\mu\text{g g}^{-1}$ )	( $\mu\text{g g}^{-1}$ )	( $\mu\text{g g}^{-1}$ )	( $\mu\text{g g}^{-1}$ )	( $\mu\text{g g}^{-1}$ )	( $\mu\text{g g}^{-1}$ )	( $\mu\text{g g}^{-1}$ )	( $\mu\text{g g}^{-1}$ )	( $\mu\text{g g}^{-1}$ )	( $\text{ng g}^{-1}$ )	( $\mu\text{g g}^{-1}$ )	
Dhofar 287	avg.	0.52	12.8	8.1	43.9	0.15	8.4	2.86	22.2	98.9		0.62								13		1.2		0.5				
NWA 032	avg.	0.36	8.5	8.7	44.7	0.11	10.9	3.08	22.8	99.1	56	0.40	42	50			142	175		11.2	6.6	1.10	1.56	0.80	5.0			1.90
NWA 773	avg.	0.03	27	4	43	0.02	5.9	0.3	19	99.3		2.7	88	210						10		0.4		0.4				
YA meteorite <sup>b</sup>	avg.	0.32	6.0	11.0	45.5	0.05	12.0	2.1	22.3	99.2	93	81	1.59	24	11	2.8	1.1	146	92	66	4.0	3.5	1.14	0.93	0.59	2.6	0.05	0.53
All Apollo 11 mare basalts	avg.	0.48	7.6	9.6	40.5	0.16	11.1	10.5	19.5	100.0	83	78	2.1	21	5.4	5.8	2.8	177	433	208	18	16	2.1	3.7	2.0	12.6	0.027	2.1
	SD	0.11	1.0	1.5	1.3	0.11	0.9	1.3	1.2		8	19	0.5	7		2.2	2.3	32	199	107	9	5	0.4	1.1	0.5	4.1		1.2
	<i>N</i>	97	89	89	29	100	89	90	89		74	62	86	78	6	18	22	17	35	74	89	85	85	82	80	73	7	65
All Apollo 12 mare basalts	avg.	0.27	10.8	9.3	45.1	0.06	10.0	3.4	20.4	100.0	50	158	3.6	46	47	3.6	1.0	120	133	70	6.8	5.0	1.13	1.35	0.65	4.0	0.036	0.78
	SD	0.10	3.5	1.6	1.6	0.01	1.6	0.8	1.2		7	30	1.0	13		1.2	0.3	30	62	23	2.3	1.2	0.38	0.398	0.18	1.0		0.23
	<i>N</i>	90	74	78	74	96	79	83	84		68	30	91	79	23	33	44	60	52	82	58	87	70	82	78	56	25	30
All Apollo 14 mare basalts	avg.	0.49	9.5	12.7	48.2	0.30	10.7	2.5	16.2	101.2	56	114	3.1	32	22	3.7	19	99	314	273	17	9	1.29	1.98	1.0	7.0	0.021	2.3
	SD	0.11	1.5	1.3	1.4	0.37	0.8	0.9	1.9		8	18	0.8	6		0.4	12	39	162	354	11	5	0.90	1.02	0.5	4.0		2.2
	<i>N</i>	94	91	90	24	87	94	91	93		93	59	93	93	2	2	24	39	46	81	95	93	94	93	93	93	3	90
All Apollo 15 mare basalts	avg.	0.27	10.4	9.1	46.3	0.05	9.8	2.1	21.2	100.1	40	202	3.9	51	58	3.8	1.0	116	90	72	5.7	3.4	0.85	0.75	0.34	2.34	0.043	0.57
	SD	0.05	2.6	1.3	1.7	0.01	1.1	0.5	1.5		5	29	1.2	12		1.0	0.9	21	34	25	2.6	0.8	0.18	0.19	0.08	0.84		0.18
	<i>N</i>	129	133	132	88	95	133	135	132		99	45	119	99	23	33	33	49	38	58	98	93	93	93	92	85	29	43
All Luna 16 mare basalts	avg.	0.52	6.4	13.4	43.8	0.18	11.7	5.0	18.7	100.2	64	75	1.56	17.5	79	3.7	1.9	404	300	335	18	13	3.27	2.53	1.13	0.60		1.9
	SD	0.02	0.5	0.2		0.04	0.3	0.2	0.4		6	10	0.12	0.9					80	2	2	0.32	0.16	0.10			0.3	
	<i>N</i>	4	4	4	1	4	4	4	4		4	4	4	4	1	1	1	1	1	4	4	4	4	4	4	1		4
All Luna 24 mare basalts	avg.	0.27	9.4	11.2	45.7	0.03	11.6	0.8	20.1	99.7	46	163	2.1	40	43	1.8		103	50	43	2.0	1.6	0.66	0.36	0.23	1.4		0.19
	SD	0.07	4.3	1.9	1.2	0.01	2.1	0.3	1.6		8	13	0.8	7				8	5	5	1.1	0.7	0.08	0.16	0.11	1.4		0.04
	<i>N</i>	19	17	17	9	12	17	17	19		13	11	19	13	5	1		4	1	3	13	13	11	12	13	12		5
Large (high-Ti) Apollo 17 mare basalts	avg.	0.39	8.4	8.9	38.9	0.06	10.5	12.1	18.9	99.0	80	105	2.95	20.3	2.0	5.1	0.70	173	216	106	5.8	8.3	1.75	2.19	1.16	7.5	0.05	0.26
	SD	0.04	1.2	0.7	1.1	0.02	0.8	1.3	0.9		5	29	0.66	4.7		1.8	0.47	33	63	80	1.3	2.5	0.44	0.66	0.31	2.2		0.12
	<i>N</i>	170	169	169	50	170	169	170	169		165	115	170	165	6	18	45	72	50	79	159	158	158	158	154	143	5	38
Apollo 17 VLT mare basalts	avg.	0.15	12.5	10.4	48.2	0.02	9.4	0.7	18.3	100.7	47	221	5.3	46						1.7	8.8	1.81	2.24	1.23	8.0		0.40	
	SD	0.04	3.0	1.2	0.7	0.01	1.1	0.2	1.7		11	30	1.0	15						1.3	2.0	0.42	0.56	0.28	1.9		0.40	
	<i>N</i>	10	10	10	4	10	10	10	10		6	6	10	6						6	9	9	9	9	9	8		1
All Apollo/Luna mare basalts <sup>c</sup>	avg.	0.35	9.4	10.6	44.6	0.11	10.6	4.7	19.1	100.1	58	140	3.1	34	36	3.9	4	170	219	158	9.5	8.2	1.6	1.9	0.96	5.4	0.036	1.1
	SD	0.12	1.8	1.6	3.1	0.09	0.8		1.4		15	52	1.1	13		1.2												

Source: Data mainly from the compilation of Haskin and Warren (1991). A large set of additional trace element data have been reported by Neal (2001), but for a few elements (Mo, Sb) his data appear spuriously high. Abbreviations: avg. = average, SD = standard deviation, *N* = number of data averaged.

<sup>a</sup>Mass-weighted means of literature data; only pristine basalts are shown (mare-dominated polymict breccias are excluded). <sup>b</sup>Mass-weighted mean of literature data for Y-793169 and Asuka-881757 probably paired mare-basaltic meteorites. <sup>c</sup>Average of the eight major Apollo/Luna varieties shown above.

**Table 3** The diversity of sampled lunar regolith compositions.

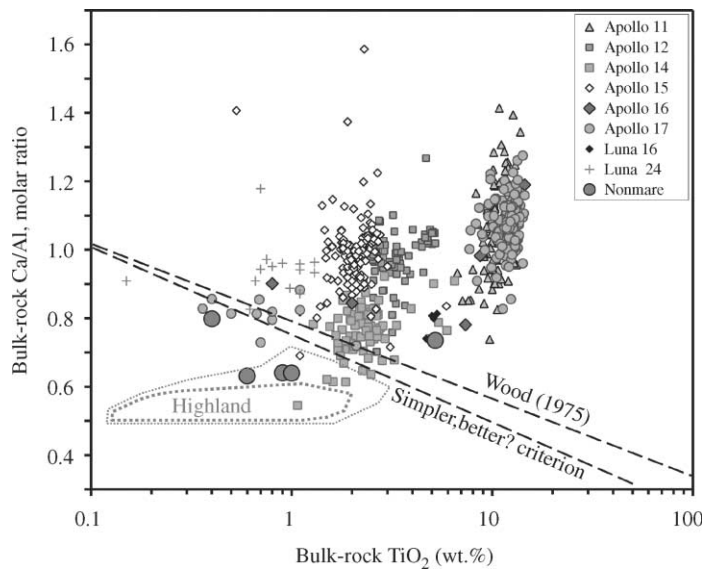
Sample	Sample type		Na <sub>2</sub> O (wt.%)	MgO (wt.%)	Al <sub>2</sub> O <sub>3</sub> (wt.%)	SiO <sub>2</sub> (wt.%)	CaO (wt.%)	TiO <sub>2</sub> (wt.%)	FeO (wt.%)	mg (mol.%)	K (mg g <sup>-1</sup> )	Sc (μg g <sup>-1</sup> )	V (μg g <sup>-1</sup> )
	Physical	Geochemical											
Ap 11 average	Soils (averaged)	Mare	0.47	7.9	12.6	42.0	11.7	7.9	16.4	46	1.37	62	70
Ap 12 average	Soils (averaged)	Mare	0.41	10.4	12.1	46.2	9.9	2.6	17.2	52	2.1	37	114
Ap 15, mare floor	Soils (averaged)	Mare	0.40	11.0	14.3	47.2	10.5	1.46	15.0	57	1.30	27	110
Ap 17, mare floor	Soils (averaged)	Mare	0.39	9.8	12.1	40.8	11.1	8.5	16.6	51	0.66	60	76
Luna 16	Core soil	Mare	0.38	8.8	15.6	44.4	11.7	3.30	16.4	49	0.95	52	80
Luna 24	Core soil	Mare	0.29	9.9	11.9	44.6	11.4	1.04	19.2	48	0.27	40	140
NWA773	Regolith breccia	Mare	0.23	13.2	10.6	46.2	10.8	0.78	17.3	58	0.83	ND	ND
QUE94281	Regolith breccia	Mainly mare	0.37	8.5	15.8	47.5	12.5	0.71	14.1	52	0.50	33	116
Yamato-793274	Regolith breccia	Mainly mare	0.38	9.1	15.3	47.9	12.2	0.61	14.2	53	0.67	33	99
Ap 14 average	Soils (averaged)	Mainly highland	0.69	9.2	17.7	48.2	11.0	1.72	10.4	61	4.3	23	51
Ap 15, Apennine Front	Core soil	Mainly highland	0.47	10.3	20.0	46.2	11.4	1.24	10.0	65	ND	18.5	65
Ap 17, South Massif	Soil 73141	Mainly highland	0.42	9.7	21.3	45.2	13.0	1.22	8.0	68	1.17	16.2	37
Luna 20	Core soil	Mainly highland	0.38	9.2	23.0	45.0	14.4	0.46	7.3	69	0.62	16.4	39
Calcalong Creek	Regolith breccia	Mainly highland	0.49	ND	20.9	ND	16.1	0.80	10.9	ND	2.0	23	57
ALH81005	Regolith breccia	Highland	0.30	8.2	25.6	45.7	15.0	0.25	5.4	73	0.19	9.1	25
Ap 14, 14076	Regolith breccia	Highland	0.44	3.3	30.5	44.1	16.8	0.33	3.8	61	0.73	7.8	17
Ap 14, 14315	Regolith breccia	Highland	0.57	7.9	22.1	47.1	13.0	0.85	7.4	65	2.6	15.6	ND
Ap 16 average	Soils (averaged)	Highland	0.48	5.8	27.1	44.7	15.5	0.58	5.2	67	1.07	10.4	20
Dar al Gani 262	Regolith breccia	Highland	0.36	4.7	27.7	44.6	16.1	0.20	4.3	66	0.42	7.6	26
Dhofar 025	Regolith breccia	Highland	0.31	6.5	26.8	44.5	15.8	0.29	4.8	71	0.48	10.0	<30
MAC88104/5	Regolith breccia	Highland	0.33	4.0	28.1	45.0	16.6	0.24	4.2	63	0.23	8.5	18
QUE93069	Regolith breccia	Highland	0.34	4.6	28.5	44.9	16.3	0.27	4.3	66	0.30	7.5	22
Yamato-791197	Regolith breccia	Highland	0.33	6.3	26.0	43.7	15.5	0.34	6.5	63	0.24	13.1	32
Average highland regolith	Conceptual		0.39	5.7	26.9	44.9	15.6	0.37	5.1	67	0.70	10.0	23

Sample	Cr (mg g <sup>-1</sup> )	Mn (mg g <sup>-1</sup> )	Co (μg g <sup>-1</sup> )	Ni (μg g <sup>-1</sup> )	Zn (μg g <sup>-1</sup> )	Ga (μg g <sup>-1</sup> )	Sr (μg g <sup>-1</sup> )	Zr (μg g <sup>-1</sup> )	Cs (μg g <sup>-1</sup> )	Ba (μg g <sup>-1</sup> )	La (μg g <sup>-1</sup> )	Ce (μg g <sup>-1</sup> )	Nd (μg g <sup>-1</sup> )
Ap 11 average	1.99	1.66	31	199	25	5.0	163	330	130	220	18.0	55	54
Ap 12 average	2.47	1.60	41	260	6	4.7	138	560	310	360	31	87	67
Ap 15, mare floor	2.53	1.45	45	216	14	4.0	138	320	170	200	21	50	30
Ap 17, mare floor	3.1	1.78	34	170	35	5.0	168	229	ND	98	8.0	24	21.8
Luna 16	2.20	1.64	32	167	26	5.1	275	253	63	185	11.2	34	24.6
Luna 24	2.91	1.97	47	129	13	1.2	91	78	52	41	3.2	8.3	6.4
NWA773	2.74	2.01	ND	ND	ND	ND	ND	ND	ND	ND	16	41	24
QUE94281	1.81	1.55	45	208	5	4.5	106	105	89	72	6.4	15.7	9.6
Yamato-793274	2.08	1.62	42	101	7	4.7	110	92	46	78	5.8	15.2	9.6
Ap 14 average	1.41	1.08	36	350	25	5.9	189	810	680	840	67	181	106
Ap 15, Apennine Front	2.01	1.11	30	162	31	5.1	145	363	260	256	99	59	34
Ap 17, South Massif	1.48	0.84	27	239	16	2.6	137	219	236	154	15.5	38	24.9
Luna 20	1.27	0.85	30	246	20	3.7	165	192	76	104	6.2	16.8	11.3
Calcalong Creek	1.30	1.12	24	360	ND	ND	ND	ND	ND	ND	20.1	52	28.8
ALH81005	0.89	0.58	21	202	9	2.7	135	27	24	28	1.98	5.2	3.2
Ap 14, 14076	0.50	0.45	15.8	231	7	10.8	175	108	146	90	8.0	18.2	11.9
Ap 14, 14315	1.24	0.78	33	430	ND	6.6	140	520	420	380	36	91	53
Ap 16 average	0.71	0.52	26	360	18	4.2	162	162	155	127	11.6	30	20.8
Dar al Gani 262	0.61	0.50	18	241	<40	4.0	210 <sup>a</sup>	33	90	200 <sup>a</sup>	2.2	6.1	3.4
Dhofar 025	0.77	0.58	15.7	141	<30	3.1	1,700 <sup>a</sup>	52	ND	120 <sup>b</sup>	3.3	8.0	5.0
MAC88104/5	0.63	0.48	14.6	148	7	3.5	151	34	38	32	2.52	6.3	4.0
QUE93069	0.57	0.47	22	295	15	3.2	149	46	41	42	3.4	8.5	5.0
Yamato-791197	0.90	0.67	19.4	178	21	5.5	135	32	67	32	2.13	5.5	3.5
Average highland regolith	0.76	0.56	20.6	247	13	4.8	149 <sup>a</sup>	113	123	100 <sup>a</sup>	7.87	19.9	12.2

<i>Sample</i>	<i>Sm</i> ( $\mu\text{g g}^{-1}$ )	<i>Eu</i> ( $\mu\text{g g}^{-1}$ )	<i>Tb</i> ( $\mu\text{g g}^{-1}$ )	<i>Dy</i> ( $\mu\text{g g}^{-1}$ )	<i>Yb</i> ( $\mu\text{g g}^{-1}$ )	<i>Lu</i> ( $\mu\text{g g}^{-1}$ )	<i>Hf</i> ( $\mu\text{g g}^{-1}$ )	<i>Ta</i> ( $\mu\text{g g}^{-1}$ )	<i>Os</i> ( $\mu\text{g g}^{-1}$ )	<i>Ir</i> ( $\mu\text{g g}^{-1}$ )	<i>Au</i> ( $\mu\text{g g}^{-1}$ )	<i>Th</i> ( $\mu\text{g g}^{-1}$ )	<i>U</i> ( $\mu\text{g g}^{-1}$ )
Ap 11 average	13.8	1.71	3.2	17	10.8	1.59	11.6	1.59	7.8	8.6	2.9	2.34	0.52
Ap 12 average	15.1	1.89	3.6	20	10.7	1.54	12.8	1.35	5.2	5.6	2.4	5.2	1.68
Ap 15, Mare	9	1.27	2.1	13	6.6	0.98	7.1	0.9	6.3	6.4	3.0	3.0	0.8
Ap 17, Mare	8.1	1.72	1.99	ND	7.2	0.99	6.8	1.18	ND	4.8	3.6	0.88	0.31
Luna 16	8.0	3.2	1.43	9.7	5.6	0.77	7.0	0.65	ND	10.3	2.4	1.12	0.30
Luna 24	2.02	0.66	0.49	3.0	1.74	0.27	1.69	0.25	7.7	5.7	6.9	0.45	0.10
NWA773	7	0.7	1.5	ND	5	0.7	ND	ND	ND	ND	ND	ND	ND
QUE94281	3.1	0.83	0.64	4.2	2.42	0.35	2.36	0.29	6.2	6.5	2.2	0.93	0.23
Yamato-793274	2.73	0.82	0.58	4.0	2.29	0.32	2.26	0.26	4.5	4.5	3.0	0.81	0.21
Ap 14 average	29.8	2.7	6.3	38	23	3.2	22	2.8	ND	17.5	5.8	13.8	3.3
Ap 15, Apennine Front	10.8	1.36	2.02	ND	7.7	1.04	8.7	1.00	ND	4.4	1.9	3.8	1.24
Ap 17, South Massif	7.0	1.2	1.50	9.3	5.4	0.80	5.2	0.75	ND	12	6	2.4	0.70
Luna 20	3.2	0.90	0.59	4.2	2.22	0.36	2.57	0.31	ND	9.5	3.6	1.06	0.37
Calalong Creek	8.7	1.20	2.16	14.2	6.4	0.98	6.8	1.12	ND	ND	ND	4.2	1.13
ALH81005	0.95	0.69	0.21	1.33	0.84	0.12	0.72	0.09	8.4	6.8	2.3	0.29	0.10
Ap 14, 14076	3.2	1.09	0.67	4.2	2.5	0.34	2.2	0.29	ND	7.9	7.4	1.34	0.34
Ap 14, 14315	14.3	1.56	3.1	19.9	10.4	1.55	11.3	1.32	ND	18.8	12.7	5.6	1.38
Ap 16 average	5.5	1.22	1.12	7.2	3.8	0.58	4.1	0.52	ND	12.2	8.0	1.97	0.57
Dar al Gani 262	1.03	0.75	0.22	1.59	0.84	0.12	0.77	0.10	ND	10.1	3.9	0.37	0.16 <sup>a</sup>
Dhofar 025	1.43	1.02	0.30	1.57	1.11	0.18	1.08	0.13	ND	5.4	4.3	0.57	0.22 <sup>a</sup>
MAC88104/5	1.15	0.79	0.24	1.49	0.97	0.14	0.86	0.11	7.3	7.2	2.7	0.39	0.10
QUE93069	1.56	0.82	0.33	1.99	1.21	0.17	1.14	0.15	21	15.6	4.5	0.53	0.13
Yamato-791197	1.06	0.77	0.25	1.56	1.01	0.15	0.88	0.10	8.2	6.7	1.4	0.33	0.11
Average highland regolith	3.34	0.97	0.71	4.54	2.51	0.37	2.56	0.31	11.3	10.1	5.2	1.27	0.4 <sup>a</sup>

<sup>a</sup> Hot-desert meteorites tend to be grossly contaminated with Ba, U, and especially Sr; these data are excluded from the “average highland regolith” calculation. ND: not determined. Data sources are too numerous to enumerate in full. Among the most noteworthy are previous compilations by [Haskin and Warren \(1991\)](#); [Jerde et al. \(1990\)](#) for Apollo 14 samples; [Korotev \(1987a\)](#), for Apennine Front core soil 15007; [Warren and Kallemeyn \(1986\)](#) for ALH81005, Luna 20 and South Massif soil (most Al-rich from Apollo 17) 73141; [Korotev and Kremser \(1992\)](#) for an average of Apollo 17 mare soils from the LM/ALSEP site near the center of the Taurus-Littrow Valley; [Jolliff et al. \(2003\)](#) for NWA773; and [Warren et al. \(2003\)](#) for other recently discovered lunar meteorites.



**Figure 2** On a plot of  $\text{TiO}_2$  versus  $\text{Ca/Al}$ , nearly all mare basalts plot above and to the right of a criterion proposed by Wood (1975) for distinguishing between mare and highland rocks, and well apart from the vast majority of highland rocks, which plot at  $\text{Ca/Al} = 0.5\text{--}0.6$  and  $\text{TiO}_2 < 2$  wt.% (0.5 is the stoichiometric plagioclase ratio; fields are based on Wood, 1975, figure 2). Five extraordinarily gabbroitic pristine highland samples are plotted as individual filled circles that straddle Wood's line: sodic ferrogabbro clast 67915c (Marti *et al.*, 1983), 14434 (Arai and Warren, 1997), 61224,11 (Marvin and Warren, 1980), 67667 (Warren and Wasson, 1978), and 73255c27 (James and McGee, 1979). Wood's (1975) criterion is  $\text{Ca/Al} = 0.786 - 0.229 \log_{10} \text{TiO}_2$  (for  $\text{Ca/Al}$  as a molar ratio and  $\text{TiO}_2$  in wt.%). Also plotted is a simpler variant proposed here,  $\text{Ca/Al} = 0.74 - 0.26 \log_{10} \text{TiO}_2$ , that seems better at including VLT mare basalts as mare samples, without significantly changing the situation for the nonmare samples.

Mare basalts are also classified on the basis of secondary compositional criteria, such as bulk-rock  $\text{Al}_2\text{O}_3$  and potassium. In the most recent and systematic variant of this scheme (Neal and Taylor, 1992), samples with  $>11$  wt.%  $\text{Al}_2\text{O}_3$  are distinguished as aluminous (or high-Al), and samples with  $>2,000$   $\mu\text{g/g}$  K are distinguished as high-K. Thus, for example, the Apollo 14 samples include a few pieces of aluminous (or more specifically aluminous, high-K, medium-Ti) mare basalt (Dasch *et al.*, 1987; Neal and Taylor, 1989). The Luna 24 VLT basalts as well as the two "YA" lunar meteorite basalts are borderline aluminous (Table 2), and the Luna 16 basalts are clearly aluminous. However, for the Luna 16 basalts, which were sampled strictly as tiny regolith particles, a caveat is in order. Most of the "bulk" analyses in the literature are uncorrected defocused-beam microprobe analyses, which tend to give spuriously high  $\text{Al}_2\text{O}_3$  (e.g., 12 such analyses by Kurat *et al.* (1976) average 16.1 wt.%  $\text{Al}_2\text{O}_3$ , whereas analyses by true bulk methods such as wet chemistry, neutron activation analysis and X-ray fluorescence are consistently close to 13.4 wt.%). The vast majority of known mare basalt types are "low-Al" and (thus) undersaturated with respect to plagioclase (Longhi, 1992).

Aside from this overall classification, mare basalts are also classified based on more subtle

distinctions among samples from a given landing site. For example, among the Apollo 12 medium-Ti mare basalts, three major groupings are distinguished, named for minerals that are especially abundant in each type: olivine, pigeonite, and ilmenite. Among Apollo 15 medium-Ti basalts, only two main types are recognized: olivine-normative and quartz-normative, which probably correspond to two distinct flows, with the olivine-normative atop the quartz-normative (Ryder and Cox, 1996). The most elaborate subclassification of a suite of basically similar mare basalts is for the high-Ti samples from Apollo 17 (Neal *et al.*, 1990). These site-specific classifications are intended to link samples with specific magma types, or even specific lava flows. It is natural to ask whether differences between the Apollo 12 olivine and Apollo 12 pigeonite basalts indicate heterogeneity within a single lava (Rhodes *et al.*, 1977) or require separate multiple lavas (Neal *et al.*, 1994). However, considering the great diversity of mare materials as a whole, the big-picture observation is that Apollo 12 pigeonite and Apollo 12 olivine basalts are only subtly different from one another.

Besides basalts, mare volcanism also produced a variety of distinctive pyroclastic glasses. Sampled pyroclastic glasses are spherules with

diameters generally between 0.03 mm and 0.3 mm. Distinguishing between these and impact-splash glasses is rarely difficult (Ryder *et al.*, 1996). Remote observations indicate that scattered large regions are veneered with pyroclastic matter. Although the largest of these “dark mantle deposits” (~10 have area >2,500 km<sup>2</sup>) occur near the rims of circular mare basins, the deposits are typically irregular-oval in shape, not arcuate. Clementine data have enabled identification of ~90 much smaller pyroclastic deposits that show similar spectral diversity but are much more widely distributed across the Moon (Gaddis *et al.*, 2000). The mare pyroclastic glasses are classified by the same titanium-, aluminum-, and potassium-based criteria as the crystalline mare basalts, and also on the expedient basis of color of the glass. High-Ti glasses tend to be orange or red, VLT glasses green, and medium-Ti glasses tan or brown; devitrification of the glass can make rapidly accumulated spherules black (which may account for the “dark” mantle deposits).

### 1.21.3.2 Chronology and Styles of Mare Volcanism

The chronology of mare volcanism is constrained primarily by isotopic ages for samples (Table 4 and Figure 3), and secondarily, but with far broader application, by photogeologic (crater-counting) methods, calibrated by extrapolation from the few isotopically dated surfaces. The oldest isotopically dated mare-type samples are high-aluminum, medium-Ti cumulate clasts, found in Apollo 14 highland breccias, whose ages extend up to 4.23 Ga (Taylor *et al.*, 1983; Shih *et al.*, 1986; Dasch *et al.*, 1987; Neal and Taylor, 1989). But in general, mare clasts within highland breccias are rare. The overall scarcity of mare basalt among the tens of thousands of diverse clasts studied from highland breccias, the scarcity of cryptomaria (regions where mare surfaces have been covered, but also sufficiently gardened to become detectable, by more recent impact cratering, Antonenko *et al.* (1995)), the sharpness of most mare–highland (and mare–mare) boundaries based on various remote-sensing data (e.g., Li and Mustard, 2000; Lucey and Steutel, 2003), and the low abundance of craters in the maria, all indicate that mare volcanism occurred mainly after the period of heavy bombardment that ended at 3.9 Ga (see below).

Most of the individual age data for mare samples are from Apollo 11, 12, 15, and 17, and these data gave rise to an early misconception (which still to some extent persists: e.g., Snyder *et al.*, 2000b) that among mare basalts, titanium content correlates with antiquity. If anything, the overall database, including photogeologic

inferences, suggests an anticorrelation between titanium and antiquity. The youngest isotopically dated mare rocks are a VLT cumulate, lunar meteorite NWA773, ~2.7 Ga, and a medium-titanium basalt, lunar meteorite NWA032, ~2.8 Ga (dated with <sup>40</sup>Ar–<sup>39</sup>Ar measurements by Fernandes *et al.*, 2002b and Fagan *et al.*, 2002; there is a caveat: these could be shock-reset ages). But the very last gasp of mare volcanism, the least cratered mare lava, is believed to be a high-Ti flow in Oceanus Procellarum (Hiesinger *et al.*, 2000). Assigning an absolute age to this surface requires a long extrapolation from rigorously dated surfaces, but Hiesinger *et al.* (2000) suggest that the age of the flow in question is ~1.3 Ga. In general, the youngest mare basalts in Procellarum tend to be high-Ti (Staid and Pieters, 2001). At the opposite extreme, the cryptomaria presumably tend to be uncommonly old, by mare standards, and remote-sensing data indicate that mare basalt in cryptomaria tends to be VLT, or at most medium-Ti (Hawke *et al.*, 2003). In short, age seems a very poor predictor of mare lava composition.

The majority of mare rock samples are noncumulate basalts, formed by melts of generally very low viscosity, of order 1 poise (calculated by method of Persikov *et al.* (1987)) in flows whose thicknesses (assuming the Imbrium region is typical) were mostly less than 10 m (Gifford and El-Baz, 1981). By one recent estimate (Hiesinger *et al.* (2002)), however, they averaged 30–60 m and ranged up to 220 m. The most widely cited method for estimating total accumulated thickness of mare lavas, based on crater submersion statistics (small, shallow craters are submerged sooner than big, deep craters), indicates that the maria are generally <0.5 km thick, and average ~1 km (DeHon, 1979). However, Hörz (1978) argued these estimates ignore prevolcanic erosion of crater depth/diameter ratio, and thus are too high by a factor of ~4. The abundance of highland component within regolith at mare-interior locales (where the highland component is probably mainly added by vertical mixing) also favors relatively thin maria (e.g., Ferrand, 1988). Even assuming DeHon’s calibration as correct, the total volume of mare basalt is only ~7 × 10<sup>6</sup> km<sup>3</sup>, or 0.03% of the lunar volume. However, it is conceivable that a larger volume of intrusive mare-like gabbros formed during the era of mare volcanism but remained unsampled, because the large post-3.9 Ga craters required to excavate them are rare.

Phenocrysts are common, especially in the Apollo 15 mare basalts, but they appear to have grown strictly during the main stage of cooling, i.e., during post-eruptive flow across the surface, and not in a deep magma chamber (Lofgren *et al.*, 1975; Walker *et al.*, 1977). The phenocrysts are

**Table 4** Summary of age constraints for mare basalts and pyroclastic glasses.

Sample	TiO <sub>2</sub> (wt.%)	Plotted age (Ga)	Ar age (Ga)	Sr age (Ga)	Nd age (Ga)	Pb age (Ga)	References
<i>Lunar meteorites</i>							
Dhofar 287	2.86	3.46			3.46 ± 0.03		Shih <i>et al.</i> (2002)
NWA 032	3.08	2.80	2.80 ± 0.02				Fagan <i>et al.</i> (2002)
NWA 773	0.30	2.7	2.7				Fernandes <i>et al.</i> (2002b)
YA meteorite	2.08	3.90	3.80 ± 0.01	3.89 ± 0.03	3.87 ± 0.06	3.94	Misawa <i>et al.</i> (1993)
<i>Apollo 11</i>							
10017	12.2	3.51		3.51 ± 0.05			BVSP (1981)
10024	12.6	3.53		3.53 ± 0.07			BVSP (1981)
10029	10.9	3.83	3.83 ± 0.03				BVSP (1981)
10062	10.5	3.86	3.79 ± 0.04	3.92 ± 0.11	3.88 ± 0.06		BVSP (1981)
<i>Apollo 12</i>							
12022	4.9	3.08	3.08 ± 0.06				BVSP (1981)
12020	2.83	3.09	3.09 ± 0.06				BVSP (1981)
12002	2.62	3.25	3.21 ± 0.05	3.29 ± 0.10			BVSP (1981)
12021	3.52	3.26		3.26 ± 0.03			BVSP (1981)
<i>Apollo 14</i>							
14053	2.72	3.93	3.93 ± 0.04				Ryder and Spudis (1980)
14072	2.57	4.04	4.04 ± 0.05	4.05 ± 0.08			Ryder and Spudis (1980)
14168	1.70	3.85	3.85 ± 0.02	3.82 ± 0.12	3.95 ± 0.17		BVSP (1981) and Shih <i>et al.</i> (1986)
14304, 113c	3 <sup>a</sup>	3.95	3.85 ± 0.04	3.95 ± 0.04			Shih <i>et al.</i> (1987)
14304, 108c	3 <sup>a</sup>	4.00		3.99 ± 0.02	4.04 ± 0.11		Shih <i>et al.</i> (1987)
14305, 122-92c	3.60	4.23		4.23 ± 0.05			Taylor <i>et al.</i> (1983)
14305, 304c	2.40	3.85	3.85 ± 0.05	3.83 ± 0.08	3.91 ± 0.16		Shih <i>et al.</i> (1986)
14321, 184c	2.41	3.95	3.95 ± 0.05	3.95 ± 0.04			Ryder and Spudis (1980)
14321, 223c	2.41	4.1		4.1			Dasch <i>et al.</i> (1987)
<i>Apollo 15</i>							
15668	2.49	3.10	3.10 ± 0.05				BVSP (1981)
15065	1.70	3.21		3.21 ± 0.04			BVSP (1981)
Ap15 green glass	0.36	3.34	3.3			3.38	Snyder <i>et al.</i> (2000) and Shih <i>et al.</i> (2001)
15385	2.19	3.35	3.35 ± 0.05				BVSP (1981)
15682	2.27	3.37		3.37 ± 0.07			BVSP (1981)
15388	3.10	3.38		3.36 ± 0.04	3.42 ± 0.07		Dasch <i>et al.</i> (1989)
15475	1.81	3.39		3.43 ± 0.15	3.37 ± 0.05		Snyder <i>et al.</i> (2000b)
<i>Apollo 17 high-Ti</i>							
71055	13.9	3.56		3.56 ± 0.09			BVSP (1981)
70017	13.4	3.59		3.59 ± 0.18			BVSP (1981)
Ap17 orange glass	8.8	3.56	3.6			3.48	Snyder <i>et al.</i> (2000) and Shih <i>et al.</i> (2001)
70215	13.1	3.79	3.79 ± 0.04				BVSP (1981)
70255	11.4	3.84	3.84 ± 0.02				BVSP (1981)
79001, 2144	9.9	3.90	3.49 ± 0.04	3.89 ± 0.04	3.92 ± 0.04		Shearer <i>et al.</i> (2001)
<i>Other samples</i>							
Apollo 17 VLT	0.71	≥4.01	?-4.01				Taylor <i>et al.</i> (1991) (p. 209)
Luna 16	5.0	Range	3.5-3.04				Snyder <i>et al.</i> (2000a) and Fernandes <i>et al.</i> (2002a)
Luna 24	0.84	Range	3.6-3.0				Snyder <i>et al.</i> (2000a) and Fernandes <i>et al.</i> (2002a)

Sources: For the sake of brevity, most of the individual data from the extensive compilation of BVSP (1981) are not reproduced here. Instead, only the two oldest and two youngest members of each major sample type are shown. This listing is intended to be nearly comprehensive for Apollo 14 (for which most data appeared after BVSP, 1981), but the samples include many shock-altered clasts, and some of the more ambiguous Sr results of Dasch *et al.* (1987) have been omitted.

<sup>a</sup> TiO<sub>2</sub> for the Shih *et al.* (1987) 14304 clasts estimated based on sum “difference” and analogy to other Apollo 14 high-Al mare basalts. Except as noted, TiO<sub>2</sub> data are from compilation of Haskin and Warren (1991) or Table 2.

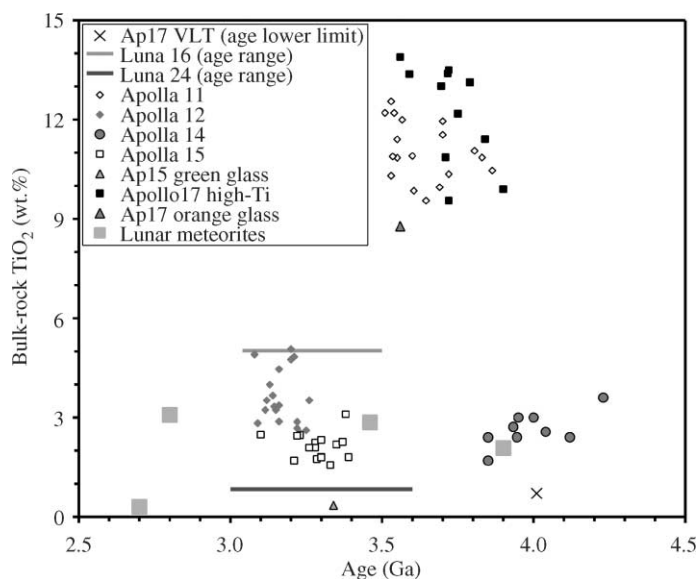


**Figure 3** Ages of mare basalts and pyroclastic glasses show no correlation with  $\text{TiO}_2$ . Age data are from previous compilations by BVSP (1981), Ryder and Spudis (1980), Fernandes *et al.* (2002a), and (for pyroclastic glasses) Shih *et al.* (2001), plus a lower limit cited for Apollo 17 VLT basalts by Taylor *et al.* (1991). The  $\text{TiO}_2$  data are averaged from the compilation of Haskin and Warren (1991). The five major Apollo basalt types are shown with small symbols because each point represents one of many available samples from the given locale, whereas each of the lunar meteorites represents (probably) our only sample from its locale.

invariably mafic, never (thus far) containing plagioclase. The absence of plagioclase in the phenocryst assemblage, and moreover its scarcity as a liquidus phase (Longhi, 1992), are powerful indications that mare magmas tended to transit directly from the mantle to the surface, and seldom paused in crustal magma chambers (cf. Wilson and Head, 2003). The aluminous mare basalts are plagioclase saturated; among those from Apollo 14, the best-documented suite of this type, many appear to have assimilated a crustal (or crust-mantle area) material, namely KREEP (Dickinson *et al.*, 1985; Neal and Taylor, 1989). But, as noted above, aluminous mare basalts are rare. Mare cumulates managed to develop, as exemplified by rocks such as 12005 (Rhodes *et al.*, 1977; Dungan and Brown, 1977), 15385 and 15387 (Ryder, 1985), 71597 (R. D. Warner *et al.*, 1977), the Apollo 14 clast that Taylor *et al.* (1983) found to be exceptionally ancient, and the NWA773 meteorite (Jolliff *et al.*, 2003). However, based on limited exsolution within their pigeonites (cf. Arai and Warren, 1999), these cumulates formed within rapidly cooling surface flows or lava ponds, and their trace-element compositions reflect relatively inefficient segregation of cumulus matter from “trapped” mare melt.

Many distinct mare melt types have been sampled via pyroclastic glasses. A compilation by Taylor *et al.* (1991) included 25 glass composition types. The process that produced the pyroclastic glasses (and dark mantle deposits)

probably has a close analogue on present-day Io. The Moon and Io are nearly identical in size and density, and in their lack of atmosphere. On Io, ongoing volcanism produces steady, long-lived plumes that probably consist of tiny, diffuse droplets, akin to the lunar pyroclastic glass spherules; these plumes have been observed to rise as high as 400 km (briefly) and spread as far as 700 km from their volcanic vents (McEwen *et al.*, 1998). The force that drives plumes like these is the explosive expansion of gas bubbles upon eruption into the near vacuum of the Ionian (or ancient lunar) atmosphere (Head and Wilson, 1992; McEwen *et al.*, 1998). The explosive gas phase on Io is probably  $\text{SO}_2$ ; the composition of the predominant gas phase during mare volcanism can only be reconstructed by inference, but it was probably dominated by CO and  $\text{CO}_2$  (Fogel and Rutherford, 1995). The precursor of these gases would be graphite, which tends to undergo oxidation if entrained in a hot magma that depressurizes during the late stages of its ascent to the surface. Lunar pyroclastic spherules have volatile-rich coatings (Chou *et al.*, 1975; Butler and Meyer, 1976; Fogel and Rutherford, 1995), and crystalline mare basalts can be highly vesicular (Ryder, 1985). Nonetheless, the smaller scale of the lunar dark mantle deposits compared to their Io analogues confirms a tendency toward relatively low proportions of volatile fuel in the lunar magmas.

Within each pyroclastic glass type, there tend to be systematic, relatively simple differentiation trends, encompassing in some cases wide ranges in chemical composition. The Apollo 14 orange glass array has MgO ranging from 14.5 wt.% down to 9.5 wt.% (Delano, 1986), and within an Apollo 14 green (VLT) glass suite, REE concentrations vary by a factor of 2 (Shearer *et al.*, 1990). But the compositional vectors of these trends do not conform to expectations from any simple “batch” partial melting or fractional crystallization model. Instead, it appears that complex processes during the formation and migration of melt in the mantle, including assimilation and fractional crystallization (AFC) involving KREEP and ilmenite cumulates, are required (Shearer *et al.*, 1996; Elkins *et al.*, 2000). (KREEP is an important material mainly associated with highland rocks, discussed in a later section.)

Initial post-Apollo views of lunar evolution envisioned that the mantle is a “layer cake” stratigraphic sequence of compositionally distinct cumulate layers (deep, low-Ti, high-*mg* cumulates, grading upward to FeO-rich, high-titanium, low-*mg* cumulates), as a result of crystallization of a primordial magma ocean. The low-titanium mare basalts were assumed to come from the deep cumulates, and the high-titanium basalts from the shallow, late-stage cumulates (Taylor and Jakes, 1974). This view now appears oversimplified. There is little correlation between the titanium abundances of mare magmas and the experimentally estimated (from the pressure of multiple-saturation of phases) depths of their source regions (Taylor *et al.*, 1991; Elkins *et al.*, 2000). Ringwood and Kesson (1976) first articulated what has become a generally accepted feature of models for mare petrogenesis: ubiquitous modification of the initial deep mantle cumulates by varying degrees of hybridization and assimilation interactions with formerly shallow material, swept down by convective stirring of the mantle. Aside from regular convective motions, many authors (e.g., Hess and Parmentier, 1995; Zhong *et al.*, 2000) have noted that the aftermath of magma ocean crystallization may have been a gravitationally unstable configuration (dense, FeO- and ilmenite-rich residual mush atop relatively FeO- and ilmenite-poor cumulates), which would imply an enhanced convective potential, and possibly a catastrophic overturn of the entire mantle. Moreover, modern theories of “polybaric” partial melting in a body as large as the Moon indicate that melting probably occurs over a range of depths, by a gradual increase in melt fraction within rising diapirs (Longhi, 1992, 2003; Shearer and Papike, 1999; Elkins *et al.*, 2000). The depth of initial melting is difficult to constrain. Beard *et al.* (1998) have inferred from Lu–Hf isotopic systematics (cf. Neal, 2001) that at high pressure,

garnet played a role in the residua of some mare basalts.

The picture that emerges from models like that of Ringwood and Kesson (1976) is an almost chaotic diversity of potential variations in the mixing between (already diverse) cumulates and “juicy” ingredients of the lunar mantle, such as downswept KREEP, during formation of precursors to mare volcanism. Nonetheless, it is often suggested that the distribution of TiO<sub>2</sub> among mare basalts is systematic, i.e., bimodal. Usually, the notion is that one mode is high-Ti, the other VLT plus medium-Ti (or low-Ti in the old nomenclature), with a gap at  $\sim 6\text{--}9$  wt.%. Giguere *et al.* (2000) interpreted Clementine TiO<sub>2</sub> data as showing that the bimodality is not significant, although they acknowledged a low-Ti/high-Ti bimodality (interpreted as a fluke) among available samples. Gillis *et al.* (2003) have proposed an alternative calibration of the Clementine TiO<sub>2</sub> data, which restores the bimodality, with the gap shifted down to 4–7 wt.%, TiO<sub>2</sub> for the Apollo and Luna sampling locations, but not for the global lunar surface. Considering the tremendous range in the TiO<sub>2</sub> data (0.3–16 wt.%), it seems most appropriate, when weighing the bimodality issue, to plot the data on a log scale. When all known samples, including lunar meteoritic samples and ignoring subtle intrasite variations among basically similar basalts (e.g., averaging all Apollo 17 high-Ti basalts together), are plotted on a log scale (Figure 4), the only bimodality appears between the VLT and medium-Ti (plus high-Ti) types; i.e., the portion of the range lacking in samples is  $\sim 1\text{--}2$  wt.%. (Unfortunately, TiO<sub>2</sub> concentrations  $< 2$  wt.% are not realistically resolvable by Clementine-style remote sensing.) Arai and Warren (1999) argue that a gap at 1–2 wt.% TiO<sub>2</sub> is more plausible, as a likely outcome of partial melting where absence versus presence of cumulus ilmenite plays a crucial role, than one at 6–9 wt.% TiO<sub>2</sub>.

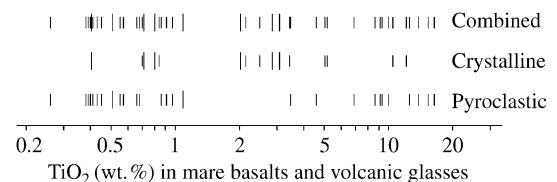


**Figure 4** Plotted on a log scale, and with fundamentally related (artificially oversampled) suites averaged together (as in Table 2), mare volcanic samples exhibit a possible bimodality in TiO<sub>2</sub> content, but with the gap in the distribution at around 1–2 wt.%, not 6–9 wt.% as commonly claimed (see text). Lunar meteoritic data, including pyroclastic glass suites (Arai and Warren, 1999), are distinguished by longer symbols.

The pyroclastic glasses tend to be far more “primitive,” in terms of MgO contents, than the crystalline basalts (Figure 5). The two types of material form a rough anticorrelation between MgO and Al<sub>2</sub>O<sub>3</sub>. But even the crystalline basalts are mostly picritic (far from plagioclase saturation), and detailed consideration of the major-element trends suggests that few, if any, of the sampled crystalline basalts are potentially related to spatially associated mare pyroclastic glasses (Longhi, 1987). Arai and Warren (1999) suggested that the glasses tend to be more MgO-rich because the fuel for explosive volcanism, graphite (density, 2.2 g cm<sup>-3</sup>), must have come from a mantle component that remained

(more or less) solid and intact through the extensive primordial (magnasphere) melting of the Moon, and thus remained MgO-rich.

### 1.21.3.3 Mare Basalt Trace-element and Isotopic Trends

Mare basalts, being young by lunar standards, are, as a rule, far less battered by impact processes than highland rocks; they are also generally closer in composition to their parent melts (i.e., the proportion of cumulates is far higher among highland rocks). Thus, mare basalts are our most suitable samples of lunar rocks that have an analogous terrestrial rock type (Figures 6 and 7). VLT and medium-Ti types are preferred for this purpose, because the high-Ti types are unlike any common variety of terrestrial basalt.

The most striking difference between mare basalt and terrestrial basalt is in their contents of volatile species. Besides H<sub>2</sub>O (practically unmeasurable in most lunar rocks), this disparity is manifested by data for volatile alkalis (sodium, potassium, rubidium, and caesium) and by trace metals such as zinc, indium, bismuth, and cadmium (Figure 6). The same trend of enormous depletions in comparison to chondritic matter and even terrestrial basalt is also shown by highland samples, but the evidence is clearest and most definitive from the mare basalts. Gross overall volatile depletion is also demonstrated by the near absence of hydrated minerals among lunar rocks. Some Apollo rocks, most impressively Apollo 16 breccia 66095, do contain surface-associated “rust” patches (mainly FeOOH,Cl), but these are suspected to be products of terrestrial oxidation, not endogenous lunar volatile processing (Papike *et al.*, 1991). Even extraordinarily “evolved” types of nonmare rock, such as a few tiny samples that are compositionally granite (a term not meant to imply the existence of lunar batholiths!) contain pyroxene, not amphibole or mica, as their mafic component (Warren *et al.*, 1983).

Mare basalts indicate that the Moon’s pattern of crust–mantle siderophile element depletions is roughly similar to that of the Earth (Figure 7). Unfortunately, for four siderophile elements, rubidium, rhodium, palladium, and platinum, no reliable data have been reported for lunar basalts. Neal *et al.* (1999, 2001) reported ICP-MS data, but their analyses show obvious artificial contamination, based on comparison with iridium data and palladium upper limits reported by Wolf *et al.* (1979). The most “noble” of the siderophile elements in Figure 7 are osmium and iridium. For noble siderophile elements, scatter among individual rocks is very great (e.g., Figure 8), but the factor-of-4 disparity between average mare and terrestrial basalt for osmium and iridium

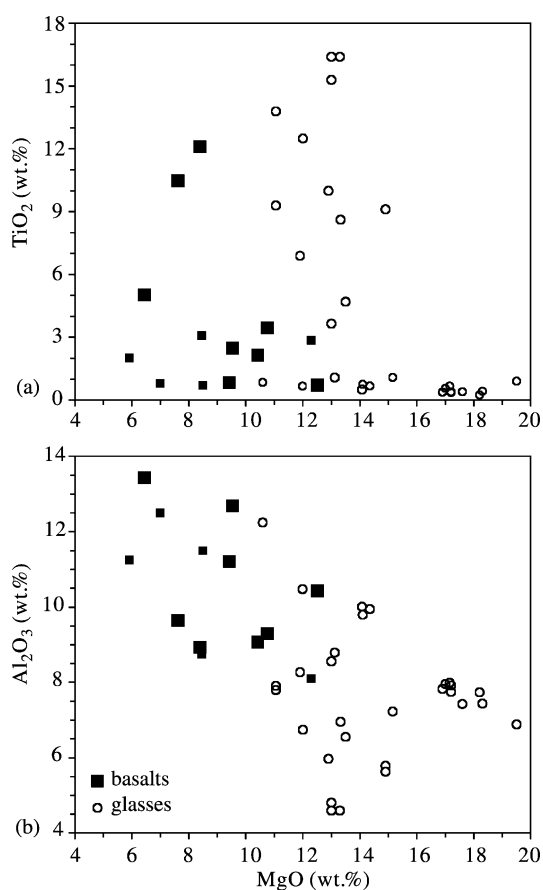


**Figure 5** Mare pyroclastic glasses tend to have far higher MgO, yet a similar range in TiO<sub>2</sub>, compared to crystalline mare basalts. For basalts, plotted data are averages of many literature analyses for basalt types (Table 2), except for lunar meteorites, which are individual rocks (shown with smaller filled squares). Other data sources are as cited by Arai and Warren (1999), i.e., primarily the compilation of Taylor *et al.* (1991); updated from Arai and Warren (1999) by adding lunar meteorites Dhofar 287 and NWA032 (but not the cumulate NWA773, 26 wt.% MgO, excluded because its composition is presumably unrepresentative of its magma type).

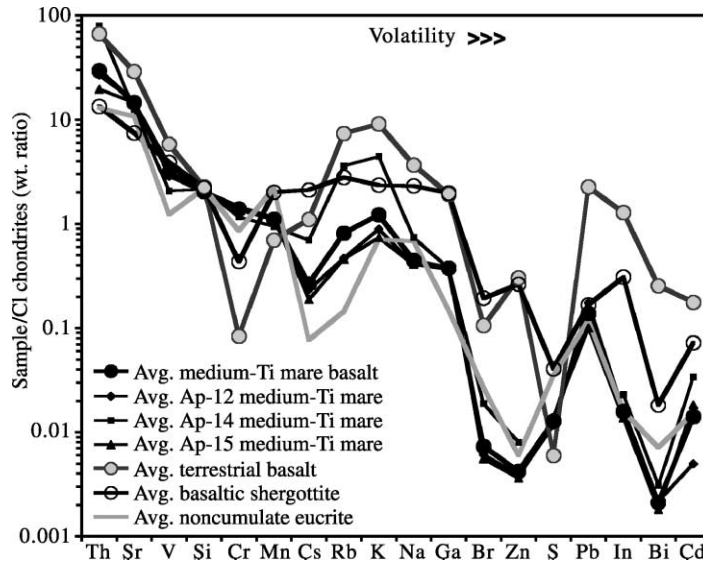


**Figure 6** Volatile element concentrations in averaged medium-Ti mare basalts, normalized to CI chondrites (Wasson and Kallemeyn, 1988). Also shown for comparison are averages for terrestrial basalts, for basaltic shergottite (martian) meteorites, and for eucrite (asteroidal) meteorites. The elements are plotted in order of thermodynamically calculated solar nebula volatility (Wasson, 1985). The mare basalt data are mainly from the compilation of Haskin and Warren (1991); a noteworthy primary source is Wolf *et al.* (1979). The plotted overall average mare basalt composition is a 4:1:4 weighting of the Apollo-12, -14, and -15 types, respectively (the Apollo 14 type has been far less well studied, and moreover may be idiosyncratically enriched in volatile-incompatible elements: Dickinson *et al.*, 1989). The average for terrestrial basalt is based on Govindaraju's (1994) compilation for USGS standards BCR-1, BHVO-1, BIR-1, and W-1, plus (given 1/5 weight) an average for MORB, based primarily on Hertogen *et al.* (1980). The average for basaltic shergottites is based on the up-to-date (internet) version of the Meyer (1998) compilation. The average for eucrites is based on a large number of references, most notably Chou *et al.* (1976), Morgan *et al.* (1978) and Paul and Lipschutz (1990).

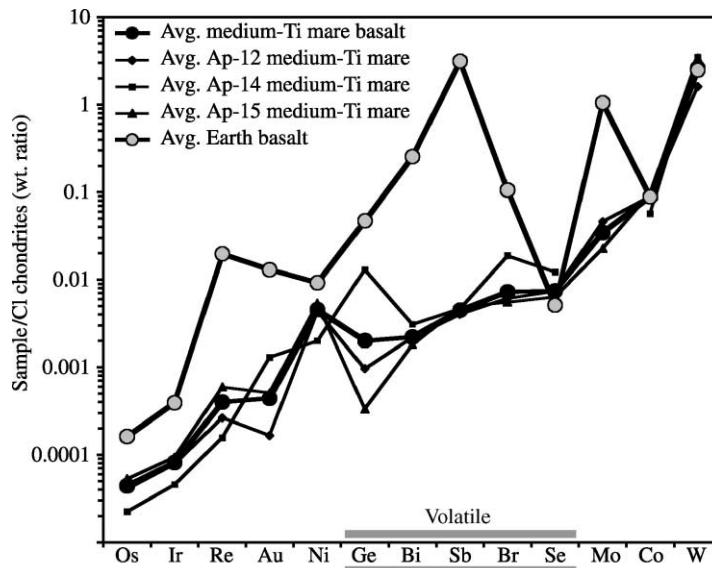


**Figure 7** Siderophile element concentrations in averaged medium-Ti mare and terrestrial basalts, normalized to CI chondrites. The elements are plotted in order of CI-depletion factors in average medium-Ti mare basalt, but for some elements volatility may account in large part for the depletion. Data are from same sources as for Figure 6. To avoid an over-complex diagram, individual terrestrial compositions are not plotted, but all show similar patterns at the scale of this diagram; the most noteworthy exceptions being low iridium ( $9 \times 10^{-6}$  times CI) and nickel ( $10^{-3}$  times CI) in BCR-1, and relatively low osmium and iridium (virtually identical to mare basalts) and antimony (0.11 times CI) in MORB.

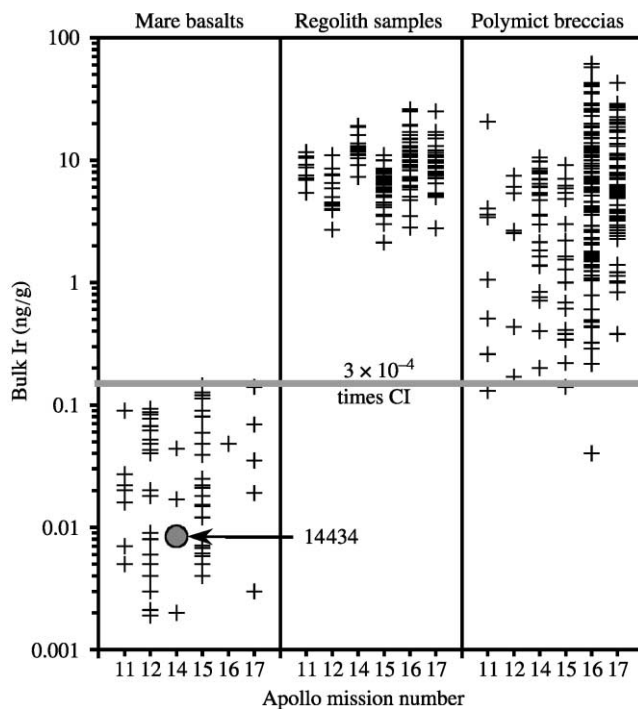


**Figure 8** Despite great scatter in the data distribution, for a highly siderophile element such as iridium data reveal a strong contrast between compositionally “pristine” rocks, as exemplified by mare basalts, and lunar materials (regolith samples and polymict breccias) contaminated by a meteoritic component. This contrast can be exploited to help identify pristine nonmare rocks. A good example is Apollo 14 diabase 14434, which has an ambiguous texture and mineralogy (monomict-brecciated but not diagnostically coarse), yet is judged very probably pristine based on its depletion in iridium (Arai and Warren, 1997).

appears real. In lunar basalt, rhenium, gold, and germanium are more “nobly” depleted than in the terrestrial regime, where these elements, particularly rhenium, tend to exhibit incompatible-lithophile tendencies (probably linked to Earth’s higher  $f_{O_2}$ ). Also, some of the lunar depletion in elements such as germanium may reflect the Moon’s general depletion of volatile elements. The same trend of strong siderophile depletions in comparison to chondritic matter, and even versus terrestrial igneous rocks, is also shown by highland samples. But for these, the evidence is far more complicated; a careful and, for siderophile elements, possibly biased selection of “pristine” rocks (see below) is required to obtain compositions representative of the endogenous igneous highland crust.

Among the highly siderophile elements, iridium and nickel contents in lunar rocks have been frequently and well determined, and both elements conform to a general pattern among planetary igneous rocks (Warren *et al.*, 1999) by showing a correlation (albeit not linear) with MgO (Figure 9). These trends represent the strongest evidence that the lunar mantle was significantly siderophile-depleted in comparison to the terrestrial mantle. Figure 9 also includes martian meteorite data, and iridium and nickel are correlated with MgO in these samples as well.

The role of sulfide-driven (chalcophile) fractionations in lunar magmatism is difficult to constrain, but sulfides presumably play a lesser role on the Moon than on Earth, because the solubility of sulfide in mafic melt increases with decreasing  $f_{O_2}$  (Peach and Mathez, 1993). Compared to lithophile elements of similar volatility, sulfur is exceptionally depleted in terrestrial and martian basalts, but not so depleted in lunar basalts (Figure 6). Medium-Ti mare basalts are clearly unsaturated with sulfide, and although high-Ti mare basalts were originally believed to be sulfide-saturated (Gibson *et al.*, 1977), Danckwerth *et al.* (1979) found them to be unsaturated, as well.

Chondrite-normalized REE patterns are shown in Figure 10. A comparable variety of patterns are found for mare pyroclastic glasses (Papike *et al.*, 1998). Most mare basalts have significant negative europium anomalies, which increase in magnitude with increasing REE content and have important implications. In the reducing lunar environment, negative europium anomalies are only to be expected in basalts that are plagioclase-saturated, i.e., left mantle residua with plagioclase, with which europium is thoroughly compatible (distribution coefficient  $D \sim 1.1-1.2$ ) when reduced to mostly  $\text{Eu}^{2+}$  (McKay and Weill, 1977). But most mare basalts (all those with  $\text{Al}_2\text{O}_3$  less than  $\sim 12$  wt.%) are not saturated with plagioclase at

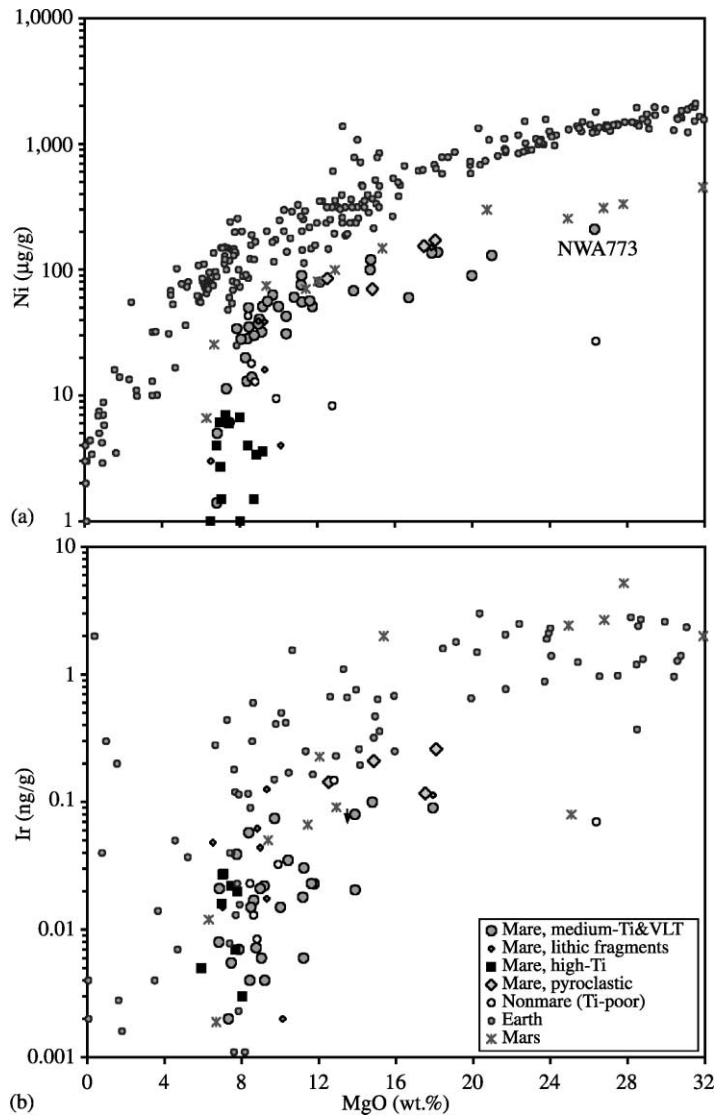


**Figure 9** (a) Nickel and (b) iridium versus MgO, for igneous rocks from the Moon, Mars, and Earth. Lunar data are mainly from the compilation of Haskin and Warren (1991), the most noteworthy addition being lunar meteorite NWA773 (nickel only; Korotev *et al.*, 2002a). Data for martian rocks are from the up-to-date (internet) version of the Meyer (1998) compilation. Data sources for terrestrial rocks are too numerous to list, but include Crocket and MacRae (1986), Brüggmann *et al.* (1987), and the compilation of Govindaraju (1994).

any pressure (Taylor *et al.*, 1991; Longhi, 1992; Papike *et al.*, 1998). The inference, therefore, is that long before the mare magmas formed, their *source regions* (i.e., much of the lunar mantle) must have been *pre-depleted* in plagioclase, presumably by formation of the highland crust. This concept has long been viewed as a significant argument in favor of a primordial lunar magma ocean (Taylor and Jakes, 1974; Warren, 1985). Shearer and Papike (1989) suggested that the negative europium anomalies could conceivably have formed without major plagioclase fractionation, because pyroxene can impart a negative europium anomaly by excluding

the relative large  $\text{Eu}^{2+}$  cation during crystallization. McKay *et al.* (1991) reported relevant  $D$  data for lunar pigeonite. Brophy and Basu (1990) applied these and earlier  $D$  results to show that accounting for the mare europium anomalies without appeal to prior plagioclase removal requires implausible assumptions about modal mineralogy and/or degree of melting in the source regions. Assimilation/mixing with KREEP swept down into the mantle may have affected many of the mare europium anomalies, but the mare basalts with the largest negative europium anomalies tend not to have KREEP-like enriched La/Sm ratios (Figure 10).

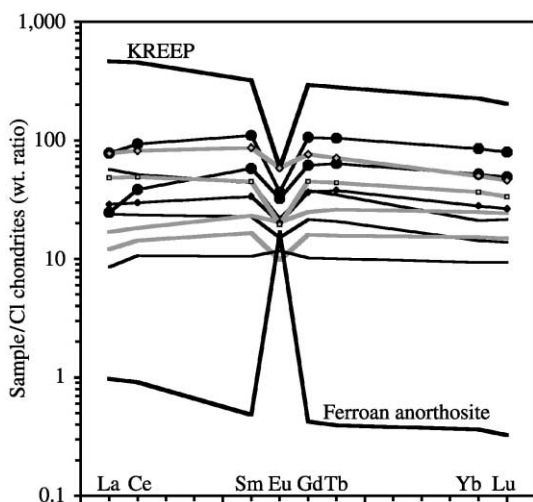


**Figure 10** Chondrite-normalized REE concentrations in mare basalts, KREEP, and a representative ferroan anorthosite. Data for mare basalt types are from Table 2, with two deliberate omissions: the NWA773 cumulate, an individual rock presumably unrepresentative of its parent magma, and the Apollo 14 type, which is a suite with notoriously diverse REE abundances, although the patterns are generally parallel to KREEP (which is plotted). Individual mare basalt types are not labeled, but symbols on some of the patterns denote relatively titanium-rich varieties; the most titanium-rich basalts (largest symbols) tend to have the lowest (often subchondritic) La/Sm ratios. Data for high-K KREEP and ferroan anorthosite 15295c41 are from Table 5 and Warren *et al.* (1990), respectively.

Data for isotopic tracer ratios,  $I_{Sr}$ ,  $\epsilon_{Nd}$ , etc., in mare basalts have been reviewed by Papike *et al.* (1998) and Snyder *et al.* (2000b). Chapter 1.20 provides an extensive discussion of lunar  $\epsilon_W$  data. Model ages based on strontium, neodymium, and lead for the mantle source regions typically cluster near 4.3–4.4 Ga, coinciding with a neodymium-based model age for urKREEP of  $4.35 \pm 0.03$  Ga (Lugmair and Carlson, 1978). Most mare basalts have positive  $\epsilon_{Nd}$ ; the exceptions are some eastern Procellarum (Apollo 12 and Apollo 14) samples whose sources probably mixed to an unusual extent with KREEP, which is extremely abundant in the Procellarum region (Lawrence *et al.*, 2002a). The Apollo 14 mare basalts also tend to have unusually high  $I_{Sr}$ , again consistent with KREEP assimilation. Low-Ti mare basalts show remarkably diverse  $\epsilon_{Hf}$  (as high as 51), again with Apollo 14 and especially Apollo 12 samples accounting for much of the range (Unruh *et al.*, 1984). Beard *et al.* (1998) inferred possible involvement of deep-mantle garnet, a suggestion also supported by Neal (2001) based on high Zr/Y and Zr/Yb ratios in some mare pyroclastic glasses. In any event, the highly diverse isotopic ratios of the mare basalts demonstrate that volcanism arose from a remarkably heterogeneous

mantle, fundamentally different from the tectonically stirred, and thus relatively homogenized, terrestrial mantle.

#### 1.21.4 THE HIGHLAND CRUST: IMPACT BOMBARDMENT AND EARLY DIFFERENTIATION

##### 1.21.4.1 Polymict Breccias and the KREEP Component

The vast majority of rocks from the sampled near-surface portion of the ancient highland crust are impactites. The proportion of highland rocks that are completely unaltered by impact processing is so minor that in this context the term “pristine” is used to denote samples (in most cases monomict breccias) that preserve in effectively unaltered form the original chemical compositions of endogenous igneous lunar rocks (Warren and Wasson, 1977; Wolf *et al.*, 1979; Ryder *et al.*, 1980; Papike *et al.*, 1998). The importance of pristine rocks in providing constraints on lunar crustal genesis will be discussed at length below, but the mixed-origin highland rocks (polymict breccias and pseudoigneous clast-poor impact-melt breccias) are important in their own way.

The polymict breccias, especially the regolith breccias, are useful as naturally produced composite samples (assembled from mostly local but otherwise random bits) of the lunar crust. The mixing involved in the genesis of these rocks diminishes their value as recorders of lunar igneous processes, but makes them ideal for constraining variations in the regional bulk composition of the crust (Table 3). The most dramatic compositional variations among these samples involve their contents of the unique lunar component, KREEP (Table 5). The chondrite-normalized REE pattern of KREEP is shown in Figure 10. Although named for its high contents of potassium, REE and potassium, KREEP is actually rich in all of the incompatible trace elements. Among the most notable are thorium and uranium, because these are the most extremely enriched (versus chondrites) in KREEP, and because (with potassium) these are the main sources of long-lived radiogenic heating within planets. Because the many hundreds of Apollo polymict impactites that are thorium- and REE-rich tend to contain all the incompatible elements in relatively constant (KREEP) ratios, Warren and Wasson (1979a) suggested that nearly all of the lunar crust’s complement of incompatible elements was derived from a common reservoir, possibly a magma ocean residuum, which they dubbed urKREEP. Note, however, that urKREEP, like KREEP, is a strictly hypothetical material.

**Table 5** Estimated composition of average “high-K” KREEP, as derived by Warren (1989).

		Warren and Wasson (1979b) KREEP	Warren (1989) KREEP (avg. high-K)	Strength of correlation with KR <sup>a</sup>	KREEP/CI chondrites wt. ratio	Uncertainty class <sup>b</sup> (see below)
Li	$\mu\text{g g}^{-1}$	56	40	Moderate +	25	III
Na	$\text{mg g}^{-1}$	6.4	7	Moderate +		II
Mg	$\text{mg g}^{-1}$	64	50 <sup>a</sup>	Moderate –		II
Al	$\text{mg g}^{-1}$	88	80	Weak –	9.3	I
Si	$\text{mg g}^{-1}$	224	235	Weak + (?)		I
P	$\text{mg g}^{-1}$	3.4	3.5	Moderate +	3.4	III
K	$\text{mg g}^{-1}$	6.9	8	Weak +	14	III
Ca	$\text{mg g}^{-1}$	68	70	Weak –	7.6	II
Sc	$\mu\text{g g}^{-1}$	23	23	None	4.0	II
Ti	$\text{mg g}^{-1}$	10	12	Very weak +	29	III
V	$\mu\text{g g}^{-1}$	43	40	Weak –		II
Cr	$\text{mg g}^{-1}$	1.3	1.2	Weak –		II
Mn	$\text{mg g}^{-1}$	1.08	1.05	None		II
Fe	$\text{mg g}^{-1}$	82	80	Weak +		II
Co	$\mu\text{g g}^{-1}$	33	25	Weak –		III
Ga	$\mu\text{g g}^{-1}$	7.5	9	Weak +		(III)
Br	$\mu\text{g g}^{-1}$	Not estimated	120	Moderate +		III
Rb	$\mu\text{g g}^{-1}$	22	22	Weak +	9.9	III
Sr	$\mu\text{g g}^{-1}$	200	200	Very weak +	25	I
Y	$\mu\text{g g}^{-1}$	300	400	Strong +	278	(II)
Zr	$\mu\text{g g}^{-1}$	1700	1,400	Strong +	368	III
Nb	$\mu\text{g g}^{-1}$	80	100	Moderate +	370	(III)
Cs	$\text{ng g}^{-1}$	2000	1000	Weak +	5.46	III
Ba	$\mu\text{g g}^{-1}$	1200	1,300	Strong +	565	II
La	$\mu\text{g g}^{-1}$	110	110	Very strong +	466	
Ce	$\mu\text{g g}^{-1}$	270	280	Very strong +	455	I
Pr	$\mu\text{g g}^{-1}$	Not estimated	37	Very strong +	398	I
Nd	$\mu\text{g g}^{-1}$	180	178	Very strong +	389	
Sm	$\mu\text{g g}^{-1}$	49	48	Very strong +	322	
Eu	$\mu\text{g g}^{-1}$	3.0	3.3	Moderate +	59	I
Gd	$\mu\text{g g}^{-1}$	57	58	Very strong +	294	
Tb	$\mu\text{g g}^{-1}$	10	10.0	Very strong +	282	
Dy	$\mu\text{g g}^{-1}$	65	65	Very strong +	265	
Ho	$\mu\text{g g}^{-1}$	14	14	Strong +	256	I
Er	$\mu\text{g g}^{-1}$	39	40	Very strong +	250	
Tm	$\mu\text{g g}^{-1}$	Not estimated	5.7	Very strong +	231	I
Yb	$\mu\text{g g}^{-1}$	36	36	Very strong +	226	
Lu	$\mu\text{g g}^{-1}$	5.0	5.0	Very strong +	204	
Hf	$\mu\text{g g}^{-1}$	37	38	Strong +	317	I
Ta	$\mu\text{g g}^{-1}$	4.0	5.0	Very strong +	313	II
W	$\mu\text{g g}^{-1}$	2.0	3.0	Strong +	30	(III)
Th	$\mu\text{g g}^{-1}$	18	22	Very strong +	759	I
U	$\mu\text{g g}^{-1}$	5	6.1	Strong +	744	I
Molar Mg/(Mg + Fe)		0.64	0.59 <sup>c</sup>	Moderate –		II

<sup>a</sup> Warren’s (1989) parameter KR is the average of sample/KREEP ratios for a large set of incompatible trace elements. <sup>b</sup> Estimated uncertainties for the average high-K KREEP composition, expressed as maximum expected percentages of deviation between “true” average and estimates: blank = 5%, I = 10%, II = 20%, III = 30%, IIII = 40%. Parentheses denote elements for which extrapolation to high KR is required.

<sup>c</sup> Mg concentrations appear to be systematically higher in Apollo-14 KREEP versus KREEP from other locales.

It is expected/inferred that none of this material remains in its original form, since almost as soon as it formed it probably was massively involved in assimilative reactions with magnesium-rich magmas (Warren, 1988; Papike *et al.*, 1996; Shervais and McGee, 1999). There may even have been a tendency for KREEP to differentiate (albeit temporarily and locally) by silicate liquid immiscibility (Neal and Taylor, 1991; Jolliff *et al.*, 1999). The few KREEP-rich rocks that are pristine are mostly basalts, or in rare cases granitic (Papike *et al.*, 1998). Despite the ephemeral nature of the hypothetical urKREEP, it is useful to compare all other lunar sample compositions to the average composition of the most concentrated “high-K” variety of polymict impactite KREEP, which occurs among Apollo 12 and especially Apollo 14 samples (Table 5).

Most of the lunar meteorite highland regolith breccias, which come from widely scattered random points, are remarkably KREEP-poor compared to the Apollo and Luna regolith samples (Table 3). The recent Lunar Prospector maps of the global distributions of thorium, uranium, potassium, and samarium (Lawrence *et al.*, 2002a; Prettyman *et al.*, 2002; Elphic *et al.*, 2000) revealed that the Apollo/Luna sampling region happens to be atypically KREEP-rich.

#### 1.21.4.2 Bombardment History of the Moon

The polymict impactites are extremely important as primary constraints on the impact bombardment of the Moon. This bombardment

history can be directly extrapolated to Earth (in early times, the tidally receding Moon was even closer to Earth), where pre-3.8 Ga crust has been virtually eliminated by vigorous geodynamism. The polymict impactite samples have yielded ages that are remarkably clustered near 3.9 Ga, especially for impact-melt breccias (Figure 11). This nearly unimodal age spectrum, which was first noted in the initial Apollo 16 sample investigations (e.g., Schaeffer and Husain, 1973; Kirsten *et al.*, 1973), represents one of the most profound discoveries of planetary sample research. It revealed that the rate of cratering (i.e., collisions between the Moon and asteroids and comets) was vastly higher  $\sim 3.9$  Gyr ago than it has been over the last 85% of solar system history. A few additional data for 3.1–3.7 Ga, derived from crater-abundance counts on mare lava terrains dated through Apollo and Luna mare basalt samples (BVSP, 1981), indicate that the cratering rate declined rapidly, by a factor of order 10, between 3.9 Ga and 3.1 Ga.

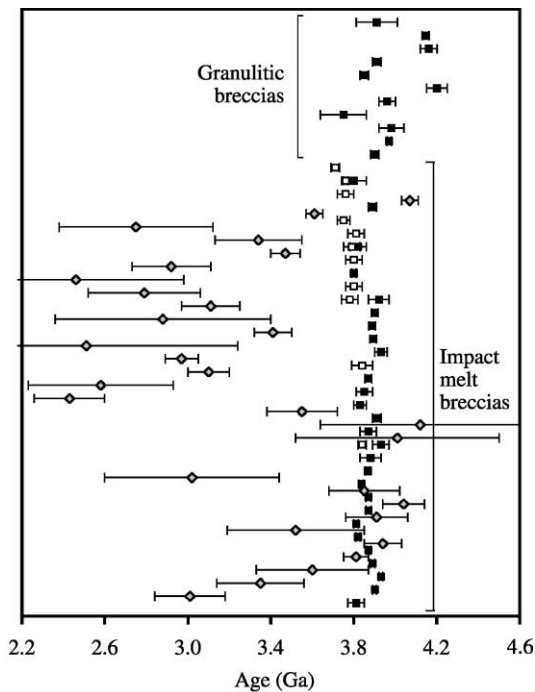


**Figure 11** Ages of lunar polymict breccias, especially impact-melt breccias, show strong clustering near 3.9 Ga. Data from argon isotopes are shown by filled symbols; from strontium isotopes by open symbols. Squares: Apollo samples, data compiled by Papike *et al.* (1998), except excluding (in order to avoid complicating the plot) five much younger ages (0.4–2.3 Ga) for impact-melt glass samples. Diamonds: clasts in four different lunar meteorites (Cohen *et al.*, 2000; Bogard *et al.*, 2000). Error bars are generally  $2\sigma$  (or unstated), but only  $1\sigma$  for the Cohen *et al.* (2000) meteorite clast data.

Based on an “Occam’s Razor” preference for simplicity, but comparatively scant evidence (indirectly inferred ages of 1.0 Ga and 0.3 Ga for the Copernicus and Tycho craters, respectively, compared versus hugely uncertain crater count data for terrains resurfaced during the formation of these craters), for many years the consensus view was that the cratering rate had probably remained approximately constant since 3.1 Ga (Guinness and Arvidson, 1977; Young, 1977; BVSP, 1981; cf. Bogard *et al.*, 1994). However, the  $^{40}\text{Ar}$ – $^{39}\text{Ar}$  ages obtained by Culler *et al.* (2000) for 155 Apollo 14 impact-glass spherules suggest that the cratering rate continued to decline by roughly a factor of two between 3.1 Ga and 2.0 Ga, and then remained roughly constant until  $\sim 0.4$  Ga, when it abruptly increased by a factor of  $3.7 \pm 1.2$ . These results should be viewed with caution. The  $<0.4$  Ga glass spherules conceivably are predominantly from one fresh crater (Cone?) near the Apollo 14 traverse area. Smaller samplings of 21 impact glasses from Apollo 16 and 17 (Zellner *et al.*, 2003; Terada *et al.*, 2002) show none younger than 0.6 Ga. The first reported ages for impact-melt clasts from lunar meteorites (Cohen *et al.*, 2000) show a comparatively diffuse cluster, spread rather evenly from 2.6 Ga to 4.0 Ga (Figure 11). Most of the Cohen *et al.* (2000) lunar meteorite data are relatively imprecise (they were obtained from tiny clasts), but these data are important because they presumably represent several very widely separated regions of the Moon. The abundance of ages  $\ll 3.9$  Ga in the Cohen *et al.* (2000) data set supports the Culler *et al.* (2000) inference that the cratering rate was still declining between 3 Ga and 2 Ga.

The bombardment history before 3.9 Ga has been most controversial. The relative scarcity of breccia ages  $>3.9$  Ga has led many (originally Tera *et al.*, 1974; in recent years most notably Ryder, 1990) to infer a spike in the global lunar cratering rate at  $\sim 3.9$  Ga; in other words, that the rate was considerably lower before 3.9 Ga. Following Tera (1974), this cratering spike concept is somewhat confusingly known as the lunar “cataclysm” hypothesis. A broader, generally accepted hypothesis known as “late heavy bombardment” simply postulates vastly higher, more destructive lunar cratering at  $\sim 3.9$  Ga, without regard to the spike question. The controversy concerns the degree to which the clustered  $\sim 3.9$  Ga ages reflect a large-factor and global spike, as opposed to a bump or inflection on a basically monotonic decline in the late-accretionary impact rate.

Skeptics of the cratering spike hypothesis have argued that the clustering of ages near 3.9 Ga may be a “stonewall” effect (Hartmann, 1975; Wetherill, 1981; Chapman *et al.*, 2002). The stonewall model invokes a saturation of the

pre-3.9 Ga crust with so many impacts that isotopic clocks were constantly being reset within a heated megaregolith, until the rocks that eventually became samples were excavated to the surface regolith (*sensu stricto*) by a few major impacts. This might seem a plausible explanation for the paucity of pre-3.9 Ga ages, if the 3.8–3.9 Ga clustering was limited to the easily reset argon age system. However, Papike *et al.* (1998) cite many strontium-based ages clustering near 3.8 Ga (Figure 11; the strontium-based cluster appears displaced by  $-0.1$  Ga from the argon-based cluster, but this may be an analytical artifact). The relevance of the impact-melt age spectrum as portrayed by Ryder (1990) and Dalrymple and Ryder (1993, 1996) can still be questioned, however, on the more fundamental grounds that these authors always assumed that only samples with classic (near-subophitic) impact-melt breccia textures are appropriate for dating impact events. J. L. Warner *et al.* (1977) suggested that on the early (pre-3.9 Ga) Moon, where the ambient crustal temperature was still relatively close to the solidus, granulitic breccias tended to form in major impacts, in analogous proportion and position to where, on the post-3.9 Ga Moon, impact-melt breccias would form. This model, from a team of leading authorities on impactite genesis, has never been effectively refuted. As was already a point of emphasis to J. L. Warner *et al.* (1977), granulitic breccias are commonly older than 3.9 Ga (Figure 11).

Critics of the cratering spike hypothesis also note (e.g., Chapman *et al.*, 2002) that the Apollo  $\sim 3.9$  Ga impact-melt samples come exclusively from sites clustered in the central nearside, and thus are likely from preponderantly just two or three impacts: Imbrium, Serenitatis, and with greater uncertainty, Nectaris. Cratering theory (Melosh, 1989; Grieve and Cintala, 1992) indicates that the proportional yield of impact melt, as opposed to solid ejecta, is vastly higher in large-basin-forming events than in smaller-scale impacts. Warren (1996) applied this principle to the particular case of the Moon.

On photogeologic–stratigraphic grounds, Nectaris is clearly older than Imbrium and Serenitatis, and two-thirds (30 out of 44) of the Moon’s still-recognizable basins appear even older than Nectaris (Wilhelms, 1987). Impact-melt breccias of Nectaris origin are presumably present among the Apollo 16 samples, acquired  $\sim 550$  km from the center of Nectaris.  $^{40}\text{Ar}$ – $^{39}\text{Ar}$  ages for Apollo 16 impact-melt breccias mostly cluster in the range 3.87–3.92 Ga (Papike *et al.*, 1998; Dalrymple *et al.*, 2001), and 3.90–3.92 Ga has become almost canonical as the age of Nectaris (e.g., Wilhelms, 1987; Dalrymple *et al.*, 2001). But, as Korotev *et al.* (2002b) have noted, the absolute age of Nectaris is unclear. A large group

(at least 13) of Apollo 16 “light matrix breccias” (these rocks were *explicitly* classified as impact-melt breccias by the authoritative Stöffler *et al.* (1980) compilation) yielded argon ages in the range 4.12–4.26 Ga (Schaeffer and Husain, 1973; Mauer *et al.*, 1978). Mauer *et al.* (1978) assumed these “group 1” samples cannot be basin-related, because they tend to be distinctly KREEP-poor compared to the other Apollo 16 impact melts; the assumption was that all impacts big enough to form basins would plumb into a KREEP layer in the lower crust. However, in light of what the Prospector data (Lawrence *et al.*, 2002a) revealed about the extreme concentration of KREEP into the Procellarum (central-eastern nearside) region, a Nectaris provenance seems more plausible for the “group 1” samples than for the more typical, younger but unsuitably KREEP-rich, impact-melt breccias from Apollo 16. Also, recent basin ejecta thickness modeling (Haskin *et al.*, 2002) suggests that ejecta from distant Imbrium and Serenitatis outweigh ejecta from the nearby but relatively small and older Nectaris, in the upper (sampled) Apollo 16 megaregolith. Considering all of these constraints, an age of  $\sim 4.2$  Ga for Nectaris seems entirely possible, if not probable.

The age of a fourth basin, Crisium, can, in principle, be constrained using Luna 20 samples. On photogeologic–stratigraphic grounds, Crisium appears similar in age to Serenitatis, i.e., older than Imbrium but younger than Nectaris (Wilhelms, 1987). Cohen *et al.* (2001) obtained argon ages for six Luna 20 rocklets and reviewed literature data (mainly from Swindle *et al.*, 1991) for 12 others. Swindle *et al.* (1991) found a loose clustering of ages at 3.75–3.90 Ga and suggested that the oldest sample in this cluster,  $3.895 \pm 0.017$  Ga, might date the Crisium impact. However, it is not even clear the sample in question is an impact-melt breccia (no thin section was made). The only two certain impact-melt breccias dated by Swindle *et al.* (1991) yielded ages of  $0.52 \pm 0.01$  Ga and  $4.09 \pm 0.02$  Ga. Among the samples dated by Cohen *et al.* (2001), most are, in this author’s opinion, probably either impact-melt breccias or annealed impact-melt breccias (genuine, pristine “gabbros” seldom have grain sizes of  $<200$   $\mu\text{m}$  like rocklet 2004D; pristine troctolites seldom have grain sizes of  $<100$   $\mu\text{m}$  like rocklet 2004C). Considering all of the 13 or so Luna 20 rocklets that have yielded  $^{40}\text{Ar}$ – $^{39}\text{Ar}$  ages (Cohen *et al.*, 2001) and are likely impact-melt breccias, the data (excluding the 0.52 Ga outlier) show an almost even distribution across the 3.75–4.19 Ga range. In other words, the age of the Crisium impact is not yet constrained beyond being probably within the range 3.8–4.2 Ga.

From a celestial-mechanical standpoint (e.g., Wetherill, 1981; Morbidelli *et al.*, 2001),

continued intense cratering as late as 3.9 Ga is plausible, but a major spike in the rate of inner solar system collisions 500 Ma after the origin of the solar system is hardly an obvious outcome from planetary accretion. Hartmann *et al.* (2000) discussed, in a conjectural way, several potential mechanisms to accomplish this.

By extrapolation to other solar system bodies, the Moon's bombardment history represents a crucial series of chronologic benchmarks for planetology. But even for application to today's mature solar system, this extrapolation is not straightforward (BVSP, 1981). Correcting for "gravitational cross-section" (i.e., the escape velocity) of the target body is straightforward, but also required is a far more complex correction for the flux and prevailing velocity of the asteroids and comets (i.e., the potential impactors) that are functions of, mainly, heliocentric distance (BVSP, 1981; Chyba, 1991). Going back in time, the extrapolation becomes even more uncertain. If the hypothesis of a 3.9 Ga cataclysm is correct, there is a slight possibility that the cataclysm was a local,  $\sim 1$  AU phenomenon (Ryder, 1990). However, Bogard (e.g., 1995; cf. Kring and Cohen, 2002) has found that ages of numerous impactite meteorites from the HED asteroid (Vesta?), and many more from the (probably) separate mesosiderite asteroid, show a similar clustering near 3.9 Ga. The sole martian meteorite older than 1.3 Ga has also yielded an argon-based age of 3.9 Ga (Ash *et al.*, 1996). Even if the cratering spike (cataclysm) hypothesis is incorrect, vastly higher inner solar system cratering rates at  $\sim 3.9$  Ga, as demonstrated primarily and still most impressively from lunar samples, are a well-established fact. Implications for evolution of Earth, including the biosphere, are profound (e.g., Kring and Cohen, 2002).

#### 1.21.4.3 Impactite and Regolith Siderophile Signatures

The siderophile elements in polymict lunar materials come almost entirely from meteoritic contamination added to the outer Moon in impacts. Siderophile elements thus may give clues to the nature of the materials that have bombarded the Moon. Unfortunately, however, the limited expanse of the Apollo/Luna sampling region, with samples dominated by just three or four major basins, again severely restricts the general applicability of this approach.

The largest basins clearly dominate the impact-melt inventory (Warren, 1996), but the degree to which they dominate the megaregolith siderophile element budget has been controversial. The Edward Anders (University of Chicago) group, in a series of papers reporting a wealth of excellent

lunar siderophile analyses (e.g., Hertogen *et al.*, 1977), interpreted some rather diffuse clustering in impactite siderophile element abundances as signatures of several different basins. For example, Wasson *et al.* (1975) and Korotev (1987a, 1994) argued that such an approach might be unreliable, because basin signatures tend to be obscured by significant siderophile contributions from smaller craters. Both views may be partly correct. The kinetic energy of impact is the main control over the basin (cavity, ejecta, and even melt) volume; and unfortunately for the aim of a simple, general answer to the basins-versus-craters controversy, the ratio of impact energy to projectile mass is sensitive to a wide-ranging and unrecoverable parameter: the collision velocity. The velocity of impact with the Moon is typically  $\sim 3$  times faster for comets than for asteroids (e.g., Chyba, 1991).

Apart from impact velocity, the problem is partially constrained by the size–frequency spectrum of projectiles striking the Moon. This size distribution conforms to a power law with number of particles proportional to  $L^{-p}$ , where  $L$  is the projectile diameter and  $p$  is a constant  $> 0$ . Numerous studies, reviewed by Melosh (1989), indicate that the slope  $p$  is 1.8 for  $L > 10$  m, to 3.5 for  $L < 10$  m. Thus (given that for large projectiles  $p \ll 3$ ; and assuming that velocity, density, and siderophile concentrations all remain roughly constant across the size spectrum), most siderophile contamination, over time, should come from a comparatively few large collisions. Realistically, however, considering the stochastic potential for overlaps, and especially the great variability of collision velocity, it may be that in most regions no single basin dominates the megaregolith siderophile budget.

In any event, the steeper ( $p > 3$ ) slope for impactor  $L < 10$  m indicates that for the regolith (*sensu stricto*), a different regime from that of impact-melt rocks prevails, with micrometeorites important, if not dominant, in determining the siderophile budget. This is demonstrated by regolith sample data for iridium, the best-studied of the "noble" siderophile elements. Mare regoliths, which form by relatively small-scale impact gardening atop intact, siderophile-poor bedrock, show a strong correlation between iridium and regolith maturity (Figure 12) (cf. Wasson *et al.*, 1975). Highland regoliths, however, show little correlation with maturity, probably because their siderophile enrichments are largely inherited from impact gardening at much larger scale, i.e., from megaregolith.

The Hertogen *et al.* (1977) interpretation of basin-dominated siderophile signatures has been refined in many subsequent works, usually emphasizing impact-melt breccias, most recently by Morgan *et al.* (2001), James (2002) and Norman *et al.* (2002a). The polymict highland

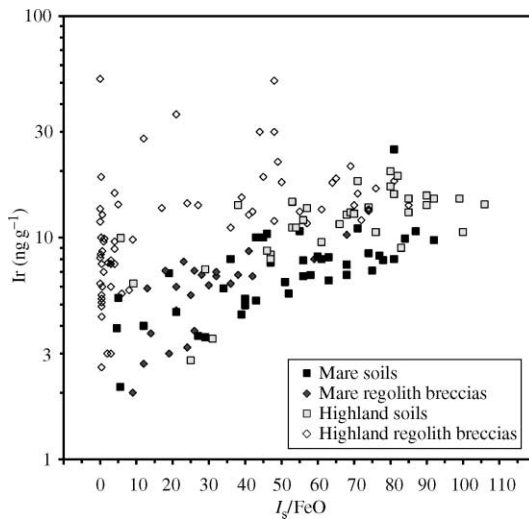


**Figure 12** Variation of iridium concentration in lunar regolith samples as a function of the maturity index  $I_s/FeO$ , which is a magnetically determined measure of the abundance of ultra-fine-grained  $Fe^0$  (which gradually accumulates through surface-regolithic processes) (Morris, 1978). The iridium data are from the compilation of Haskin and Warren (1991). A few soils of mixed mare–highland provenance (Apollo 17 stations 2 and 3) are excluded for the sake of clarity. Mare regolith samples show a strong positive correlation between iridium and  $I_s/FeO$ . Highland regolith samples feature generally higher iridium, and only a very weak correlation versus  $I_s/FeO$ .

impactites from the Apollo 14, 15, and 16 sites, where the siderophile components should be dominated by some combination of Imbrium, Serenitatis and (possibly, for Apollo 16 only) Nectaris ejecta, tend to feature remarkably non-chondritic siderophile patterns: Au/Ir is typically 3 times, and Ni/Ir 2 times, the CI-chondritic ratios. The polymict impactites from Apollo 17, presumably dominated by ejecta from adjacent Serenitatis, feature similar but less extremely high Au/Ir and Ni/Ir. Among chondrites (Wasson and Kallemeyn, 1988), only the EH enstatite type has Au/Ir approaching the typical Apollo 14, 15, and 16 ratio. Korotev (1987b) and Korotev *et al.* (1998) has conjectured that high-Au/Ir and high-Ni/Ir iron meteorites (akin to the IAB type) impacted at both Serenitatis and the Apollo 16 region. Morgan *et al.* (2001) argue that the high Au/Ir signature of late lunar accretion matches the composition they infer for the latest major accretion on Earth.

Ringwood *et al.* (1987) advocated a very different interpretation of the high Ni/Ir ratios in Apollo 16 impactites. These authors assumed that the meteoritic components have chondritic Ni/Ir, implying by mass balance (i.e., stripping away the meteoritic component based on iridium)

a high nickel concentration for the indigenous highland crust. This model appears implausible in view of nickel and iridium systematics in lunar highland meteorites, which tend to feature chondritic Ni/Ir, implying that the Apollo 16 site happens to be unrepresentative (Warren *et al.*, 1989, 2003).

Attempts to use siderophile element data to constrain the amount of material added to the Moon after origin of its crust (Ryder, 1999; Hartmann *et al.*, 2000) are plagued with tremendous uncertainties. The most straightforward approach is to average breccia data in the hope that the samples are representative of some portion of the lunar crust. Unfortunately, siderophile elements are unevenly distributed, and available samples may be grossly unrepresentative. For example, a single Apollo 14 rock that consists of metal with noritic silicates (Albrecht *et al.*, 1995) has 1,780  $\mu\text{g/g}$  Ir, or 150 times the mean highland (Apollo 14 and 16) regolith concentration, which itself may be significantly enriched by surface-micrometeoritic processing (Figure 12). This metal-rich rock suggests that meteoritic impactor siderophile components have tended to accumulate in dense metal at the bottom of large impact melts. It seems unrealistic to expect subsequent gardening to stir the crust so well that the uppermost megaregolith is representative of the whole.

To utilize data for regolith samples, Ryder (1999) invoked a dubious “correction” of the observed iridium concentrations by assuming that, in each soil from a terrain older than the lavas atop which the Apollo 11 regolith formed (i.e., 3.6 Ga), 8.9 ng/g of iridium, the concentration found in the Apollo 11 regolith, was added by surface-micrometeoritic processing. This method ignored the high maturity ( $I_s/FeO = 78$ : Morris, 1978) of the sparsely sampled Apollo 11 regolith. A less-mature regolith atop the same Tranquillitatis lava would have a much lower iridium concentration. Ryder’s method (cf. Hartmann *et al.*, 2000) resulted in an estimate that an average highland regolith contains only 0.5 wt.% of CI-chondritic equivalent (i.e., 2.6 ng/g of iridium) as a pre-3.6 Ga meteoritic component. Considering that the mare trend on Figure 12 extends from  $\sim 3$  to  $\sim 11$  ng/g (the low end is not zero, because no mare soil is free of debris sprayed off the highlands), while the highland regoliths average  $\sim 15$  ng/g (with no clear correlation with maturity), it seems a more realistic estimate for the contribution of pre-3.6 Ga Ir in average highland soil would be 8–12 ng/g, i.e., 2 wt.% of CI-chondritic equivalent. In any event, a long extrapolation would be needed to relate any surface regolith constraint to the content of meteoritic siderophiles in the crust as a whole.

#### 1.21.4.4 Pristine Highland Rocks: Distinctiveness of the Ferroan Anorthositic Suite

Making the distinction between pristine rocks and polymict breccias is a crucial first step in any attempt to accurately gauge the original diversity, and thus the igneous processes involved in genesis, of the nonmare lunar crust (the terms nonmare and highland are essentially synonymous; arguably “highland” is an awkward term for virtually all of the Moon’s crust, most of which is at levels lower than, including directly beneath, the veneers of “lowland” mare basalt). The vast majority of nonmare rocks are polymict breccias, and, unfortunately, identifying the pristine exceptions is seldom as easy as we would like it to be. In rare cases, vestiges of a coarse igneous cumulate texture, more consistent with an endogenous igneous origin than with an impact-melt origin, are preserved (e.g., Dymek *et al.*, 1975; Warren and Wasson, 1980b). But the most straightforward and generally applicable criterion is based on siderophile elements. Nonpristine rocks, i.e., products of meteorite impact-induced mixing, generally contain enough meteoritic debris to impart high concentrations of siderophile elements such as iridium, in comparison to the levels characteristic of pristine rocks, as exemplified by mare basalts (Figure 8). Warren and Wasson (1977) suggested  $3 \times 10^{-4}$  times the CI chondritic concentration as the “cutoff” level.

It should be emphasized that this siderophile cutoff should never be construed as an upper limit, *sine qua non*, and nor should data below the cutoff be taken as complete proof of pristine composition. In evaluating suspected pristine samples all relevant traits, such as texture and mineralogy (silicates in gross disequilibrium, or more obviously FeNi metal with typical meteoritic kamacite composition, can be indicators of impact mixing), other aspects of bulk composition (absence of KREEP contamination can be a mildly favorable indicator of pristinity) and isotopic data (an extremely old age can be mildly favorable) should be assessed, if possible (cf. Ryder *et al.*, 1980; Warren, 1993). Of course, a fine-grained texture, disequilibrium (zoned) silicates, and KREEP contamination, all are inevitable (but fortunately, high siderophile concentrations are not), if the pristine rock happens to be KREEP basalt.

The rate of discovery of pristine nonmare rocks has been limited by the scarcity of large lunar rock samples. Identification of a coarse cumulate or otherwise “plutonic” texture is difficult without a thin section at least several mm across, and determination of trace siderophile elements becomes increasingly difficult (and prone to the “nugget” effect) if available sample mass falls below  $\sim 0.1$  g. Lunar geochemists must resist

a temptation to overestimate the likelihood that new samples may be pristine. As a rather severe example, Snyder *et al.* (1995) classified 12 out of 18 small rock clasts from Apollo 14 as “probably pristine,” even though “[n]one of the samples... are texturally pristine,” and their siderophile data included no concentration (or limit) lower than  $6 \times 10^{-4}$  times CI, and even that level was approached for only one of the 12 samples in question. Rocklet 14286, which arguably might pass for an uncommonly fine-grained pristine norite, except that it contains a huge mass of meteoritic kamacite (Albrecht *et al.*, 1995), indicates that potential pristine rocks should be evaluated with great caution.

When pristine rocks alone are considered, a remarkable geochemical bimodality is manifested within the nonmare crust. During the 1970s, petrologists gradually noticed that the most anorthositic pristine rocks tend to feature distinctively low *mg* in comparison to otherwise comparable nonmare rocks. Dowty *et al.* (1974) coined the term “ferroan anorthosite” and Warner *et al.* (1976) were the first to postulate a separate “magnesium-rich plutonic” suite to account for nearly all other pristine nonmare rocks. In more recent usage, the original terms may be replaced with “ferroan anorthositic suite” (or simply “ferroan suite”) and “Mg-suite,” but their basic meanings have not changed. The distinctiveness of the ferroan anorthositic (FA) suite was first noticed on the basis of mineral composition data, namely plots of plagioclase  $\text{Ca}/(\text{Ca} + \text{Na})$  versus mafic silicate *mg*. Essentially the same pattern is found by simply plotting bulk-rock *mg* versus  $\text{Na}/(\text{Na} + \text{Ca})$  (Figure 13(a)). The Mg-suite rocks distribute along a normal fractionation path, with  $\text{Na}/(\text{Na} + \text{Ca})$  increasing as *mg* decreases, to form a diagonal trend on Figure 13(a). The FA suite forms a distinct cluster to the low  $\text{Na}/(\text{Na} + \text{Ca})$ , low-*mg* side of the Mg-suite trend; and there is a noticeable gap (or at least, a sparsely populated region) between the two groups. Warren and Kallemeyn (1984) found the same bimodality using other plagiophile element ratios, such as Ga/Al or Eu/Al, in place of  $\text{Na}/(\text{Na} + \text{Ca})$ . Most impressive is Eu/Al (Figure 13(b)), which results in a wide gap between the two pristine rock groups.

Besides having distinctive combinations of *mg* and plagiophile ratios, FA suite rocks tend to be more anorthositic than other types of pristine rocks (Figure 14). Not all of the ferroan pristine rocks are anorthosites, *sensu stricto* (>90 vol.% plagioclase, Stöfler *et al.*, 1980), but prevalence of low *mg* among the most anorthositic components of the crust is borne out by major-element variations among regolith samples (Figure 15). The obvious yet far-reaching implication (Warren and Wasson, 1980a) is that the FA suite, and no other adequately

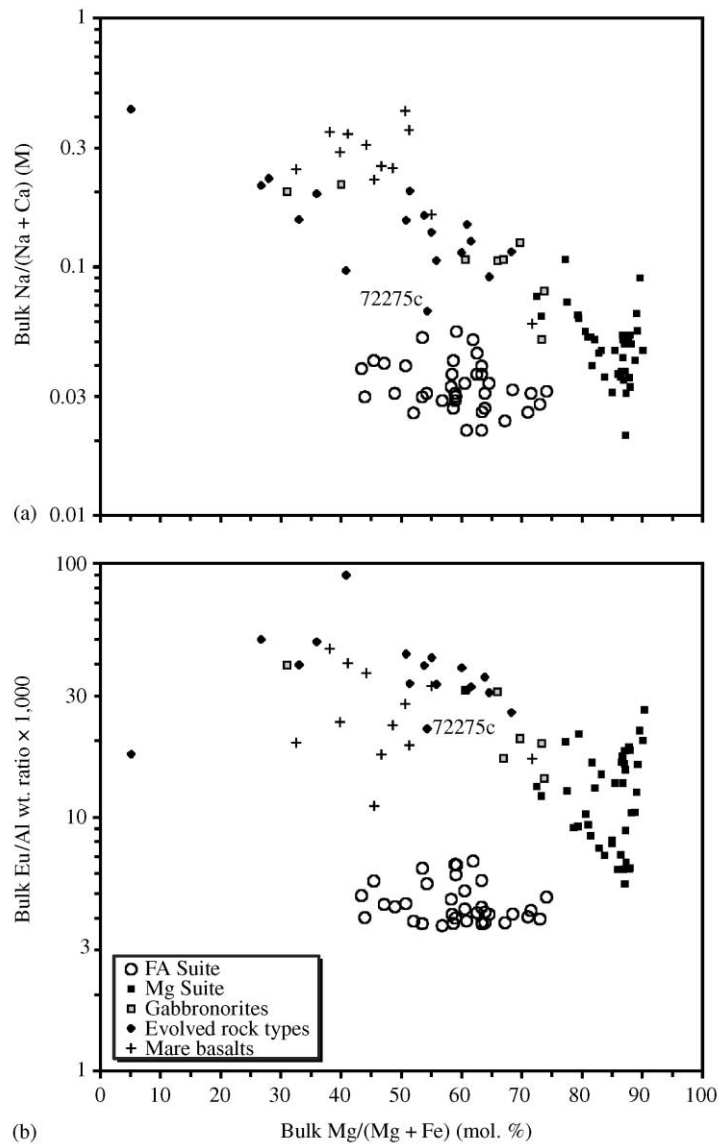


**Figure 13** Examples of the geochemical bimodality of pristine nonmare rocks: (a) Na/(Na + Ca) and (b) Eu/Al versus bulk-rock *mg*. The category “evolved rocks” here includes such rock types as granite, felsite, quartz, monzodiorite, and KREEP basalt. The database used for these diagrams comprises all known nonmare rocks with “pristinity confidence index”  $\geq 6$  as compiled by Warren (1993); more recent data sources include Arai and Warren (1997), Jolliff *et al.* (1999), Zeigler *et al.* (2000) (gabbronorite 62283,7-15 only), Neal and Kramer (2003), plus a few unpublished analyses by the author. On the Eu/Al diagram (b), the single gray diamond represents quartz monzodiorite 14161; its actual Eu/Al ( $\times 1,000$ ) is 126 (Jolliff *et al.*, 1999), but it is plotted at a slightly lower value (90) to avoid compressing the y-axis of the diagram. For gabbronorite 62283,7-15, the *mg* ratio is inferred to be  $\sim 40$  mol.% based on published mineralogy (source Zeigler *et al.*, 2000).

sampled type of pristine lunar rock (note that Figure 14 includes no samples smaller than 1 g), would have been buoyant over its parental magma. If the magma ocean hypothesis (see below) has any validity, the FA suite represents the only rock type plausibly formed as magma ocean flotation crust; and the manifestly sunken cumulates of the Mg-suite must come from intrusions that were emplaced into an older, FA-dominated crust.

In the few FA suite rocks that (as sampled) contain more than 1–2% mafic silicates, the mafics are typically a mix of olivine and coarsely exsolved low-Ca pyroxene (igneous pigeonite) (Taylor *et al.*, 1991; Papike *et al.*, 1991, 1998). Another apparent geochemical discontinuity between the ferroan anorthositic and Mg-suites is manifested by Ni–Co systematics in olivine (Shearer *et al.*, 2001b). Early models designed to

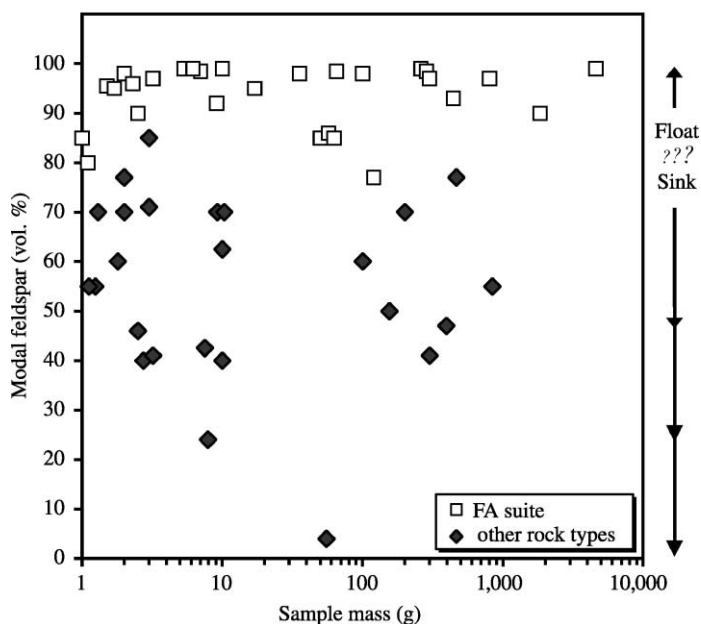


**Figure 14** Ferroan suite rocks tend to be more anorthositic than any other type of pristine lunar rock. Most of the “other” large pristine rocks are troctolitic and noritic cumulates of the magnesium suite (source Warren, 1993).

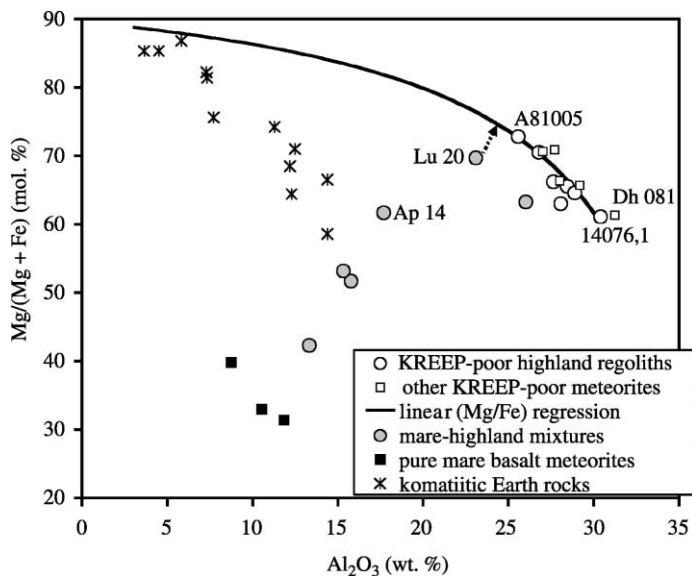


**Figure 15** *mg* versus  $Al_2O_3$  for lunar meteorites and averaged highland regolith samples from Apollo and Luna sites. The data set used for KREEP-poor highland regoliths comprises lunar meteorite breccias ALH81005, DaG 262, Dhofar 025, MAC88105, and QUE93069, Apollo 14 sample 14076,1 (Jerde *et al.*, 1990), and average Apollo 16 station 11 regolith (Korotev, 1981). The other KREEP-poor lunar meteorites are polymict breccias DaG 400, Dhofar 026, Dhofar 081, NWA 482, and Y-82192. The mare–highland mixture lunar meteorites shown are EET87521, QUE94281, and Y-793274. The pure mare basalts are Asuka-881757, NWA 032, and Y-793169. Data for komatiitic Earth rocks are from BVSP (1981). Curve represents an extrapolated linear regression for all of the plotted KREEP-poor highland samples. Also shown is the position inferred for the pure highland component of the Luna 20 regolith sample.

account for all pristine nonmare rocks as magma ocean flotation cumulates (Wood, 1975; Longhi and Boudreau, 1979) assumed that the mafic silicates formed from locally high proportions of trapped melt. However, the more mafic members

of the FA suite, such as 62236 (Borg *et al.*, 1999) and 62237 (Warren and Wasson, 1978), have only slightly higher REE concentrations than the purest anorthosites, indicating that the mafics are almost purely cumulus (or geochemically equivalent

“adcumulus”) material; i.e., in FA rocks the trapped melt components are uniformly low.

FA suite rocks have distinctive but not entirely uniform compositions, and James *et al.* (1989) suggested a subclassification of the suite into four “subgroups” based on subtly different *mg* ratios of mafic silicates and alkali contents of plagioclase. Obviously, such terms can be useful for descriptive purposes, but our sampling of the FA suite (mainly from one site, Apollo 16) is probably inadequate for assessing whether the proposed subgroups reflect compositional discontinuities within the suite, or apparent divisions, due to nonrepresentative sampling, of a compositional continuum.

Most of the other pristine nonmare rocks are Mg-suite rocks: troctolitic, noritic, and gabbro-noritic rocks that, based on evidence from a few texturally pristine samples (e.g., Dymek *et al.*, 1975; Marvin and Warren, 1980), probably all formed as cumulates. The highest-*mg* cumulates include several with ultramafic modes, but only one of these, dunite 72415 (Dymek *et al.*, 1975), has a mass >1 g (Figure 14), so many of them may actually be grossly unrepresentative samples of troctolites. High-Ca pyroxene apparently

formed relatively late in the crystallization sequence of most Mg-suite magmas; gabbro-norites are relatively rare, and they tend to have lower *mg* and higher Na/(Na + Ca) than norites (Figure 13(a)). They were first recognized as a distinctive subdivision of the Mg-suite (James and Flohr, 1983). As reviewed by Papike *et al.* (1998; cf. Shervais and McGee, 1999), the most evolved pristine rock types, alkali (high Na/Ca) suite rocks and rare granites (and similar quartz monzodiorites; also fine-grained felsites), may be extreme differentiates related to the Mg-suite and/or KREEP. Some of the best-sampled granitic rocks show clear millimeter-scale effects of silicate liquid immiscibility (Warren *et al.*, 1987; Jolliff *et al.*, 1999).

Isotopic studies have constrained the chronology of genesis of the various types of pristine rock. Results are summarized in Figure 16. Dating the REE- and rubidium-poor FA suite poses a severe analytical challenge, but argon isotopes seem far more prone than Sm–Nd and Rb–Sr to undergo resetting during the slow cooling and intense shock that ancient pristine rocks have typically endured. Considering the likelihood that the FA suite represents flotation crust from the

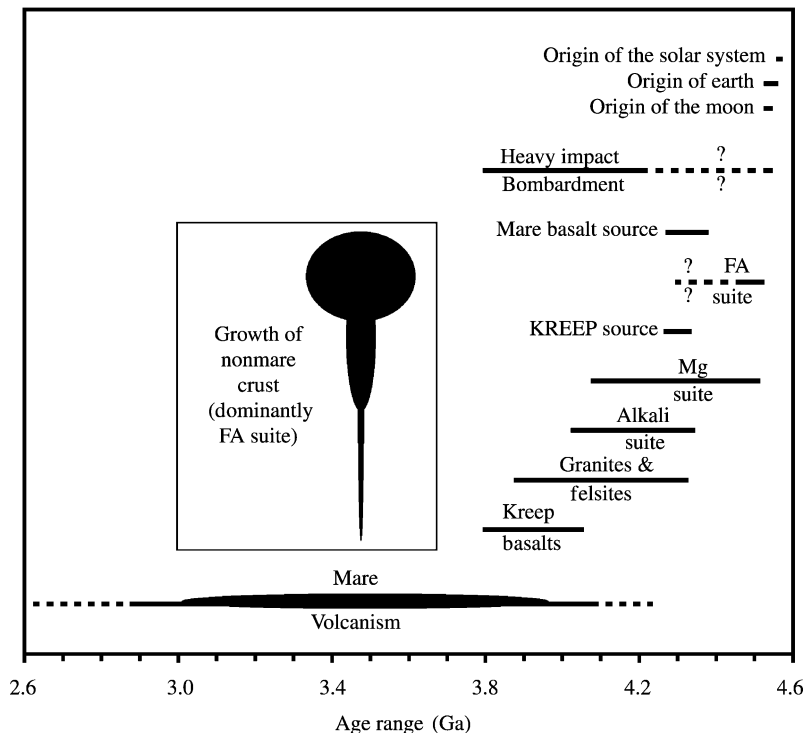


**Figure 16** Summary of the chronology of lunar crustal genesis, based mainly on data previously reviewed by Papike *et al.* (1998) and in Chapter 1.20. Other noteworthy sources include Carlson and Lugmair (1979) and Shih *et al.* (1992) for KREEP and mare basalt ages, including source model ages; and Borg *et al.* (1999) for the lowest of arguably accurate/relevant ages for a ferroan anorthositic (FA) suite rock (~4.29 Ga, for 62236). The inset cartoon indicates (roughly) the relative volume of crust produced at the various stages; i.e., the main volume of the crust probably formed as FA suite flotation cumulate, whereas evolved rocks like granites and KREEP basalts are probably volumetrically minor.

putative magma ocean, Sm–Nd isochron ages obtained for FA samples have been surprisingly diverse, ranging from  $4.56 \pm 0.07$  (Alibert *et al.*, 1994) down to  $\sim 4.29$  Ga (for 62236: Borg *et al.*, 1999). However, Norman *et al.* (2002b) inferred that the plagioclase in these rocks might have been compositionally modified, most likely during a large-impact event many hundreds of millions of years after igneous crystallization. When Norman *et al.* (2002b) constructed an Sm–Nd isochron using mafic silicates only (from four different FA samples, including 62236), they found an age of  $4.456 \pm 0.040$  Ga; they suggest that this may be closer to the true igneous crystallization age than any of the previous individual FA rock isochrons.

As reviewed by Papike *et al.* (1998) and Snyder *et al.* (2000b), Mg-suite rock ages distribute fairly evenly across a range from  $\sim 4.5$  Ga (very close to the age of the Moon itself, but all of the oldest Mg-suite ages are strontium-based, and thus plagued by uncertainty associated with the decay constant) down to  $\sim 4.1$  Ga. In a very general way, as illustrated in Figure 16, the sequence of typical or median age for the various major pristine rock types appears to be: FA suite, Mg-suite, gabbro-norite (subset of the Mg-suite), alkali suite, granites and felsites, KREEP basalts, mare basalts.

Before leaving the topic of pristine rocks, it should be noted that not only might individual samples be misclassified as pristine, but conceivably, particularly in the light of 14286 (Albrecht *et al.*, 1995), whole classes of putatively pristine rocks may actually be products of uncommonly large impact-melt ponds engendered by basin-forming impacts (Delano and Ringwood, 1978). The Mg-suite rocks are probably the most likely candidates for such an impact-melt genesis (A. E. Ringwood, 1993, personal communication; Hess, 1994). The diverse Mg-suite ages (Figure 16) imply that any impact-melt model is inconsistent with the bombardment cataclysm hypothesis, at least in its extreme form as advocated by Ryder (1990), because most ages should be the same in such a model. However, even if Ryder (1990) overstates the case for a cataclysm, the finite number of old basins is a major stumbling block for the Mg-suite-as-impact-melt-products hypothesis, because the hypothesis requires derivation of each Mg-suite sample through a combination of two major impacts. Impact 1 is required to form an exceptionally large pond of impact melt that yields the Mg-suite cumulates. Impact 2 is required to excavate the cumulates and add them to the surface regolith. Two overlapping basins are probably required for such a scenario. If Procellarum originally formed as an impact basin (a question that may never be resolved; see, e.g., Wilhelms, 1987), cumulates from its central

“sheet” of impact melt, indistinguishable from truly pristine rocks, may well have been excavated by subsequent events like Imbrium. However, as noted by Warren *et al.* (1996), in an event as gigantic and early as the putative Procellarum impact, the distinction between pristine and nonpristine becomes blurred and potentially even misleading, because most of the energy in the impact melt is inherited from the very warm (and deep) target region, and the mantle beneath the point of impact probably does not respond in a strictly passive way to the aftermath of such a colossal near-surface heating event.

#### 1.21.4.5 The Magma Ocean Hypothesis

The original inspiration for the lunar magma ocean hypothesis (Wood *et al.*, 1970) was a discovery that among  $\sim 1,700$  tiny (nearly all  $< 2$  mm) rocklets from the Apollo 11 Mare Tranquillitatis soil, a distinctive minority (5%) of exotic (i.e., highland) origin had anorthositic or “anorthositic gabbro” mineralogy or composition. Based on these few tiny samples, Wood *et al.* (1970) inferred that the Moon’s main, highland crust formed as a globe-wide “surface layer of floating anorthite crystals” over a zone of “gabbroic liquid, of composition near the eutectic value of the Moon as a whole.” Wood *et al.* (1970) admitted that their samples were “much too fine grained to have formed in such a grand event.” They nonetheless claimed to discern consistent cumulate textures. From a modern perspective, one of their crystalline samples (“40–2”) shows what is arguably a brecciated cumulate texture; most are fine-grained granulitic breccias. In any event, Wood *et al.* (1970) saw that “the cumulate interpretation must [also] be based on the specialized compositions of anorthositic rocks.”

The most impressive argument for a lunar magma ocean is still that same straightforward observation: the bulk composition of the globe-wide highland crust is far too anorthositic to have formed by piecemeal aggregation of basaltic partial melts ascended from the deeper interior. The normative plagioclase contents of internally generated partial melts are constrained by phase equilibria (e.g., Longhi and Pan, 1988) to be less than  $\sim 55$  wt.%, whereas the highly anorthositic ( $\sim 75$  wt.% normative plagioclase) composition of the global lunar crust has been amply confirmed in recent years by lunar meteorites (Table 3) and remote sensing (Lucey *et al.*, 2000a; Prettyman *et al.*, 2002).

Warren’s (1985) review cited numerous other lines of evidence favoring the magma ocean hypothesis. Warren’s (1985) second argument, the extreme antiquity of many pristine nonmare rocks, has been strengthened by recent work on

FA suite chronology (Norman *et al.*, 2002b). But a more impressive argument, which I would now rank ahead of that one, is based on the geochemical bimodality of the pristine nonmare rocks (Figure 13). The singularly low-*mg* composition of the FA suite must reflect a special process of origin. Warren (1986) argued that a deep, originally ultramafic magma ocean is the only plausible scenario for engendering a global component of low-*mg* cumulate anorthosite while burying the comparable (or larger) volume of low-*mg* mafic (sunken) cumulates that must have formed simultaneously, but are so deep that they are absent among sampled lunar rocks. This scenario accounts for the peculiarly low *mg* of the flotation crust, *provided* that the initial magma ocean was ultramafic, so that onset of (copious) plagioclase crystallization was preceded by extensive fractional crystallization of mafic silicates, driving down the *mg* and driving up the density, yet not fractionating plagiophile ratios, such as  $\text{Na}/(\text{Na} + \text{Ca})$ , of the residual melt. A similarly low-*mg*, low- $(\text{Na}/(\text{Na} + \text{Ca}))$  composition was probably never reproduced by subsequent, post-magma-ocean magmatism, because these magmas originated by (more or less) conventional partial melting of the mantle, and thus were already at or near plagioclase saturation even as they ascended into the crust.

Even if the parent Mg-suite magmas of some of the highest-*mg* dunites and troctolites initially reached the crust undersaturated in plagioclase, assimilation of ferroan anorthositic country rock by superheated, adiabatically decompressed melt may have curtailed the extent of the fractional crystallization of mafic silicates prior to plagioclase saturation (Warren, 1996; Ryder, 1991). Warren (1986) constructed a rather detailed model of this proposed AFC process. Without explicitly finding fault with Warren's (1986) model, Hess (1994) argued that such assimilation could not be very extensive. The main difference between the two model approaches is probably that Warren (1986) assumed that real-world assimilation would seldom involve total melting. The assimilation could be mostly physical; i.e., plagioclase grains that became loosened by disaggregation of anorthositic wall rock (at, say, 30% melting), and after a while settled at the base of a Mg-suite intrusion, might be impossible to distinguish from plagioclase grown entirely from the parent melt. In any event, as Hess (1994) suggested, assimilation would not be needed, provided the initial melts were sufficiently magnesian; this might, however, require that the source regions included high-*mg* cumulates from the early stages of magma ocean crystallization.

Another key argument in support of the magma-ocean hypothesis, formulated by various authors in the mid-1970s (most notably Taylor and Jakes,

1974), holds that the prevalence of negative europium anomalies among plagioclase-poor mare basalts implies predepletion of mare basalt source regions in massive proportions of plagioclase with positive europium anomalies. As discussed above, the assumption that the mare basalt europium anomalies can only reflect plagioclase fractionation has been challenged, but it still appears sound (Brophy and Basu, 1990).

Warren (1985) also cited the uniformity of the trace-element pattern of KREEP, suggesting derivation from the residuum (urKREEP) of a single, global magma. This argument has been weakened slightly, because remote sensing (Lawrence *et al.*, 2002a; cf. Warren, 2003) and lunar meteorites (Table 3) have revealed that KREEP is only abundant in one relatively small area, i.e., the Procellarum–Imbrium region. However, the same revelation about KREEP distribution reinforces another of Warren's (1985) arguments in favor of a magma ocean (“petrochemistry correlated with longitude”). The extremely heterogeneous distribution of KREEP stands in stark contrast to the almost uniform (anorthositic) major-element composition of the global crust. Both the Procellarum–Imbrium region and the giant, nearly antipodal South Pole Aitken basin have exceptionally mafic (noritic) compositions, yet strong KREEP enrichment is found only at Procellarum–Imbrium (Lawrence *et al.*, 2002a; Pieters *et al.*, 2001). Thus, the Procellarum–Imbrium KREEP anomaly is not simply a by-product of the large-scale cratering of that region. The uniqueness of the Procellarum–Imbrium region suggests that a globe-wide, extremely KREEP-concentrated magmatic plumbing system, such as a declining magma ocean, channeled and concentrated incompatible elements into this one region. The failure of KREEP to concentrate as well into the South Pole Aitken basin may be a consequence of origin of KREEP at a later stage, after the magma ocean had already nearly completely solidified.

Many authors have constructed detailed models for the crystallization of a lunar magma ocean (e.g., Longhi and Boudreau, 1979; Brophy and Basu, 1990; Snyder *et al.*, 1992; cf. the review of Warren, 1985). One key constraint is that silicate adiabats have small  $dP/dT$  relative to melting curves, so crystallization occurs primarily along the base of the magma ocean (Thomson, 1864). This is important, because pressures of the order 0.1–4 GPa enhance stability of pyroxene at the expense of olivine. It is commonly assumed that the lunar magma ocean produced mainly olivine until late in its crystallization sequence. However, it is likely that even the early cumulates consisted largely of pyroxene (Warren and Wasson, 1979b), with important compositional implications for the initial magma ocean, for its early and deep

cumulates, and for the bulk-Moon composition. All models indicate that the late magma ocean becomes (because of its low  $f_{\text{O}_2}$ ) highly enriched in FeO, which gives the FA suite parent melt a high density, and, in turn, allowed a considerable proportion of mafic silicate to be rafted within the FA flotation crust, as modeled quantitatively by Warren (1990).

As reviewed by Shearer and Papike (1999), the origin of the other major class of ancient pristine rocks, the Mg-suite, is widely ascribed to more conventional layered intrusions, emplaced in the FA crust during and shortly after the magma ocean waned to the final dregs of urKREEP (e.g., Warren and Wasson, 1980a; Ryder, 1991; Papike *et al.*, 1996). In a variant of this model, Hess (1994) suggested that the layered intrusions might have formed as impact melts in a few of the largest lunar accretionary events (cf. the previous section). The Mg-suite plutonism may have been triggered by the enhanced convective potential that many authors (e.g., Warren and Wasson, 1980a; Ryder, 1991; Hess, 1994; Hess and Parmentier, 1995; Zhong *et al.*, 2000) have noted would likely ensue if the magma ocean crystallized into a gravitationally unstable configuration: dense, FeO- and ilmenite-rich residual mush atop relatively FeO- and ilmenite-poor early cumulates. The Mg-suite plutons would inevitably interact extensively with urKREEP stewing at the base of the FA crust; this seems a major advantage of the model, because pristine KREEP basalts have relatively high *mg* ratios (Warren, 1988), and Mg-suite cumulates appear to have formed from remarkably KREEP-rich parent melts (e.g., Papike *et al.*, 1996; Shervais and McGee, 1999).

One obvious reason for skepticism regarding the magma ocean hypothesis is the colossal energy input that is required to engender a fully molten layer encompassing a large portion of the Moon (e.g., Wetherill, 1981). Another widely cited basis for skepticism stems from recent neodymium isotopic studies of ferroan anorthositic suite rocks. Until very recently, part of the problem lay in the young apparent ages (younger than Mg-suite rocks of manifest non-magma-ocean origin) for samples such as 62236,  $\sim 4.29$  Ga (Borg *et al.*, 1999). As discussed above, Norman *et al.* (2002b) seem to have largely eliminated this aspect of the neodymium-isotope based concern. These authors found that neodymium isotopic data from four FA suite rocks define a “robust” isochron, aged  $4.456 \pm 0.040$  Ga. However, the neodymium isotopic data still pose a dilemma, because the same isochron implies a positive initial  $\varepsilon_{\text{Nd}}$  of  $+0.8 \pm 1.4$ . More significantly, Norman *et al.* (2002b) also report an initial  $\varepsilon_{\text{Nd}}$  of  $+0.8 \pm 0.5$  for an individual FA suite sample 67215c, and

endorse a value of  $+0.9 \pm 0.5$  for sample 60025 (Carlson and Lugmair, 1988). These positive initial  $\varepsilon_{\text{Nd}}$  ratios imply derivation of the FA suite from material that had spent the prior few tens of Ma (between origin of the solar system and igneous crystallization) with a remarkably fractionated, light REE-depleted Sm/Nd ratio.

The potential seriousness of the problem is illustrated in Figure 17. The magnitude of the required light REE depletion is inversely related to the duration assumed for  $^{147}\text{Sm}$  decay prior to isotopic closure. Assuming crystallization at  $4.456 \pm 0.040$  Ga (Norman *et al.*, 2002b), the maximum duration of the decay at fractionated Sm/Nd is 110 Ma, and  $\sim 80$  Ma is more realistic, since the solar system formed at 4.566 Ga, and it probably took 20–30 Ma just to form the Moon (Chapter 1.20). A straightforward calculation (Dickin, 1995) yields the implied Sm/Nd ratio of the parent material as a function of assumed initial  $\varepsilon_{\text{Nd}}$  and duration of  $^{147}\text{Sm}$  decay (Figure 17). The implied Sm/Nd for the FA parent material is  $\sim 1.3$  times chondritic, and 1.14 times chondritic even at the extreme low end of the quoted 60025  $\varepsilon_{\text{Nd}}$  uncertainty range. These may sound like minor fractionations, but samarium and neodymium are separated by just two atomic numbers. Extrapolation suggests that the ratio of the heaviest REE versus the lightest, Lu/La or even Yb/Ce, would be more strongly nonchondritic than Sm/Nd. Assuming  $\log(\text{REE concentration})$  scales linearly with atomic number, an Sm/Nd ratio of 1.3 times chondritic suggests Ce/Yb  $\sim 0.21$  times chondrites. The right side of Figure 17 indicates how the implied source Sm/Nd ratios translate into (approximate) source Ce/Yb based on more detailed modeling (see caption). Assuming 80 Ma of decay at fractionated Sm/Nd after the formation of the source, for the source to so quickly reach an  $\varepsilon_{\text{Nd}}$  of  $+0.8$  implies the Sm/Nd of the source is 1.38 times chondritic, and its Ce/Yb is only  $\sim 0.14$  times chondritic.

The severity of this  $\varepsilon_{\text{Nd}}$  conundrum appeared even worse before Norman *et al.* (2002b) adduced their revised interpretation of the neodymium isotopic data for the FA suite. Results for 62236 led Borg *et al.* (1999) to question the viability of the magma ocean hypothesis, where the positive initial  $\varepsilon_{\text{Nd}}$  of  $3.1 \pm 0.9$  was seen as even more problematic than the young ( $\sim 4.29$  Ga) apparent age. While an age can be reset by shock and/or thermal processes, strongly positive  $\varepsilon_{\text{Nd}}$  ratio was claimed to be a firmly established trait of the FA suite. No conventional magmasphere model predicts light REE depletion at any point in the magma ocean’s evolution, and least of all in its later stages. On the contrary, magma ocean crystallization models (e.g., Snyder *et al.*, 1992)

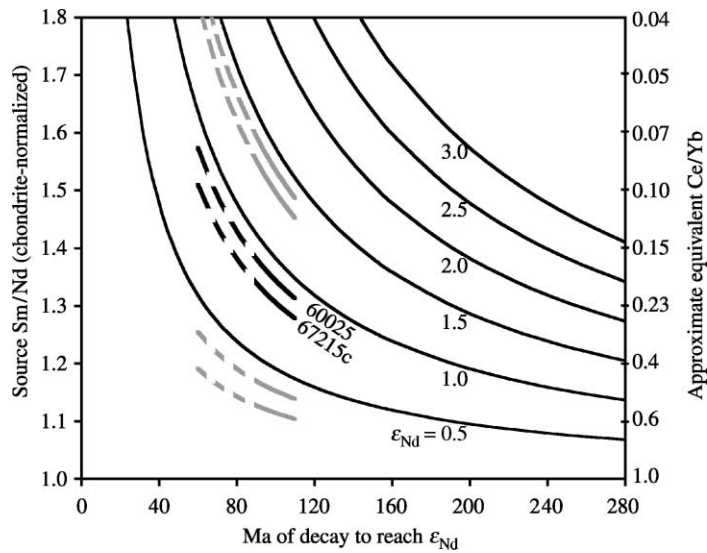


**Figure 17** Source Sm/Nd required for development of a range of target  $\epsilon_{Nd}$  versus time, where the former is calculated by rearrangement of equation 4.2 of Dickin (1995). As discussed in the text, these trends have important implications for origin of ferroan anorthosites with positive  $\epsilon_{Nd}$ , such as 60025 and 67215c (Norman *et al.*, 2002b). Black curves labeled 60025 and 67215c correspond to the nominal  $\epsilon_{Nd}$  of these samples (Norman *et al.*, 2002b) and the decay periods shown on the x-axis; unlabeled grey curves show limits implied by the quoted  $\epsilon_{Nd}$  uncertainties. The curves for 60025 and 67915c end at 110 Ma, because if their age is 4.456 Ga (Norman *et al.*, 2002b) they formed only 110 Ma after origin of the solar system. Shown at right are approximate Ce/Yb ratios, extrapolated from Sm/Nd based on modeling the FA source material as residual solids engendered by 0–6 wt.% “continuous” (1 wt.% porosity) partial melting (Albarède, 1995) of a plausible “primitive Moon mantle” with initially 60% olivine, 12% plagioclase, and 28% pigeonite, and applying distribution coefficients from Phinney and Morrison (1990), Kennedy *et al.* 1993, and McKay *et al.* 1991. Similar Ce/Yb would be implied by a variety of models; for example, under the simple assumption that  $\log(\text{REE concentration})$  scales linearly with atomic number, Sm/Nd ratios of 1.2, 1.4, and 1.6 would correspond to Ce/Yb = 0.33, 0.13, and 0.06, respectively.

indicate that crystallization of pyroxene tends to enrich light REE over heavy REE as the magma ocean evolves to approach plagioclase saturation (i.e., FA suite flotation). Based on the older age and less extreme  $\epsilon_{Nd}$  results implied by their revised interpretation, Norman *et al.* (2002b) reverted toward acceptance of the hypothesis that the FA suite formed as a magma ocean flotation crust, and speculated that the positive initial  $\epsilon_{Nd}$  ratio for the FA suite may have arisen because bulk Moon might have a subchondritic Nd/Sm ratio. However, the magnitude of the implied Ce/Yb fractionation (Figure 17) seems far in excess of what can be plausibly invoked without enormously depleting the Moon in light REE and other incompatible elements relative to cosmochemically similar refractory lithophile major elements (aluminum and calcium). Based on remote-sensing data (Lawrence *et al.*, 2002a; Prettyman *et al.*, 2002), incompatible elements are certainly not depleted by more than a factor of 2 relative to aluminum and calcium. As an alternative solution to the positive  $\epsilon_{Nd}$  conundrum, Norman *et al.* (2002b) conceded that the canonical value for CHUR-Nd (i.e., the zero point on the  $\epsilon_{Nd}$  scale) may not be “precisely representative” for lunar material.

#### 1.21.4.6 Alternative Models

Models have been proposed that invoke no magma ocean, although not in any detail for many years. Walker (1983) reviewed the evidence for petrogenetic diversity among the various types of pristine rocks, and suggested that the lunar crust formed by “serial magmatism” as a series of flows and plutons. However, Walker offered little justification for his implicit assumption that the entire lunar magma ocean hypothesis should be rejected simply because important (yet subordinate to the FA suite) components of the crust formed by processes other than magma ocean cumulate flotation. Walker conceded that a magma ocean is implied “if the bulk crust... [is] significantly more feldspathic than internally generated partial melt.” As discussed above, recent data amply confirm that the bulk composition of the crust (or at least its upper half) has ~75 wt.% plagioclase.

Wetherill (1981) argued that accretional heating could not melt a large fraction of the Moon; and yet, he suggested, it might have produced the Moon’s anorthositic crust. In this model, the Moon is zone-refined by production of many regional magma chambers as the central impact melts of the biggest accretionary events.

As the Moon grows, these impact-melt plutons differentiate so that incompatible elements and low-density plagioclase concentrate upward. Melting is discontinuous in space and time, but the ultimate, cumulative effect is a global surface layer of anorthosite. Similar models were earlier (and briefly) mentioned by Wetherill himself, by *Alfvén and Arrhenius* (1976), and by *Hess et al.* (1977).

The most detailed variant of this type of a model was proposed by *Longhi and Ashwal* (1985). In their model, the upward concentration of anorthosite is enhanced by diapiric detachment and ascent of feldspathic portions of the layered impact-melt plutons of the *Wetherill* (1981) model. Partial melting, partly due to pressure release, would lubricate the diapirs and enhance their potential for poking through the cool, mostly solid near-surface layer, and would be consistent with an argument (*Haskin et al.*, 1981) that ferroan anorthosites may be residual solids from episodic partial melting. Through the years (e.g., *Borg et al.*, 1999), this anorthosite diapirism model has been widely cited as the strongest competition for the magma ocean hypothesis. However, the diapirism model has some serious drawbacks. It implies that the anorthositic early crust should consist mainly of annealed (and possibly sheared and deformed) relict. But among the few pristine anorthositic (FA suite) samples that show little brecciation, only one, 15415, shows an annealed texture consistent with a relict origin (*Taylor et al.*, 1991). The majority of the samples (e.g., 62237, *Dymek et al.*, 1975, 66035c; *Warren and Wasson*, 1980b; 64435c, *James et al.*, 1989) have igneous textures. Also, in common with all other published models for early lunar petrogenesis without a magma ocean, the diapirism model seems ill-suited to account for the geochemical bimodality of pristine rocks, i.e., the observation that nearly all of the pristine rocks with the distinctive “ferroan” geochemical signature (*Figure 13*) are anorthosites (*Figure 14*), and vice versa. Why should such a relationship have developed, and in such consistent way, if the crust formed by aggregation of diapirically mobilized components from many separate, isolated intrusions? Highly inconsistent geochemical data seem inevitable, considering that the original plutons are supposed to form and crystallize at variety of depths (i.e., pressures), and would be prone to diverse fates, due to regional remelting events during the prolonged but spotty accretional heating of the Moon. By the same token, the diapirism model also seems ill-suited to account for the characteristic uniformity of the KREEP component (*Warren and Wasson*, 1979a). *Longhi* (2002) recently advocated a deep, primordial magma ocean, citing evidence for major depletion

of aluminum in the source region of VLT-mare pyroclastic glasses.

*Shirley* (1983) proposed a model that is, in some respects, intermediate between “serial” magmatic models and the magma ocean hypothesis. In this model, only a relatively thin zone near the top of the system is fully molten; the rest of the differentiating system, or at least a large portion immediately below the magma ocean, is a convective, mostly crystalline mush that *Shirley* (1983) called “magmifer.” In a quasi-steady state, the magmifer continually bleeds partial melt into the magma ocean, which replenishes the mush layer by precipitating mafic crystals, while simultaneously floating buoyant anorthosite to form a FA suite crust. *Warren* (1985) suggested the term magmasphere for the combined (magmifer + thin magma ocean) partially molten system. This model has an obvious thermal advantage: most of the Moon can be differentiated by the magmasphere, without fully melting the differentiated volume. Realistically, any “magma ocean” must have some magmifer/magmasphere characteristics, but it is unclear whether a lunar magmifer could sustain itself against upward percolation of buoyant melt (*McKenzie*, 2000) over a thick enough depth range, with a large enough fraction of melt, to have any appreciable effect. A major role for equilibration between the magma ocean and a thick magmifer would have a major disadvantage: it would dampen, if not cancel, the potential for early fractional crystallization of ultramafic, plagioclase-undersaturated magma (see above) to engender the peculiarly low-*mg* ratio of the FA suite pristine rocks. It would also tend to reduce the tendency for heterogeneity to develop in the mantle (the magmifer is well-stirred, like a melt-lubricated variant of Earth’s present-day asthenosphere), and thus come into conflict with evidence (e.g., *Figure 1*; hafnium isotopic data, *Unruh et al.*, 1984; *Beard et al.*, 1998) for extreme heterogeneity in the source mantle for mare basalts.

### 1.21.5 THE BULK COMPOSITION AND ORIGIN OF THE MOON

A vast literature exists concerning attempts to divine the bulk composition of the Moon, and to assess the implications for models of lunar origin of the Moon and Earth. The most obvious areas of compositional contrast versus Earth are the gross depletion in FeNi (i.e., core matter) implied by the Moon’s low bulk density, and the lunar volatile depletions, which were discussed above (*Figure 6*). The FeNi depletion is a key advantage of the popular giant impact model, according to which the Moon originated as a form of giant impact spall after a collision between

the protoearth and a doomed Mars-sized, or larger, body (e.g., Cameron and Ward, 1976; Canup and Asphaug, 2001).

More controversial (although sometimes cited as proven fact) have been claims (e.g., Taylor and Jakes, 1974; Taylor, 1982) that the bulk Moon is enriched roughly twofold in the cosmochemically refractory lithophile elements (a class that includes the REEs, the heat sources thorium and uranium, and the major elements aluminum, calcium, and titanium), and that compared to Earth's primitive mantle, the Moon's silicate *mg* ratio is much lower, i.e., its FeO concentration is much higher. Neither of these claims has been confirmed by recent lunar science developments, which include the advent of global thorium and samarium maps (Lawrence *et al.*, 2002a; Prettyman *et al.*, 2002), data from lunar meteorites, and some radically changed interpretations of the Apollo seismic database.

Starting with Cameron and Ward (1976), the putative refractory enrichments have been claimed as an advantage of the high temperatures implied by most variants of the giant impact model of Earth–Moon origin. It has often been claimed, or implied, that the well-documented lunar volatile depletions (Figure 6) are so great that they must represent a unique signature of origin by giant impact. However, an effectively identical overall volatile depletion pattern is found for the eucrite meteorites (Figure 6), which are products of an asteroid (or asteroids) that presumably was never involved in an Earth–Mars scale collision (Chapter 1.11). Another common misconception holds that the bulk-Moon volatile depletions imply a significant degree of refractory enrichment. In fact, total depletion of every constituent with cosmochemical volatility (solar nebular condensation temperature, Wasson, 1985) between those of SiO<sub>2</sub> and H<sub>2</sub>O, from even the most volatile-rich (CI) type of chondrite, would increase the concentrations of all elements more refractory than silicon by a factor of only 1.22. For ten other types of chondrites (Jarosewich, 1990), the increase would be merely a factor of 1.02–1.09 (average 1.05).

Until recently, the canonical interpretation of the Apollo seismic data was that the thickness of the crust in the central nearside (Apollo 12 and Apollo 14) region is 60 km, and the global average thickness ~73 km (e.g., Taylor, 1982). Recent, more thorough processing of the Apollo lunar seismic data set suggests the central nearside crustal thickness is only ~30 km (Chenet *et al.*, 2002) or perhaps ~38 km (Khan and Mosegaard, 2002). Wiczorek (2003) calculates from global mass distribution constraints that the thickness cannot be less than 33 km; but in any case, the required aluminum and calcium to account for the lunar crust now appears greatly reduced. Meanwhile, the global

thorium map (Lawrence *et al.*, 2002a; cf. Warren, 2003) and lunar meteorites (Table 3) have revealed that the Apollo (central nearside) sampling region is highly unrepresentative for KREEPy refractory lithophile elements, again relaxing the need to invoke refractory enrichments.

The anticorrelation between Al<sub>2</sub>O<sub>3</sub> and *mg* shown by KREEP-poor highland regolith samples, including new lunar meteorites (Figure 15), extrapolates to a high, Earth-like *mg* for the mafic component of the highland crust. As noted by Warren (2003), this and other evidence (e.g., the extremely high *mg* of some Mg-suite rocks, Figure 13) is difficult to reconcile with a bulk Moon that is greatly enriched in FeO compared to Earth's primitive mantle. Warren (2003) argues that, apart from volatile and siderophile element constituents, plus possibly chromium and vanadium, available constraints imply a high degree of compositional similarity between the Moon and Earth's primitive mantle.

The precise oxygen isotopic match between Earth and the Moon (Wiechert *et al.*, 2001) is a powerful constraint. Chromium isotopes also show a noteworthy match (Lugmair and Shukolyukov, 1998). It is not obvious, however, that such a precise oxygen isotopic match should be seen as a confirmation of the giant impact model. In many variants of the model, most of the material that ultimately forms the Moon is derived not from the protoearth, but from the Mars-sized intruder. In the estimation of Canup and Asphaug, 2001), the intruder's contribution was probably ~80 wt.%. Considering the easily measurable difference between the real Mars and Earth in terms of oxygen isotopes (Clayton and Mayeda, 1996), the giant impact model seems to require a remarkable degree of similarity between the putative giant impactor and the final Earth. Another cause for concern is the likelihood (Warren, 1992) that geochemical stratification in the impactor would have resulted in a Moon, i.e., the orbiting spall from the giant impact, with an idiosyncratic (e.g., thorium- and light REE-enriched) bulk composition.

## ACKNOWLEDGMENTS

The author is indebted to Steve Simon and Andy Davis for helpful reviews. This research was supported by NASA grant NAG5-4215.

## REFERENCES

- Adler I., Trombka J. I., Schmadebeck R., Lowman P., Blodgett H., Yin L., Eller E., Podwysocki M., Weidner J. R., Bickel A. L., Lum R. K. L., Gerard J., Gorenstein P., Bjorkholm P., and Harris B. (1973) Results of the Apollo 15 and 16 x-ray experiment. *Proc. 4th Lunar Sci. Conf.* 2, 2783–2792.

- Albarède F. (1995) *Introduction to Geochemical Modeling*. Cambridge University Press, Cambridge, 543pp.
- Albrecht A., Herzog G. F., Klein J., Middleton R., Schultz L., Weber H. W., Kallemeyn G. W., and Warren P. H. (1995) Trace elements,  $^{26}\text{Al}$  and  $^{10}\text{Be}$ , and noble gases in lunar rock 14286. In *Lunar Planet. Sci. XXVI*. The Lunar and Planetary Institute, Houston, pp. 13–14.
- Alfvén H. and Arrhenius G. (1976) *Evolution of the Solar System*. NASA, 599p.
- Alibert C., Norman M. D., and McCulloch M. T. (1994) An ancient age for a ferroan anorthosite clast from lunar breccia 67016. *Geochim. Cosmochim. Acta* **58**, 2921–2926.
- Andre C. G. and El-Baz F. (1981) Regional chemical setting of the Apollo 16 landing site and the importance of the Kant Plateau. *Proc. 12th Lunar Planet. Sci. Conf.*, 767–779.
- Antonenko I., Head J. W., Mustard J. F., and Hawke B. R. (1995) Criteria for the detection of lunar cryptomaria. *Earth Moon Planet.* **69**, 141–172.
- Arai T. and Warren P. H. (1997) “Large” (1.7 g) compositionally pristine diabase 14434: a lithology transitional between Mg-gabbro and high-Al mare basalt. *Meteorit. Planet. Sci.* **32**, A7–A8.
- Arai T. and Warren P. H. (1999) Lunar meteorite QUE94281: glass compositions and other evidence for launch pairing with Yamato-793274. *Meteorit. Planet. Sci.* **34**, 209–234.
- Arnold (1979) Ice in the Lunar polar regions. *J. Geophys. Res.* **84**, 5659–5668.
- Ash R. D., Knott S. F., and Turner G. (1996) A 4-yr shock age for a Martian meteorite and implications for the cratering history of Mars. *Nature* **380**, 57–59.
- Bandermann L. W. and Singer S. F. (1973) Calculation of meteoroid impacts on Moon and Earth. *Icarus* **19**, 108–113.
- Beard B. L., Taylor L. A., Scherer E. E., Johnson C. M., and Snyder G. A. (1998) The source region and melting mineralogy of high-titanium and low-titanium lunar basalts deduced from Lu–Hf isotope data. *Geochim. Cosmochim. Acta* **62**, 525–544.
- Benoit P. H., Sears D. W. G., and Symes S. J. K. (1996) The thermal and radiation exposure history of lunar meteorites. *Meteorit. Planet. Sci.* **31**, 869–875.
- Bielefeld M. J., Andre C. G., Eliason E. M., Clark P. E., Adler I., and Trombka J. I. (1977) Imaging of lunar surface chemistry from orbital X-ray data. *Proc. 8th Lunar Sci. Conf.*, 901–908.
- Bogard D. D. (1995) Impact ages of meteorites: a synthesis. *Meteoritics* **30**, 244–268.
- Bogard D. D., Garrison D. H., Shih C.-Y., and Nyquist L. E. (1994)  $^{39}\text{Ar}$ – $^{40}\text{Ar}$  dating of two lunar granites—the age of Copernicus. *Geochim. Cosmochim. Acta* **58**, 3093–3100.
- Bogard D. D., Garrison D. H., and Nyquist L. E. (2000) Argon-39–Argon-40 ages of lunar highland rocks and meteorites. In *Lunar Planet. Sci. XXXI*, #1138. The Lunar and Planetary Institute, (CD-ROM).
- Borg L., Norman M., Nyquist L., Bogard D., Snyder G., Taylor L., and Lindstrom M. (1999) Isotopic studies of ferroan anorthosite 62236: a young lunar crustal rock from a light rare-earth-element-depleted source. *Geochim. Cosmochim. Acta* **63**, 2679–2691.
- Brophy J. G. and Basu A. (1990) Europium anomalies in mare basalts as a consequence of mafic cumulate fractionation from an initial lunar magma. *Proc. 20th Lunar Planet. Sci. Conf.*, 25–30.
- Brügmann G. E., Arndt N. T., Hofmann A. W., and Tobschall H. J. (1987) Noble metal abundances in komatiite suites from Alexo, Ontario and Gorgona Island, Columbia. *Geochim. Cosmochim. Acta* **51**, 2159–2169.
- Butler P., Jr. and Meyer C., Jr. (1976) Sulfur prevails in coatings on glass droplets: Apollo 15 green and brown glasses and Apollo 17 orange and black (devitrified) glasses. *Proc. 7th Lunar Sci. Conf.*, 1561–1582.
- BVSP (1981) *Basaltic Volcanism on the Terrestrial Planets*. Pergamon, New York, 1286p.
- Cameron A. G. W. and Ward W. R. (1976) The origin of the moon. In *Lunar Sci. VII*. The Lunar Science Institute, Houston, pp. 120–122.
- Canup R. M. and Asphaug E. (2001) Origin of the Moon in a giant impact near the end of the Earth’s formation. *Nature* **412**, 708–712.
- Carlson R. W. and Lugmair G. W. (1979) Sm–Nd constraints on early lunar differentiation and the evolution of KREEP. *Earth Planet. Sci. Lett.* **45**, 123–132.
- Carlson R. W. and Lugmair G. W. (1988) The age of ferroan anorthosite 60025: oldest crust on a young Moon? *Earth Planet. Sci. Lett.* **90**, 119–130.
- Chapman C. R., Cohen B. A., and Grinspoon D. H. (2002) What are the real constraints on commencement of the late heavy bombardment? In *Lunar Planet. Sci. XXXIII*, #1627. The Lunar and Planetary Institute, Houston (CD-ROM).
- Chenet H., Gagnepain-Beyneix J., and Lognonne P. (2002) A new geophysical view of the Moon. In *Lunar Planet. Sci. XXXIII*, #1684. The Lunar and Planetary Institute, Houston (CD-ROM).
- Chou C.-L., Boynton W. V., Sundberg L. L., and Wasson J. T. (1975) Volatiles on the surface of Apollo 15 green glass and trace-element distributions among Apollo 15 soils. *Proc. 6th Lunar Sci. Conf.*, 1701–1727.
- Chou C. L., Boynton W. V., Bild R. W., Kimberlin J., and Wasson J. T. (1976) Trace element evidence regarding a chondritic component in howardite meteorites. *Proc. 7th Lunar Sci. Conf.*, 3501–3518.
- Chyba C. F. (1991) Terrestrial mantle siderophiles and the lunar impact record. *Icarus* **92**, 217–233.
- Clayton R. N. and Mayeda T. K. (1996) Oxygen isotopic studies of achondrites. *Geochim. Cosmochim. Acta* **60**, 1999–2017.
- Cohen B. A., Swindle T. D., and Kring D. A. (2000) Support for the lunar cataclysm hypothesis from lunar meteorite impact melt ages. *Science* **290**, 1754–1756.
- Cohen B. A., Snyder G. A., Hall C. M., Taylor L. A., and Nazarov M. A. (2001) Argon-40–Argon-39 chronology and petrogenesis along the eastern limb of the Moon from Luna 16, 20, and 24 samples. *Meteorit. Planet. Sci.* **36**, 1345–1366.
- Crider D. H. and Vondrak R. R. (2000) The solar wind as a possible source of lunar polar hydrogen deposits. *J. Geophys. Res.* **105**, 26773–26782.
- Crocket J. H. and MacRae W. E. (1986) Platinum-group element distribution in komatiitic and tholeiitic volcanic rocks from Munro Township, Ontario. *Econ. Geol.* **81**, 1242–1251.
- Culler T. S., Becker T. A., Muller R. A., and Renne P. R. (2000) Lunar impact history from  $^{40}\text{Ar}/^{39}\text{Ar}$  dating of glass spherules. *Science* **287**, 1785–1788.
- Cushing J. A., Taylor G. J., Norman M. D., and Keil K. (1999) The granulitic impactite suite-impact melts and metamorphic breccias of the earliest lunar crust. *Meteorit. Planet. Sci.* **34**, 185–195.
- Dalrymple G. B. and Ryder G. (1993)  $^{40}\text{Ar}/^{39}\text{Ar}$  age spectra of Apollo 15 impact melt rocks by laser step heating and their bearing on the history of lunar basin formation. *J. Geophys. Res.* **98**, 13085–13095.
- Dalrymple G. B. and Ryder G. (1996) Argon-40/argon-39 age spectra of Apollo 17 highlands breccia samples by laser step heating and the age of the Serenitatis basin. *J. Geophys. Res.* **101**, 26069–26084.
- Dalrymple G. B., Ryder G., Duncan R. A., and Huard J. J. (2001)  $^{40}\text{Ar}$ – $^{39}\text{Ar}$  ages of Apollo 16 impact melt rocks by laser step heating. In *Lunar Planet. Sci. XXXII*, #1225. The Lunar and Planetary Institute, Houston (CD-ROM).
- Danckwerth P. A., Hess P. C., and Rutherford M. J. (1979) The solubility of sulfur in high-TiO<sub>2</sub> mare basalts. *Proc. 10th Lunar Planet. Sci. Conf.*, 517–530.
- Dasch E. J., Shih C.-Y., Bansal B. M., Wiesmann H., and Nyquist L. E. (1987) Isotopic analysis of basaltic fragments from lunar breccia 14321: chronology and petrogenesis of

- pre-imbrium mare volcanism. *Geochim. Cosmochim. Acta* **51**, 3241–3254.
- Dasch E. J., Ryder G., Shih C. Y., Wiesmann H., Bansal B. M., and Nyquist L. E. (1989) Time of crystallization of a unique A15 basalt. In *Lunar Planet. Sci. XX*. The Lunar and Planetary Institute, Houston, pp. 218–219.
- DeHon R. A. (1979) Thickness of the western mare basalts. *Proc. 10th Lunar Planet. Sci. Conf.*, 2935–2955.
- Delano J. W. (1986) Pristine lunar glasses: criteria, data, and implications. *Proc. 16th Lunar Planet. Sci. Conf.*, D201–D213.
- Delano J. W. and Ringwood A. E. (1978) Siderophile elements in the lunar highlands: nature of the indigenous component and implications for the origin of the Moon. *Proc. 9th Lunar Planet. Sci. Conf.*, 111–159.
- Dickin A. P. (1995) *Radiogenic Isotope Geology*. Cambridge University Press, Cambridge, p.78.
- Dickinson T., Taylor G. J., Keil K., Schmitt R. A., Hughes S. S., and Smith M. R. (1985) Apollo 14 aluminous mare basalts and their possible relationship to KREEP. *Proc. 15th Lunar Planet. Sci. Conf.*, C365–C374.
- Dickinson T., Taylor G. J., Keil K., and Bild R. W. (1989) Germanium abundances in lunar basalts: evidence of mantle metasomatism? *Proc. 19th Lunar Planet. Sci. Conf.*, 189–198.
- Dowty E., Prinz M., and Keil K. (1974) Ferroan anorthosite: a widespread and distinctive lunar rock type. *Earth Planet. Sci. Lett.* **24**, 15–25.
- Dungan M. A. and Brown R. W. (1977) The petrology of the Apollo 12 limonite basalt suite. *Proc. 8th Lunar Sci. Conf.*, 1339–1382.
- Dymek R. F., Albee A. L., and Chodos A. A. (1975) Comparative petrology of lunar cumulate rocks of possible primary origin: dunite 72415, troctolite 76535, norite 78235, and anorthosite 62237. *Proc. 6th Lunar Sci. Conf.*, 301–341.
- Elkins L. T., Fernandes V. A., Delano J. W., and Grove T. L. (2000) Origin of lunar ultramafic green glasses; constraints from phase equilibrium studies. *Geochim. Cosmochim. Acta* **64**, 2339–2350.
- Elphic R. C., Lawrence D. J., Feldman W. C., Barraclough B. L., Maurice S., Binder A. B., and Lucey P. G. (2000) Lunar rare earth element distribution and ramifications for FeO and TiO<sub>2</sub>: Lunar Prospector neutron spectrometer observations. *J. Geophys. Res.* **105**, 20333–20345.
- Eugster O., Polnau E., Salerno E., and Terribilino D. (2000) Lunar surface exposure models for meteorites Elephant Moraine 96008 and Dar al Gani 262 from the Moon. *Meteorit. Planet. Sci.* **35**, 1177–1182.
- Fagan T. J., Taylor G. J., Keil K., Bunch T. E., Wittke J. H., Korotev R. L., Jolliff B. L., Gillis J. J., Haskin L. A., Jarosewich E., Clayton R. N., Mayeda T. K., Fernandes V. A., Burgess R., Turner G., Eugster O., and Lorenzetti S. (2002) Northwest Africa 032: product of lunar volcanism. *Meteorit. Planet. Sci.* **37**, 371–394.
- Feldman W. C., Maurice S., Lawrence D. J., Little R. C., Lawson S. L., Gasnault O., Wiens R. C., Barraclough B. L., Elphic R. C., Prettyman T. H., Steinberg J. T., and Binder A. B. (2001) Evidence for water ice near the lunar poles. *J. Geophys. Res.: Planets* **106**, 23231–23251.
- Fernandes V. A., Burgess R., and Turner G. (2002a) Age determination of lunar regolith samples from the Luna 16 and 24 cores using IR step heating. In *Lunar Planet. Sci. XXXIII*, #1753. The Lunar and Planetary Institute, Houston (CD-ROM).
- Fernandes V. A., Burgess R., and Turner G. (2002b) North West Africa 773 (NWA773): Ar–Ar studies of breccia and cumulate lithologies. In *The Moon Beyond 2002: Next Steps in Lunar Science and Exploration*, #3033 (eds. D. J. Lawrence and M. B. Duke). Lunar and Planetary Institute, Houston.
- Ferrand W. H. (1988) Highland contamination and minimum basalt thickness in northern Mare Fecunditatis. *Proc. 18th Lunar Planet. Sci. Conf.*, 319–329.
- Fogel R. A. and Rutherford M. J. (1995) Magmatic volatiles in primitive lunar glasses: I. FTIR and EPMA analyses of Apollo 15 green and yellow glasses and revision of the volatile-assisted fire-fountain theory. *Geochim. Cosmochim. Acta* **59**, 201–215.
- Gaddis L. R., Hawke B. R., Robinson M. S., and Coombs C. (2000) Compositional analyses of small lunar pyroclastic deposits using clementine multispectral data. *J. Geophys. Res.* **105**, 4245–4262.
- Gault D. E. (1983) The terrestrial accretion of lunar material. In *Lunar Planet. Sci. XIV*. The Lunar and Planetary Institute, Houston, pp. 243–244.
- Gibson E. K., Brett R., and Andrawes F. (1977) Sulfur in lunar mare basalts as a function of bulk composition. *Proc. 8th Lunar Sci. Conf.*, 1417–1428.
- Gifford A. W. and El-Baz F. (1981) Thicknesses of mare flow fronts. *Moon Planets* **24**, 391–398.
- Giguere T. A., Taylor G. J., Hawke B. R., and Lucey P. G. (2000) The titanium contents of lunar mare basalts. *Meteorit. Planet. Sci.* **35**, 193–200.
- Gillis J. J., Jolliff B. L., and Elphic R. C. (2003) A revised algorithm for calculating TiO<sub>2</sub> from Clementine UVVIS data: a synthesis of rock, soil, and remotely sensed TiO<sub>2</sub> concentrations. *J. Geophys. Res.: Planets* **108** (E2), art. no. 5009.
- Gladman B. J., Burns J. A., Duncan M., Lee P., and Levison H. F. (1996) The exchange of impact ejecta between terrestrial planets. *Science* **271**, 1387–1392.
- Govindaraju K. (1994) 1994 compilation of working values and sample description for 383 geostandards. *Geostand. Newslett.* **18**, 1–158.
- Grieve R. A. F. and Cintala M. J. (1992) An analysis of differential impact melt-crater scaling and implications for the terrestrial record. *Meteoritics* **27**, 526–538.
- Guinness E. A. and Arvidson R. E. (1977) On the constancy of the lunar cratering flux over the past  $3.3 \times 10^9$  yr. *Proc. 8th Lunar Sci. Conf.*, 3475–3494.
- Hartmann W. K. (1975) “Lunar cataclysm”: a misconception? *Icarus* **24**, 181–187.
- Hartmann W. K., Ryder G., Dones L., and Grinspoon D. (2000) The time-dependent intense bombardment of the primordial Earth/Moon system. In *Origin of the Earth and Moon* (eds. R. M. Canup and K. Righter). University of Arizona Press, Tucson, pp. 493–512.
- Haskin L. A. and Warren P. H. (1991) Chemistry. In *Lunar Sourcebook, A User's Guide to the Moon* (eds. G. Heiken, D. Vaniman, and B. M. French). Cambridge University Press, Cambridge, UK, pp. 357–474.
- Haskin L. A., Lindstrom M. M., Salpas P., and Lindstrom D. J. (1981) On compositional variations among lunar anorthosites. *Proc. 12th Lunar Planet. Sci. Conf.*, 41–66.
- Haskin L. A., Korotev R. L., Gillis J. J., and Jolliff B. L. (2002) Stratigraphies of Apollo and Luna highland landing sites and provenances of materials from the perspective of basin impact ejecta modelling. In *Lunar Planet. Sci. XXXIII*, #1364. The Lunar and Planetary Institute, Houston (CD-ROM).
- Hawke B. R., Lawrence D. J., Blewett D. T., Lucey P. G., Smith G. J., Taylor G. J., and Spudis P. D. (2003) Remote sensing studies of geochemical and spectral anomalies on the nearside of the Moon. In *Lunar Planet. Sci. XXXIV*, #1598. The Lunar and Planetary Institute, Houston (CD-ROM).
- Head J. W. and Wilson L. (1992) Lunar mare volcanism: stratigraphy, eruption conditions, and the evolution of secondary crusts. *Geochim. Cosmochim. Acta* **56**, 2155–2175.
- Hertogen J., Janssens M. J., and Palme H. (1980) Trace elements in ocean ridge basalt glasses: implications for fractionations during mantle evolution and petrogenesis. *Geochim. Cosmochim. Acta* **44**, 2125–2143.

- Hertogen J., Janssens M. J., Takahashi H., Palme H., and Anders E. (1977) Lunar basins and craters: evidence for compositional changes of bombarding population. *Proc. 8th Lunar Sci. Conf.*, 17–45.
- Hess P. C. (1994) Petrogenesis of lunar troctolites. *J. Geophys. Res.* **99**, 19083–19093.
- Hess P. C. and Parmentier E. M. (1995) A model for the thermal and chemical evolution of the Moon's interior: implications for the onset of mare volcanism. *Earth Planet. Sci. Lett.* **134**, 501–514.
- Hess P. C., Rutherford M. J., and Campbell H. W. (1977) Origin and evolution of LKFM basalt. *Proc. 8th Lunar Sci. Conf.*, 2357–2374.
- Hiesinger H., Head J. W., Wolf U., and Neukum G. (2000) Lunar mare basalts in oceanus procellarum: initial results on age and composition. In *Lunar Planet. Sci. XXXI*, #1278. The Lunar and Planetary Institute, Houston (CD-ROM).
- Hiesinger H., Head J. W., III, Wolf U., Jaumann R., and Neukum G. (2002) Lunar mare basalt flow units: thicknesses determined from crater size-frequency distributions. *Geophys. Res. Lett.* **29**, 8891–8894.
- Hörz F. (1978) How thick are lunar mare basalts? *Proc. 9th Lunar Planet. Sci. Conf.*, 3311–3331.
- James O. B. (2002) Distinctive meteoritic components in lunar “cataclysm” impact-melt breccias. In *Lunar Planet. Sci. XXXIII*, #1210. The Lunar and Planetary Institute, Houston (CD-ROM).
- James O. B. and Flohr M. K. (1983) Subdivision of the Mg-suite noritic rocks into Mg-gabbro-norites and Mg-norites. *Proc. Lunar Planet. Sci. Conf.*, A603–A614.
- James O. B. and McGee J. J. (1979) Consortium breccia 73255: genesis and history of two coarse-grained “norite” clasts. *Proc. 10th Lunar Planet. Sci. Conf.*, 713–743.
- James O. B., Lindstrom M. M., and Flohr M. K. (1989) Ferroan anorthosite from lunar breccia 64435: implications for the origin and history of lunar ferroan anorthosites. *Proc. 19th Lunar Planet. Sci. Conf.*, 219–243.
- Jarosewich E. (1990) Chemical analyses of meteorites: a compilation of stony and iron meteorite analyses. *Meteoritics* **25**, 323–337.
- Jerde E. A., Morris R. V., and Warren P. H. (1990) In quest of lunar regolith breccias of exotic provenance—a uniquely anorthositic sample from the Fra Mauro (Apollo 14) highlands. *Earth Planet. Sci. Lett.* **98**, 90–108.
- Jolliff B. L., Floss C., McCallum I. S., and Schwartz J. M. (1999) Geochemistry, petrology, and cooling history of 14161,7373: a plutonic lunar sample with textural evidence of granitic-fraction separation by silicate-liquid immiscibility. *Am. Mineral.* **84**, 821–837.
- Jolliff B. L., Korotev R. L., Zeigler R. A., Floss C., and Haskin L. A. (2003) Northwest Africa 773: lunar mare breccia with a shallow-formed olivine cumulate, very-low-Ti heritage, and a KREEP connection. In *Lunar Planet. Sci. XXXIV*, #1935. The Lunar and Planetary Institute, Houston (CD-ROM).
- Keller L. P. and McKay D. S. (1997) The nature and origin of rims on lunar grains. *Geochim. Cosmochim. Acta* **61**, 2331–2341.
- Kennedy A. K., Lofgren G. E., and Wasserburg G. J. (1993) An experimental study of trace element partitioning between olivine, orthopyroxene, and melt in chondrules. *Earth Planet. Sci. Lett.* **115**, 177–195.
- Khan A. and Mosegaard K. (2002) An inquiry into the lunar interior: a nonlinear inversion of the Apollo lunar seismic data. *J. Geophys. Res.* **107**, E63.1–E63.23.
- Kirsten T., Horn P., and Kiko J. (1973) <sup>39</sup>Ar–<sup>40</sup>Ar dating and rare gas analysis of Apollo 16 rocks and soils. *Proc. 4th Lunar Sci. Conf.*, 1757–1784.
- Korotev R. L. (1981) Compositional trends in Apollo 16 soils. *Proc. 12th Lunar Planet. Sci. Conf.*, 577–605.
- Korotev R. L. (1987a) Mixing levels, the Apennine front soil component, and compositional trends in the Apollo 15 soils. *Proc. 17th Lunar Planet. Sci. Conf.*, E411–E431.
- Korotev R. L. (1987b) The meteoritic component of Apollo 16 noritic impact melt breccias. *Proc. 17th Lunar Planet. Sci. Conf.*, E491–E512.
- Korotev R. L. (1994) Compositional variation in Apollo 16 impact melt breccias and inferences for the geology and bombardment history of the central highlands of the Moon. *Geochim. Cosmochim. Acta* **58**, 3931–3969.
- Korotev R. L. and Kremser D. T. (1992) Compositional variations in Apollo 17 soils and their relationship to the geology of the Taurus-Littrow site. *Proc. 22nd Lunar Planet. Sci. Conf.*, 275–301.
- Korotev R. L., Haskin L. A., and Jolliff B. L. (1998) Ir/Au ratios and the origin of Apollo 17 and other Apollo impact-melt breccias. In *Lunar Planet. Sci. XXIX*, #1231. The Lunar and Planetary Institute, Houston (CD-ROM).
- Korotev R. L., Gillis J. J., Haskin L. A., and Jolliff B. L. (2002a) On the age of the Nectaris basin. In *The Moon Beyond 2002: Next Steps in Lunar Science and Exploration*, #3029 (eds. D. J. Lawrence and M. B. Duke). The Lunar and Planetary Institute, Houston.
- Korotev R. L., Zeigler R. A., Jolliff B. L., and Haskin L. A. (2002b) Northwest Africa 773—an unusual rock from the lunar maria. *Meteorit. Planet. Sci.* **37**, A81.
- Korotev R. L., Jolliff B. L., Zeigler R. A., and Haskin L. A. (2003) Compositional evidence for launch pairing of the YQ and elephant moraine lunar meteorites. In *Lunar Planet. Sci. XXIV*, #1357. The Lunar and Planetary Institute, Houston.
- Kring D. A. and Cohen B. A. (2002) Cataclysmic bombardment throughout the inner solar system. *J. Geophys. Res.* **107**, E2.4.1–E2.4.6.
- Kurat G., Kracher A., Keil K., Warner R., and Prinz M. (1976) Composition and origin of Luna 16 aluminous mare basalts. *Proc. 7th Lunar Sci. Conf.* **2**, 1301–1322.
- Lawrence D. J., Feldman W. C., Barraclough B. L., Binder A. B., Elphic R. C., Maurice S., and Thomsen D. R. (1998) Global elemental maps of the Moon: the Lunar Prospector gamma-ray spectrometer. *Science* **281**, 1484–1489.
- Lawrence D. J., Elphic R. C., Feldman W. C., Gasnault O., Maurice S., and Prettyman T. H. (2002a) Small-area thorium enhancements on the lunar surface. In *Lunar Planet. Sci. XXXIII*, #1970. The Lunar and Planetary Institute, Houston (CD-ROM).
- Lawrence D. J., Feldman W. C., Elphic R. C., Little R. C., Prettyman T. H., Maurice S., Lucey P. G., and Binder A. B. (2002b) Iron abundances on the Lunar surface as measured by the Lunar Prospector gamma-ray and neutron spectrometers. *J. Geophys. Res.* **107**, E12.13.1–E12.13.26.
- Le Bas M. J. (2001) Report of the working party on the classification of the lunar igneous rocks. *Meteorit. Planet. Sci.* **36**, 1183–1188.
- Li L. and Mustard J. F. (2000) Compositional gradients across mare–highland contacts: importance and geological implication of lateral transport. *J. Geophys. Res.* **105**, 20431–20450.
- Lindsay J. F. (1992) Extraterrestrial soils: the lunar experience. *SDEDP* **2**, 41–70.
- Lindstrom M. M. and Lindstrom D. J. (1986) Lunar granulites and their precursor anorthositic norites of the early lunar crust. *Proc. 16th Lunar Planet. Sci. Conf.*, D263–D276.
- Lofgren G. E., Donaldson C. H., and Usselman T. M. (1975) Geology, petrology, and crystallization of Apollo 15 quartz-normative basalts. *Proc. 6th Lunar Sci. Conf.*, 79–100.
- Longhi J. (1987) On the connection between mare basalts and picritic volcanic glasses. *Proc. Lunar 17th Planet. Sci. Conf.*, E349–E360.
- Longhi J. (1992) Experimental petrology and petrogenesis of mare volcanics. *Geochim. Cosmochim. Acta* **56**, 2235–2251.
- Longhi (2002) The extent of early lunar differentiation. In *Lunar Planet. Sci. XXXIII*, #2069. The Lunar and Planetary Institute, Houston.

- Longhi J. (2003) Green glasses: new pressure calibration, new ascent mechanism, new calculations, same story. In *Lunar Planet. Sci. XXXIV*, #1528. The Lunar and Planetary Institute, Houston (CD-ROM).
- Longhi J. and Ashwal L. D. (1985) Two-stage models for lunar and terrestrial anorthosites: petrogenesis without a magma ocean. *Proc. 15th Lunar Planet. Sci. Conf.*, C571–C584.
- Longhi J. and Boudreau A. E. (1979) Complex igneous processes and the formation of the primitive lunar crustal rocks. *Proc. 10th Lunar Planet. Sci. Conf.*, 2085–2105.
- Longhi J. and Pan V. (1988) A reconnaissance study of phase boundaries in low-alkali basaltic liquids. *J. Petrol.* **29**, 115–147.
- Lucey P. G. and Steutel D. (2003) Global mineral maps of the Moon. In *Lunar Planet. Sci. XXXIV*, #1051. The Lunar and Planetary Institute, Houston (CD-ROM).
- Lucey P. G., Blewett D. T., and Hawke B. R. (1998) Mapping the FeO and TiO<sub>2</sub> content of the lunar surface with multispectral imagery. *J. Geophys. Res.* **103**, 3679–3699.
- Lucey P. G., Blewett D. T., and Jolliff B. L. (2000a) Lunar iron and titanium abundance algorithms based on final processing of Clementine ultraviolet-visible images. *J. Geophys. Res.* **105**, 20297–20305.
- Lucey P. G., Blewett D. T., Taylor G. J., and Hawke B. R. (2000b) Imaging of lunar surface maturity. *J. Geophys. Res.* **105**, 20377–20386.
- Lugmair G. W. and Carlson R. W. (1978) The Sm–Nd history of KREEP. *Proc. 9th Lunar Planet. Sci. Conf.*, 689–704.
- Lugmair G. W. and Shukolyukov A. (1998) Early solar system timescales according to <sup>53</sup>Mn–<sup>53</sup>Cr systematics. *Geochim. Cosmochim. Acta* **62**, 2863–2886.
- Marti K., Aeschlimann U., Eberhardt P., Geiss J., Grögler N., Jost D. T., Laul J. C., Ma M. S., Schmitt R. A., and Taylor G. J. (1983) Pieces of the ancient lunar crust: ages and composition of clasts in consortium breccia 67915. *Proc. 14th Lunar Planet. Sci. Conf.*, B165–B175.
- Marvin U. B. and Warren P. H. (1980) A pristine eucrite-like gabbro from Descartes and its exotic kindred. *Proc. 11th Lunar Planet. Sci. Conf.*, 507–521.
- Mauer P. P. E., Geiss J., Grögler N., Stettler A., Brown G. M., Peckett A., and Krähenbühl U. (1978) Pre-imbrian craters and basins: ages, compositions, and excavation depths of Apollo 16 breccias. *Geochim. Cosmochim. Acta* **42**, 1687–1720.
- McEwen A. S., Keszthelyi L. P., Spencer J. R., Schubert G., Matson D. L., Lopes-Gautier R. M. C., Klaasen K. P., Johnson T. V., Head J. W., III, Geissler P. E., Fagents S., Davies A. G., Carr M. H., Breneman H. H., and Belton M. J. S. (1998) High-temperature silicate volcanism on Jupiter's moon Io. *Science* **281**, 87–90.
- McKay G. A. and Weill D. F. (1977) KREEP petrogenesis revisited. *Proc. 8th Lunar Sci. Conf.*, 2339–2355.
- McKay G., Le L., and Wagstaff J. (1991) Constraints on the origin of the mare basalt europium anomaly: REE partition coefficients for pigeonite. In *Lunar Planet. Sci. XXII*. The Lunar and Planetary Institute, Houston, (CD-ROM), pp. 883–884.
- McKenzie D. (2000) Constraints on melt generation and transport from V-series activity ratios. *Chem. Geol.* **162**, 81–94.
- Melosh H. J. (1989) *Impact Cratering: A Geologic Process*. Oxford University Press, New York, 245p.
- Meyer C. (1998) *Mars Meteorite Compendium—1998*. NASA Johnson Space Center, 237p.
- Misawa K., Tatsumoto M., Dalrymple G. B., and Yanai K. (1993) An extremely low U/Pb source in the Moon: U–Th–Pb, Sm–Nd, Rb–Sr, and <sup>40</sup>Ar–<sup>39</sup>Ar systematics of lunar meteorite Asuka 881757. *Geochim. Cosmochim. Acta* **57**, 4687–4702.
- Morbidelli A., Petit J. M., Gladman B., and Chambers J. E. (2001) A plausible cause of the late heavy bombardment. *Meteorit. Planet. Sci.* **36**, 371–380.
- Morgan J. W., Higuchi H., Takahashi H., and Hertogen J. (1978) A “chondritic” eucrite parent body: inference from trace elements. *Geochim. Cosmochim. Acta* **42**, 27–38.
- Morgan J. W., Walker R. J., Brandon A. D., and Horan M. F. (2001) Siderophile elements in Earth's upper mantle and lunar breccias: data synthesis suggests manifestations of the same late influx. *Meteorit. Planet. Sci.* **36**, 1257–1275.
- Morris R. V. (1978) The surface exposure (maturity) of lunar soils: some concepts and I<sub>2</sub>/FeO compilation. *Proc. Lunar 9th Planet. Sci. Conf.*, 2287–2297.
- Neal C. R. (2001) Interior of the Moon: the presence of garnet in the primitive deep lunar mantle. *J. Geophys. Res.* **106**, 27865–27885.
- Neal C. R. and Kramer G. (2003) The composition of KREEP: a detailed study of KREEP basalt 15386. In *Lunar Planet. Sci. XXXIV*, #2023. The Lunar and Planetary Institute, Houston (CD-ROM).
- Neal C. R. and Taylor L. A. (1989) Metasomatic products of the lunar magma ocean: the role of KREEP dissemination. *Geochim. Cosmochim. Acta* **53**, 529–541.
- Neal C. R. and Taylor L. A. (1991) Evidence for metasomatism of the lunar highlands and the origin of whitlockite. *Geochim. Cosmochim. Acta* **55**, 2965–2980.
- Neal C. R. and Taylor L. A. (1992) Petrogenesis of mare basalts: a record of lunar volcanism. *Geochim. Cosmochim. Acta* **56**, 2177–2211.
- Neal C. R., Taylor L. A., Hughes S. S., and Schmitt R. A. (1990) The significance of fractional crystallization in the petrogenesis of Apollo 17 type A and B high-Ti basalts. *Geochim. Cosmochim. Acta* **54**, 1817–1833.
- Neal C. R., Hacker M. D., Snyder G. A., Taylor L. A., Liu Y.-G., and Schmitt R. A. (1994) Basalt generation at the Apollo 12 site: Part I. New data, classification, and re-evaluation. *Meteoritics* **29**, 334–348.
- Neal C. R., Jain J. C., Snyder G. A., and Taylor L. A. (1999) Platinum group elements from the ocean of storms: evidence of two cores forming? (abstract). In *Lunar Planet. Sci. XXX*, #1003. The Lunar and Planetary Institute, Houston (CD-ROM).
- Neal C. R., Ely J. C., and Jain J. C. (2001) The siderophile element budget of the Moon: a reevaluation, Part I. In *Lunar Planet. Sci. XXXII*, #1658. The Lunar and Planetary Institute, Houston (CD-ROM).
- Neukum G., Ivanov B. A., and Hartmann W. K. (2001) Cratering records in the inner solar system in relation to the lunar reference system. *Space Sci. Rev.* **96**, 55–86.
- Nishiizumi K., Okazaki R., Park J., Nagao K., Masarik J., and Finkel R. C. (2002) Exposure and terrestrial histories of Dhofar 019 martian meteorite. In *Lunar Planet. Sci. XXXIII*, #1366. The Lunar and Planetary Institute, Houston (CD-ROM).
- Norman M. D., Benne V. C., and Ryder G. (2002a) Incorporation of siderophile elements into impact melts from lunar basins: PGE@Serenitatis.nasa.org. In *Lunar Planet. Sci. XXXIII*, #1176. The Lunar and Planetary Institute, Houston (CD-ROM).
- Norman M. D., Borg L. E., Nyquist L. E., and Bogard D. D. (2002b) Crystallization age and impact resetting of ancient lunar crust from the Descartes terrane. In *The Moon Beyond 2002: Next Steps in Lunar Science and Exploration*, #3028 (eds. D. J. Lawrence and M. B. Duke). The Lunar and Planetary Institute, Houston.
- Papike J., Taylor L., and Simon S. (1991) Lunar minerals. In *Lunar Sourcebook: A User's Guide to the Moon* (eds. G. Heiken, D. Vaniman, and B. M. French). Cambridge University Press, Cambridge, pp. 121–181.
- Papike J. J., Fowler G. W., Shearer C. K., and Layne G. D. (1996) Ion microprobe investigation of plagioclase and orthopyroxene from lunar Mg suite norites: implications for calculating parental melt REE concentrations and for assessing post-crystallization REE redistribution. *Geochim. Cosmochim. Acta* **60**, 3967–3978.

- Papike J. J., Ryder G., and Shearer C. K. (1998) Lunar samples. *Rev. Mineral.* **36**, 5.1–5.234.
- Paul R. L. and Lipschutz M. E. (1990) Chemical studies of differentiated meteorites: I. Labile trace elements in Antarctic and non-Antarctic eucrites. *Geochim. Cosmochim. Acta* **54**, 3185–3195.
- Peach C. L. and Mathez E. A. (1993) Sulfide melt-silicate melt distribution coefficients for nickel and iron and implications for the distribution of other chalcophile elements. *Geochim. Cosmochim. Acta* **57**, 3013–3021.
- Persikov E. S., Bukhtiyarov P. G., and Kalinicheva T. V. (1987) Effects of composition, temperature, and pressure on magma fluidity. *Geokhimiya* **3**(3), 483–498.
- Phinney W. C. and Morrison D. A. (1990) Partition coefficients for calcic plagioclase: implications for Archean anorthosites. *Geochim. Cosmochim. Acta* **54**, 2025–2043.
- Pieters C. M., Head J. W., III, Gaddis L., Jolliff L., and Duke M. (2001) Rock types of South Pole-Aitken basin and extent of basaltic volcanism. *J. Geophys. Res.* **106**, 28001–28022.
- Pieters C. M., Stankevich D. G., Shkuratov Y. G., and Taylor L. A. (2002) Statistical analysis of the links between lunar mare soil mineralogy, chemistry and reflectance. *Icarus* **155**, 285–298.
- Prettyman T. H., Feldman W. C., McKinney G. W., Binder A. B., Elphic R. C., Gasnault O. M., Maurice S., and Moore K. R. (2002) Library least squares analysis of Lunar Prospector gamma-ray spectra. In *Lunar Planet. Sci. XXXIII*, #2012. The Lunar and Planetary Institute, Houston (CD-ROM).
- Quaide W. L. and Oberbeck V. R. (1975) Development of the mare regolith: some model considerations. *Moon* **13**, 27–55.
- Rhodes J. M., Blanchard D. P., Dungan M. A., Brannon J. C., and Rodgers K. V. (1977) Chemistry of Apollo 12 mare basalts: magma types and fractionation processes. *Proc. 8th Lunar Sci. Conf.*, 1305–1338.
- Ringwood A. E. and Kesson S. E. (1976) A dynamic model for mare basalt petrogenesis. *Proc. 7th Lunar Sci. Conf.*, 1697–1722.
- Ringwood A. E., Seifert S., and Wänke H. (1987) A komatiite component in Apollo 16 highland breccias: implications for the nickel–cobalt systematics and bulk composition of the Moon. *Earth Planet. Sci. Lett.* **81**, 105–117.
- Ryder G. (1985) *Catalog of Apollo 15 Rocks* (Curatorial Facility Publication 20787). NASA Johnson Space Center, 1296p.
- Ryder G. (1990) Lunar samples, lunar accretion and the early bombardment of the Moon. *EOS* **71**, 313–323.
- Ryder G. (1991) Lunar ferroan anorthosites and mare basalt sources: the mixed connection. *Geophys. Res. Lett.* **18**, 2065–2068.
- Ryder G. (1999) Meteoritic abundances in the ancient lunar crust. In *Lunar Planet. Sci. XXX*, #1848. The Lunar and Planetary Institute, Houston (CD-ROM).
- Ryder G. and Cox B. T. (1996) An Apollo 15 mare basalt fragment and lunar mare provinces. *Meteorit. Planet. Sci.* **31**, 50–59.
- Ryder G. and Spudis P. D. (1980) Volcanic rocks in the lunar highlands. In *Proceedings of the Conference on the Lunar Highlands Crust* (eds. J. J. Papike and R. B. Merrill). Pergamon, New York, pp. 353–375.
- Ryder G., Norman M. D., and Score R. A. (1980) The distinction of pristine from meteorite-contaminated highlands rocks using metal compositions. *Proc. 11th Lunar Planet. Sci. Conf.*, 471–479.
- Ryder G., Delano J. W., Warren P. H., Kallemeyn G. W., and Dalrymple G. B. (1996) A glass spherule of equivocal impact origin from the Apollo 15 landing site: unique target mare basalt. *Geochim. Cosmochim. Acta* **60**, 693–710.
- Schaeffer O. A. and Husain L. (1973) Early lunar history: ages of 2 to 4 mm soil fragments from the lunar highlands. *Proc. 4th Lunar Sci. Conf.*, 1847–1864.
- Schultz P. H. and Mendell W. (1978) Orbital infrared observations of lunar craters and possible implications for impact ejecta emplacement. *Proc. 9th Lunar Planet. Sci. Conf.*, 2857–2884.
- Shearer C. K. and Papike J. J. (1989) Is plagioclase removal responsible for the negative Eu anomaly in the source regions of mare basalts. *Geochim. Cosmochim. Acta* **53**, 3331–3336.
- Shearer C. K. and Papike J. J. (1999) Magmatic evolution of the Moon. *Am. Mineral.* **84**, 1469–1494.
- Shearer C. K., Papike J. J., Simon S. B., Shimizu N., Yurimoto H., and Sueno S. (1990) Ion microprobe studies of trace elements in Apollo 14 volcanic glass beads: comparisons to Apollo 14 mare basalts and petrogenesis of picritic magmas. *Geochim. Cosmochim. Acta* **54**, 851–867.
- Shearer C. K., Papike J. J., and Layne G. D. (1996) Deciphering basaltic magmatism on the Moon from the compositional variations in Apollo 15 very low-Ti picritic magmas. *Geochim. Cosmochim. Acta* **60**, 509–528.
- Shearer C. K., Borg L., Ryder G., Papike J. J., and Nyquist L. (2001a) Deciphering ages of impacted glass beads using a crystal chemical-ion microprobe approach. An example using the Apollo 17 Group D basalt. In *Lunar Planet. Sci. XXXII*, #1851. The Lunar and Planetary Institute, Houston (CD-ROM).
- Shearer C. K., Papike J. J., and Hager J. (2001b) Chemical dichotomy of the Mg-suite. Insights from a comparison of trace elements in silicates from a variety of lunar basalts. In *Lunar Planet. Sci. XXXII*, #1643. The Lunar and Planetary Institute, Houston (CD-ROM).
- Shervais J. W. and McGee J. J. (1999) KREEP cumulates in the western lunar highlands: ion and electron microprobe study of alkali-suite anorthosites and norites from Apollo 12 and 14. *Am. Mineral.* **84**, 806–820.
- Shih C.-Y., Nyquist L. E., Bogard D. D., Bansal B. M., Wiesmann H., Johnson P., Shervais J. W., and Taylor L. A. (1986) Geochronology and petrogenesis of Apollo 14 very high potassium basalts. *Proc. 16th Lunar Planet. Sci. Conf.*, D214–D228.
- Shih C.-Y., Nyquist L. E., Bogard D. D., Dasch E. J., Bansal B. M., and Wiesmann H. (1987) Geochronology of high-K aluminous mare basalt clasts from Apollo 14 breccia 14304. *Geochim. Cosmochim. Acta* **51**, 3255–3271.
- Shih C.-Y., Nyquist L. E., Bansal B. M., and Wiesmann H. (1992) Rb–Sr and Sm–Nd chronology of an Apollo 17 KREEP basalt. *Earth Planet. Sci. Lett.* **108**, 203–215.
- Shih C.-Y., Nyquist L. E., Reese Y., Wiesmann H., and Schwandt C. (2001) Rb–Sr and Sm–Nd isotopic constraints on the genesis of lunar green and orange glasses. In *Lunar Planet. Sci. XXXII*, #1401. The Lunar and Planetary Institute, Houston (CD-ROM).
- Shih C.-Y., Nyquist L. E., Reese Y., Wiesmann H., Nazarov M. A., and Taylor L. A. (2002) The chronology and petrogenesis of the mare basalt clast from lunar meteorite Dhofar 287: Rb–Sr and Sm–Nd isotopic studies. In *Lunar Planet. Sci. XXXIII*, #1344. The Lunar and Planetary Institute, Houston (CD-ROM).
- Shirley D. N. (1983) A partially molten magma ocean model. *Proc. 13th Lunar Planet. Sci. Conf.* A519–A527.
- Shkuratov Y., Pieters C., Omelchenko V., Stankevich D., Kaydash V., and Taylor L. (2003) Estimates of the lunar surface composition with clementine images and LSCC data. In *Lunar Planet. Sci. XXXIV*, #1258. The Lunar and Planetary Institute, Houston (CD-ROM).
- Shoemaker E. M., Hait M. H., Swann G. A., Schleicher D. L., Schaber G. G., Sutton R. L., Dahlem D. H., Goddard E. N., and Waters A. C. (1970) Origin of the lunar regolith at Tranquillity base. *Proc. Apollo 11 Lunar Sci. Conf.*, 2399–2412.
- Simonds C. H., Warner J. L., Phinney W. C., and McGee P. E. (1976) Thermal model for impact breccia lithification: Manicouagan and the moon. *Proc. 7th Lunar Sci. Conf.*, 2509–2528.
- Snyder G. A., Taylor L. A., and Neal C. R. (1992) The sources of mare basalts: a model involving lunar magma ocean

- crystallization, plagioclase flotation and trapped instantaneous residual liquid. *Geochim. Cosmochim. Acta* **56**, 3809–3823.
- Snyder G. A., Neal C. R., Taylor L. A., and Halliday A. N. (1995) Processes involved in the formation of magnesian-suite plutonic rocks from the highlands of Earth's Moon. *J. Geophys. Res.* **100**, 9365–9388.
- Snyder G. A., Hall C. M., Taylor L. A., Nazarov M. A., and Semenova T. S. (2000a)  $^{40}\text{Ar}$ – $^{39}\text{Ar}$  geochronology of “new” basalts from Mare Fecunditatis and Mare Crisium. In *Lunar Planet. Sci.* **XXXI**, #1222. The Lunar and Planetary Institute, Houston (CD-ROM).
- Snyder G. A., Borg L. E., Nyquist L. E., and Taylor L. A. (2000b) Chronology and isotopic constraints on lunar evolution. In *Origin of the Earth and Moon* (eds. R. Canup and K. Righter). University of Arizona Press, Tucson, pp. 361–395.
- Staid M. I. and Pieters C. M. (2001) Mineralogy of the last lunar basalts: results from Clementine. *J. Geophys. Res.* **106**, 27887–27900.
- Starukhina L. V. and Shkuratov Y. G. (2000) The lunar poles: water ice or chemically trapped hydrogen? *Icarus* **147**, 585–587.
- Stewart D. B. (1975) Apollonian metamorphic rocks—the products of prolonged subsolidus equilibration. In *Lunar Sci. VI*. The Lunar Science Institute, Houston, pp. 774–776.
- Stöffler D., Knöll H.-D., Marvin U. B., Simonds C. H., and Warren P. H. (1980) Recommended classification and nomenclature of lunar highland rocks—a committee report. In *Proceedings of the Conference on the Lunar Highlands Crust* (eds. R. B. Merrill and J. J. Papike). Pergamon, New York, pp. 51–70.
- Swindle T. D., Spudis P. D., Taylor G. J., Korotev R. L., Nichols R. H., Jr., and Olinger C. T. (1991) Searching for Crisium basin ejecta: chemistry and ages of Luna 20 impact melts. *Proc. 21st Lunar Planet. Sci. Conf.*, 167–181.
- Taylor G. J., Warren P., Ryder G., Delano J., Pieters C., and Lofgren G. (1991) Lunar rocks. In *Lunar Sourcebook: A User's Guide to the Moon* (eds. G. Heiken, D. Vaniman, and B. M. French). Cambridge University Press, Cambridge, pp. 183–284.
- Taylor L. A., Shervais J. W., Hunter R. H., Shih C. Y., Nyquist L., Bansal B., Wooden J., and Laul J. C. (1983) Pre-4.2 AE mare basalt volcanism in the lunar highlands. *Earth Planet. Sci. Lett.* **66**, 33–47.
- Taylor S. R. (1982) *Planetary Science: A Lunar Perspective*. Lunar and Planetary Institute, Houston, 512p.
- Taylor S. R. and Jakes P. (1974) The geochemical evolution of the Moon. *Proc. 5th Lunar Planet. Sci. Conf.*, 1287–1305.
- Tera F. (1974) Isotopic evidence for a terminal lunar cataclysm. *Earth Planet. Sci. Lett.* **22**, 1–21.
- Tera F., Papanastassiou D. A., and Wasserburg G. J. (1974) Isotopic evidence for a terminal lunar cataclysm. *Earth Planet. Sci. Lett.* **22**, 1–21.
- Terada K., Saiki T., Hidaka H., Hashizume K., and Sano Y. (2002) *In-situ* ion microprobe U–Pb dating of glass spherules from Apollo 17 lunar soils. In *Lunar Planet. Sci.* **XXXIII**, #1481. The Lunar and Planetary Institute, Houston.
- Thalman C., Eugster O., Herzog G. F., Klein J., Krähenbühl U., Vogt S., and Xue S. (1996) History of lunar meteorites Queen Alexandra Range 93069, Asuka 881757, and Yamato 791639 based on noble gas abundances, radionuclide concentrations, and chemical composition. *Meteorit. Planet. Sci.* **31**, 857–868.
- Thomson W. (1864) On the secular cooling of the Earth. *Trans. Roy. Soc. Edinburgh* **23**, 157–169.
- Tompkins S. and Pieters C. M. (1999) Mineralogy of the lunar crust: results from clementine. *Meteorit. Planet. Sci.* **34**, 25–41.
- Unruh D. M., Stille P., Patchett P. J., and Tatsumoto M. (1984) Lu–Hf and Sm–Nd evolution in lunar mare basalts. *Proc. 14th Lunar Planet. Sci. Conf.*, B459–B477.
- Vaniman D., Dietrich J., Taylor G. J., and Heiken G. (1991) Exploration, samples, and recent concepts of the Moon. In *Lunar Sourcebook: A User's Guide to the Moon* (eds. G. Heiken, D. Vaniman, and B. M. French). Cambridge University Press, Cambridge, pp. 5–26.
- Walker D. (1983) Lunar and terrestrial Crust Formation. *Proc. 14th Lunar Planet. Sci. Conf.*, B17–B25.
- Walker D., Longhi J., Lasaga A. C., Stolper E. M., Grove T. L., and Hays J. F. (1977) Slowly cooled microgabbros 15555 and 15065. *Proc. 8th Lunar Sci. Conf.*, 1521–1548.
- Warner J. L., Simonds C. H., and Phinney W. C. (1976) Genetic distinction between anorthosites and Mg-rich plutonic rocks: new data from 76255 (abstract). *Lunar Sci. VII*. The Lunar Science Institute, Houston, pp. 915–917.
- Warner J. L., Phinney W. C., Bickel C. E., and Simonds C. H. (1977) Feldspathic granulitic impactites and pre-final bombardment lunar evolution. *Proc. 8th Lunar Sci. Conf.* **2**, 2051–2066.
- Warner R. D., Keli K., and Taylor G. J. (1977) Coarse-grained basalt 71597: a product of partial olivine accumulation. *Proc. 8th Lunar Sci. Conf.*, 1429–1442.
- Warren P. H. (1985) The magma ocean concept and lunar evolution. *Ann. Rev. Earth Planet. Sci.* **13**, 201–240.
- Warren P. H. (1986) Anorthosite assimilation and the origin of the Mg/Fe-related bimodality of pristine Moon rocks: support for the magmasphere hypothesis. *Proc. 16th Lunar Planet. Sci. Conf.*, D331–D343.
- Warren P. H. (1988) The origin of pristine KREEP: effects of mixing between urKREEP and the magmas parental to the Mg-rich cumulates. *Proc. 18th Lunar Planet. Sci. Conf.*, 233–241.
- Warren P. H. (1989) KREEP: major-element diversity, trace-element uniformity (almost). In *Workshop on Moon in Transition: Apollo 14, KREEP, and Evolved Lunar Rocks* (Technical Report 89-03) (eds. G. J. Taylor and P. H. Warren). Lunar and Planetary Institute, Houston, pp. 149–153.
- Warren P. H. (1990) Lunar anorthosites and the magma ocean hypothesis: importance of FeO enrichment in the parent magma. *Am. Mineral.* **75**, 46–58.
- Warren P. H. (1992) Inheritance of silicate differentiation during lunar origin by giant impact. *Earth Planet. Sci. Lett.* **112**, 101–116.
- Warren P. H. (1993) A concise compilation of key petrologic information on possibly pristine nonmare Moon rocks. *Am. Mineral.* **78**, 360–376.
- Warren P. H. (1996) Global inventory of lunar impact melt as a function of parent crater size. In *Lunar Planet. Sci.* **XXVII**. The Lunar and Planetary Institute, Houston, pp. 1379–1380.
- Warren P. H. (2003) “New” lunar meteorites: II. Implications for composition of the global lunar surface, of the lunar crust, and of the bulk Moon. *Meteorit. Planet. Sci.* **38** (submitted).
- Warren P. H. and Kallemeyn G. W. (1984) Pristine rocks (8th foray): “Plagiophile” element ratios, crustal genesis, and the bulk composition of the Moon. *Proc. 15th Lunar Planet. Sci. Conf.* C16–C24.
- Warren P. H. and Kallemeyn G. W. (1986) Geochemistry of lunar meteorite Yamato-791197: comparison with ALHA81005 and other lunar samples. *Proc. NIPR Symp. Antarct. Meteorit. (Tokyo)* **10**, 3–16.
- Warren P. H. and Wasson J. T. (1977) Pristine nonmare rocks and the nature of the lunar crust. *Proc. 8th Lunar Sci. Conf.*, 2215–2235.
- Warren P. H. and Wasson J. T. (1978) Compositional-petrographic investigation of pristine nonmare rocks. *Proc. 9th Lunar Planet. Sci. Conf.*, **1**, 185–217.
- Warren P. H. and Wasson J. T. (1979a) Effects of pressure on the crystallization of a “chondritic” magma ocean and implications for the bulk composition of the Moon. *Proc. 10th Lunar Planet. Sci. Conf.*, **2**, 2051–2083.

- Warren P. H. and Wasson J. T. (1979b) The origin of KREEP. *Rev. Geophys. Space Phys.* **17**, 73–88.
- Warren P. H. and Wasson J. T. (1980a) Early lunar petrogenesis, oceanic and extraoceanic. In *Proceedings of the Conference on the Lunar Highlands Crust* (eds. R. B. Merrill and J. J. Papike). Pergamon, New York, pp. 81–99.
- Warren P. H. and Wasson J. T. (1980b) Further foraging for pristine nonmare rocks: correlations between geochemistry and longitude. *Proc. 11th Lunar Planet. Sci. Conf.*, 431–470.
- Warren P. H., Taylor G. J., Keil K., Shirley D. N., and Wasson J. T. (1983) Petrology and chemistry of two “large” granite clasts from the Moon. *Earth Planet. Sci. Lett.* **64**, 175–185.
- Warren P. H., Jerde E. A., and Kallemeyn G. W. (1987) Pristine Moon rocks: a “large” felsite and a metal-rich ferroan anorthosite. *Proc. 17th Lunar Planet. Sci. Conf.*, E303–E313.
- Warren P. H., Jerde E. A., and Kallemeyn G. W. (1989) Lunar meteorites: siderophile element contents, and implications for the composition and origin of the Moon. *Earth Planet. Sci. Lett.* **91**, 245–260.
- Warren P. H., Jerde E. A., and Kallemeyn G. W. (1990) Pristine Moon rocks: an alkali anorthosite with coarse augite exsolution from plagioclase, a magnesian harzburgite, and other oddities. *Proc. 20th Lunar Planet. Sci. Conf.*, 31–59.
- Warren P. H., Jerde E. A., and Kallemeyn G. W. (1991) Pristine Moon rocks: Apollo 17 anorthosites. *Proc. 21st Lunar Planet. Sci. Conf.*, 51–61.
- Warren P. H., Claeys P., and Cedillo-Pardo E. (1996) Mega-impact melt petrology (Chicxulub, Sudbury, and the Moon): effects of scale and other factors on potential for fractional crystallization and development of cumulates. In *The Cretaceous-Tertiary Event and Other Catastrophes in Earth History*, Spec. Pap. 307 (eds. G. Ryder, D. Fastovsky, and S. Gartner). Geological Society of America, Boulder, CO, pp. 105–124.
- Warren P. H., Kallemeyn G. W., and Kyte F. T. (1999) Origin of planetary cores: evidence from highly siderophile elements in martian meteorites. *Geochim. Cosmochim. Acta* **63**, 2105–2122.
- Warren P. H., Ulf-Möller F., and Kallemeyn G. W. (2003) “New” lunar meteorites: I. Impact melt and regolith breccias and large-scale heterogeneities of the upper lunar crust. *Meteorit. Planet. Sci.* **38** (submitted).
- Wasson J. T. (1985) *Meteorites: Their Record of Early Solar System History*. Freeman, New York, 267p.
- Wasson J. T. and Kallemeyn G. W. (1988) Compositions of chondrites. *Phil. Trans. Roy. Soc. London* **A325**, 535–544.
- Wasson J. T., Boynton W. V., Chou C.-L., and Baedecker P. A. (1975) Compositional evidence regarding the influx of interplanetary materials onto the lunar surface. *Moon* **13**, 121–141.
- Wetherill G. W. (1981) Nature and origin of basin-forming projectiles. In *Multi-ring Basins* (eds. P. H. Schultz and R. B. Merrill). Pergamon, New York, pp. 1–18.
- Wiechert U., Halliday A. N., Lee D.-C., Snyder G. A., Taylor L. A., and Rumble D. (2001) Oxygen isotopes and the Moon-forming giant impact. *Science* **294**, 345–348.
- Wieczorek M. A. (2003) The thickness of the lunar crust: how low can you go? In *Lunar Planet. Sci. XXXIV*, #1330. The Lunar and Planetary Institute, Houston, CD-ROM.
- Wilhelms D. E. (1987) *The Geologic History of the Moon (USGS Professional Paper 1348)*. US Geological Survey, 302p.
- Wilson L. and Head J. W., III (2003) Depth generation of magmatic gas on the Moon and implications for pyroclastic eruptions. *Geophys. Res. Lett.* **30** (12), 1605.
- Wolf R. and Anders E. (1980) Moon and Earth: compositional differences inferred from siderophiles, volatiles, and alkalis in basalts. *Geochim. Cosmochim. Acta* **44**, 2111–2124.
- Wolf R., Woodrow A., and Anders E. (1979) Lunar basalts and pristine highland rocks: comparison of siderophile and volatile elements. *Proc. 10th Lunar Planet. Sci. Conf.*, 2107–2130.
- Wood J. A. (1975) Lunar petrogenesis in a well-stirred magma ocean. *Proc. 6th Lunar Sci. Conf.*, 1087–1102.
- Wood J. A., Dickey J. S., Marvin U. B., and Powell B. N. (1970) Lunar anorthosites and a geophysical model of the Moon. *Proc. Apollo 11 Lunar Sci. Conf.*, 965–988.
- Young R. A. (1977) The lunar impact flux, radiometric age correlation, and dating of specific lunar features. *Proc. 8th Lunar Sci. Conf.*, 3457–3474.
- Zeigler R. A., Jolliff B. L., Korotev R. L., and Haskin L. A. (2000) Petrology, geochemistry, and possible origin of monomict mafic lithologies of the Cayley plains. In *Lunar Planet. Sci. XXXI*, #1859. The Lunar and Planetary Institute, Houston (CD-ROM).
- Zellner N. E. B., Spudis P. D., Delano J. W., Whittet D. C. B., and Swindle T. D. (2003) Geochemistry and impact history at the Apollo 16 landing site. In *Lunar Planet. Sci. XXXIV*, #1157. The Lunar and Planetary Institute, Houston (CD-ROM).
- Zhong S., Parmentier E. M., and Zuber M. T. (2000) A dynamic origin for the global asymmetry of lunar mare basalts. *Earth Planet. Sci. Lett.* **177**, 131–140.